Edge Localized Modes (ELMs) and their control by Resonant Magnetic Perturbations (RMPs)

François Orain[1],

M.Hoelzl[1], A.Lessig[1], M.Bécoulet[2], G.T.A.Huijsmans[2], N.Schwarz[1], M.Dunne[1], E.Viezzer[1], M.Bécoulet[2], G.T.A.Huijsmans[2], S.Pamela[3], W.Suttrop[1], M.Willensdorfer[1], S.Guenter[1], E.Strumberger[1], K.Lackner[1] and the ASDEX Upgrade team[1]

[1]Max-Planck-Institut für Plasmaphysik, Garching, Germany
[2]CEA, IRFM, 13108 Saint-Paul-Lez-Durance, France
[3]CCFE, Culham Science Centre, Oxon, OX14 3DB, UK

Outline

- Introduction: ELMs and RMPs
- The JOREK code
- ELM dynamics
- ELM control by RMPs
- Conclusion and Outlook

Outline

- Introduction: ELMs and RMPs
  - ➔ High-confinement regime and ELMs
  - ➔ ELM control by RMPs
- The JOREK code
- ELM dynamics
- ELM control by RMPs
- Conclusion and Outlook

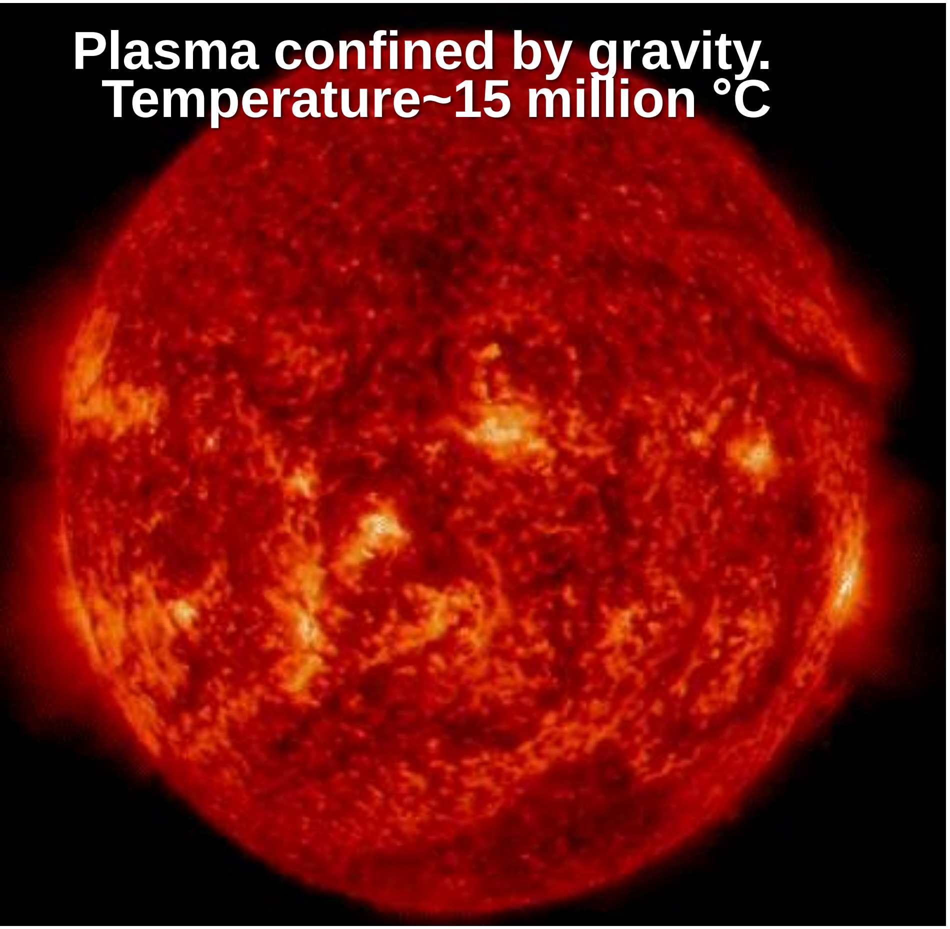

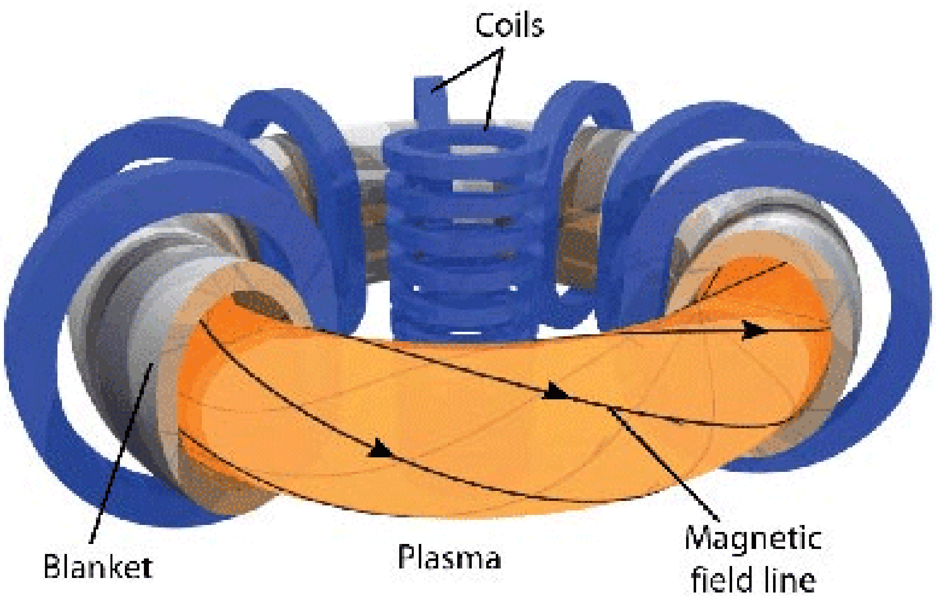

<u>Challenge:</u>
<u>Magnetic confinement of the plasma</u>

Temperature~100 million °C

Magnetic structure in tokamaks

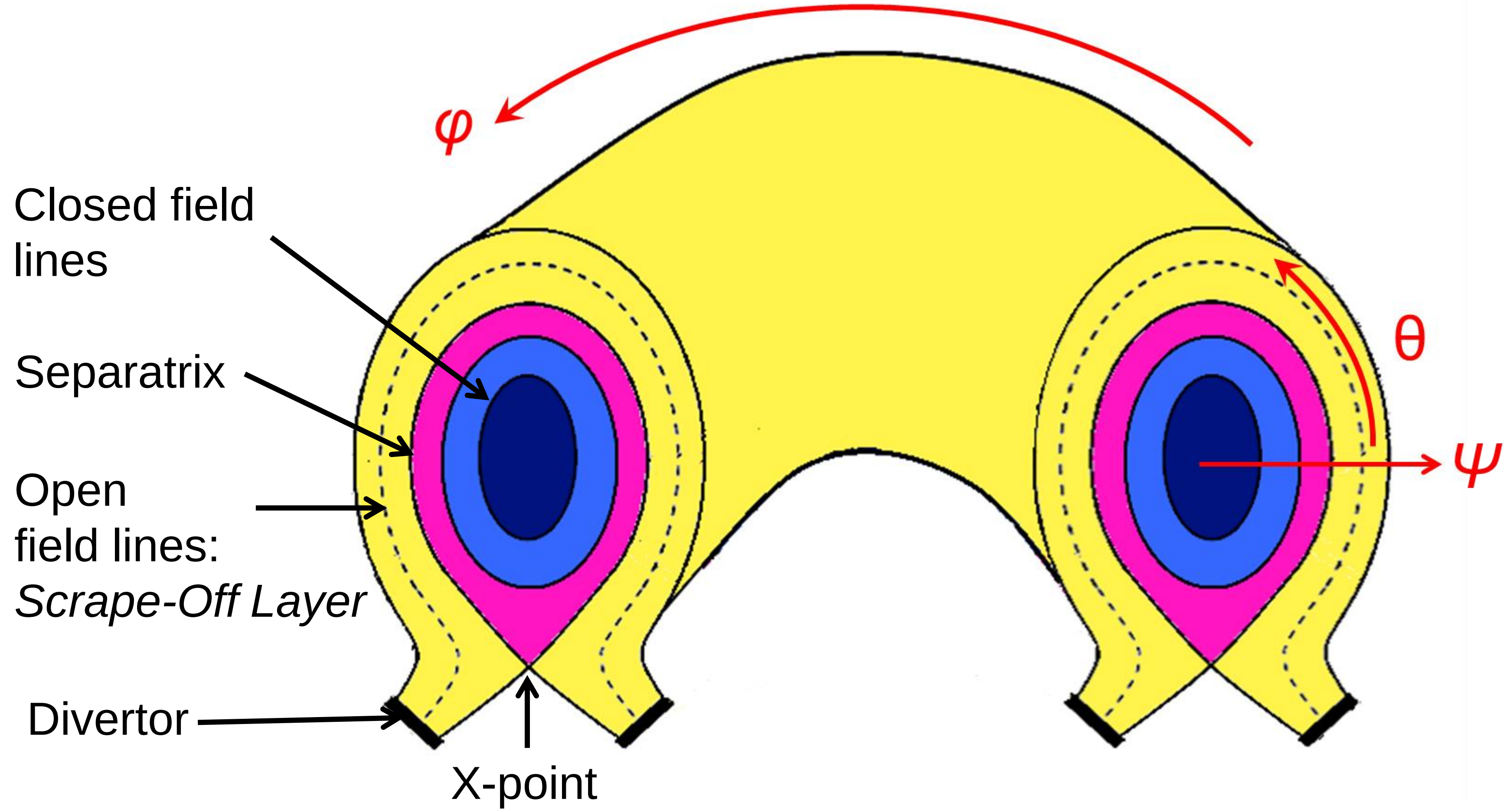

Magnetic structure in tokamaks

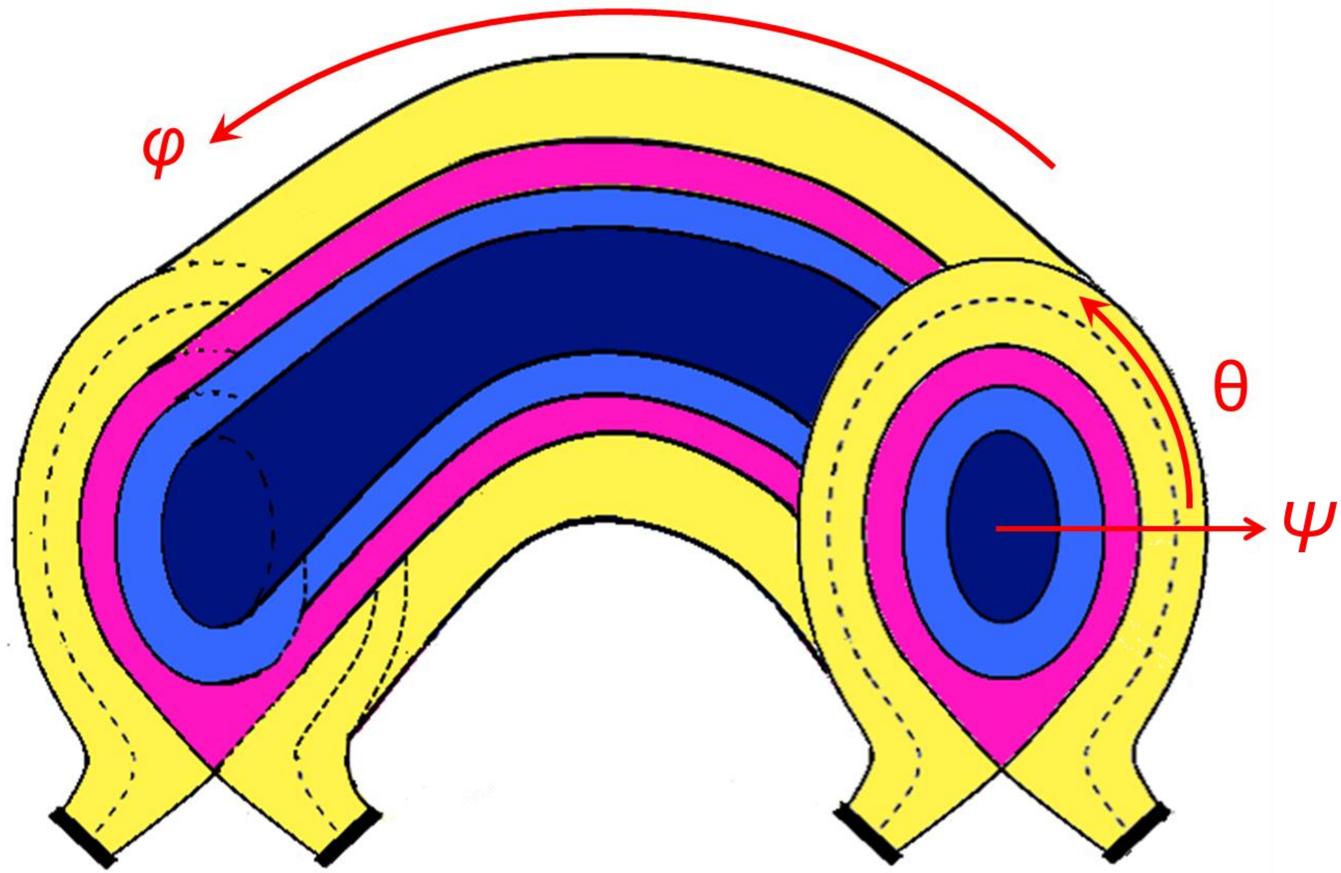

Magnetic surfaces nested into each other: → // transport >> ⊥ transport

→ Poloidal flux ψ labels magnetic surfaces

→ Equilibrium profiles T, $n \approx$ 1D = $f(\psi)$

Magnetic structure in tokamaks

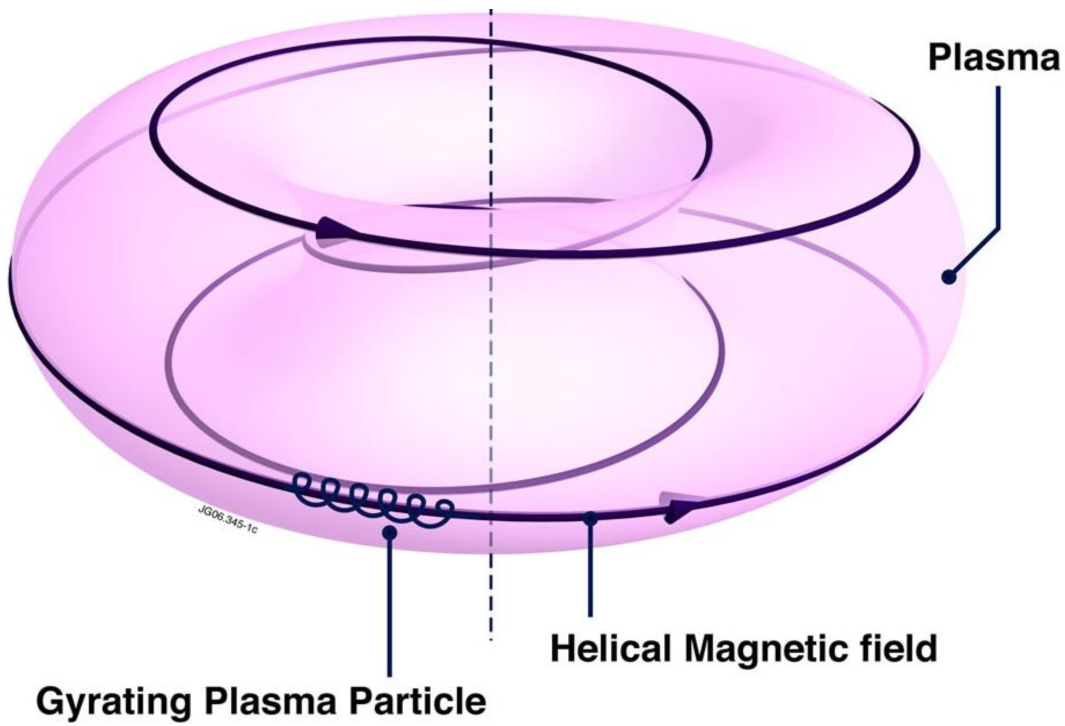

→ Safety factor q characterizes helicity of field lines:

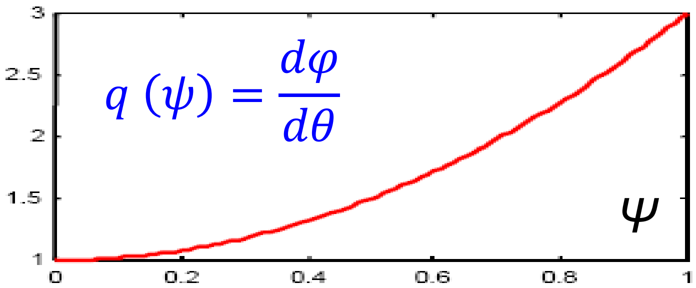

→ Field lines close on themselves
on resonant surfaces $q = m/n$

H-mode: improved confinement in X-point configuration

❖ **Improved confinement due to external transport barrier**

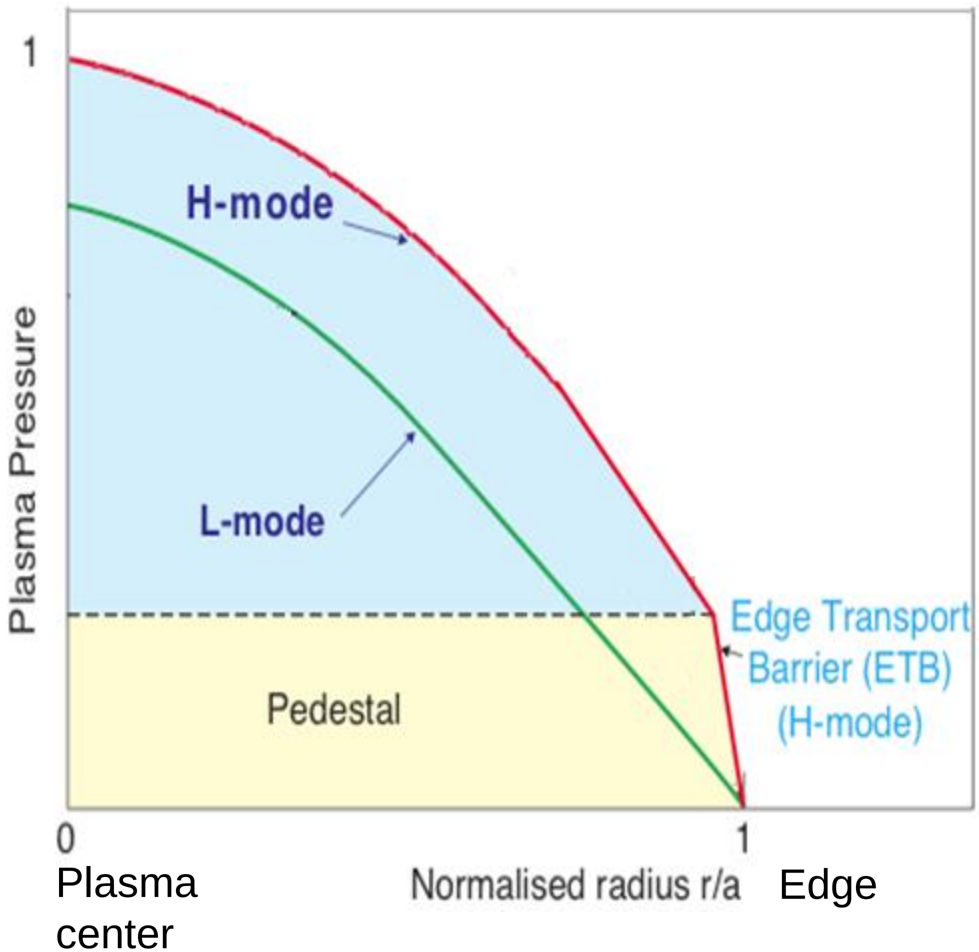

❖ Radial transport = turbulent
→ turbulence stabilized at the edge
→ External transport barrier
→ Pressure profile on a "pedestal"
→ **Improved confinement**

<u>H-mode:</u> improved confinement in X-point configuration

❖ <u>Improved confinement due to external transport barrier</u>

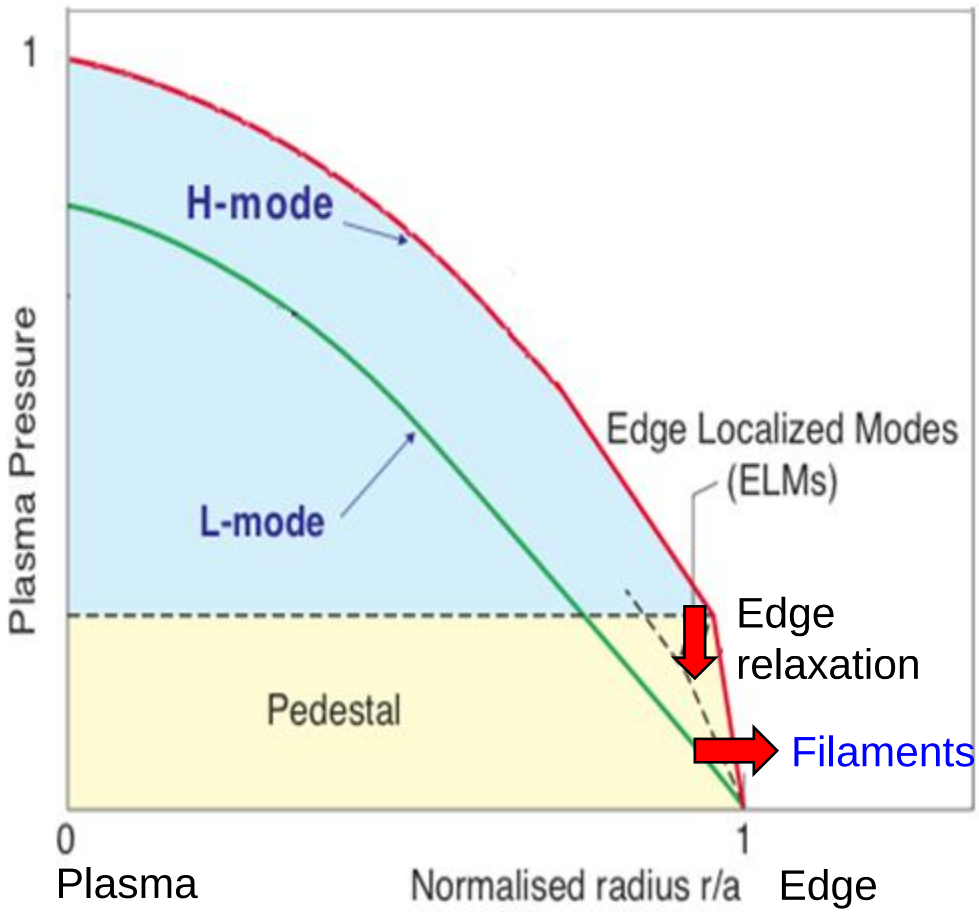

Edge relaxation

Filaments expelled from bulk plasma

Plasma center

Edge

❖ Radial transport = turbulent
→ turbulence stabilized at the edge
→ External transport barrier
→ Pressure profile on a "pedestal"
→ **<u>Improved confinement</u>**

❖ BUT quasiperiodic relaxations of the edge plasma **<u>due to Edge Localized Modes (ELMs)</u>**

Somehow analogous to solar eruptions…

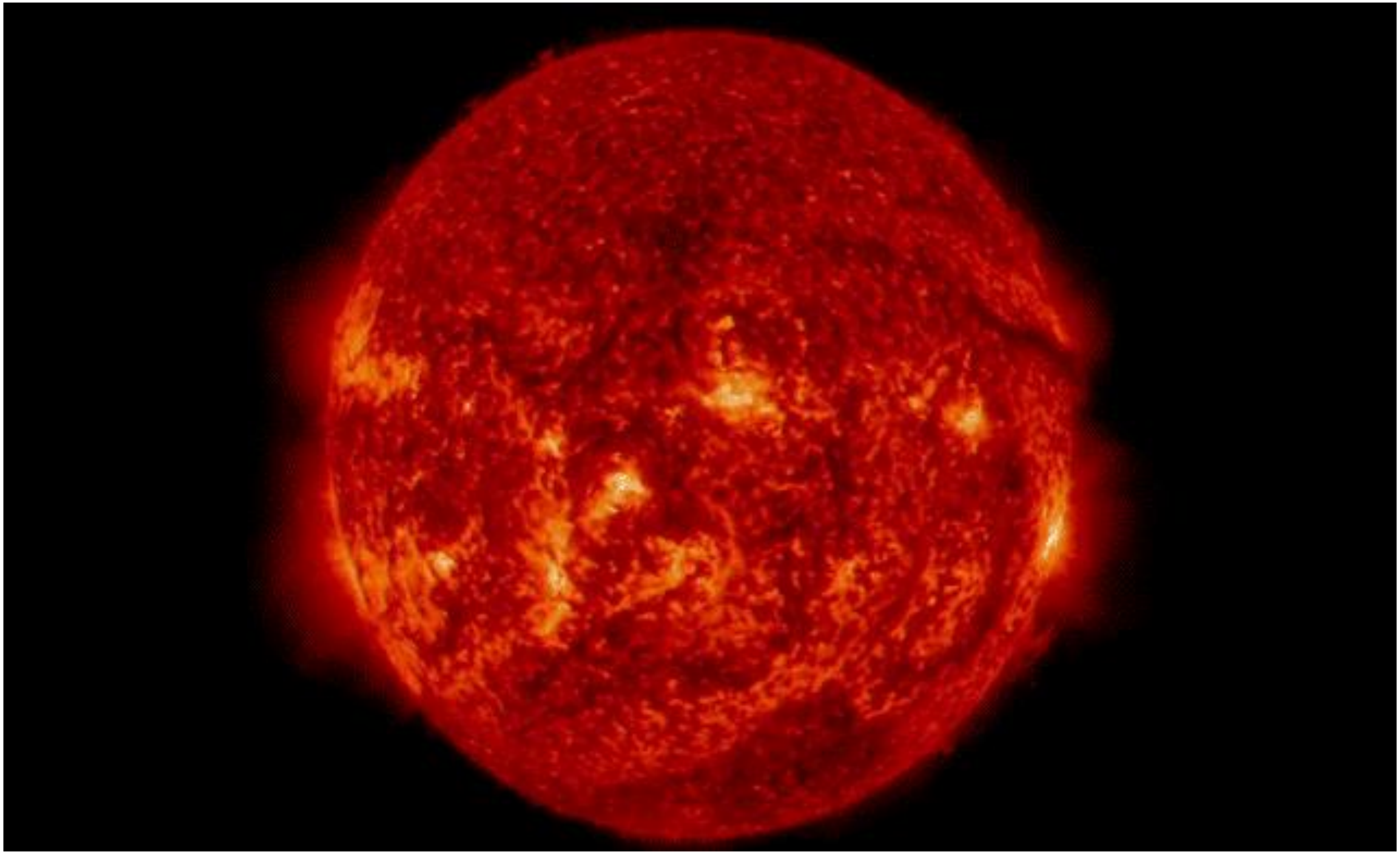

[NASA 2014]

… are the Edge Localized Modes (ELMs) in tokamaks

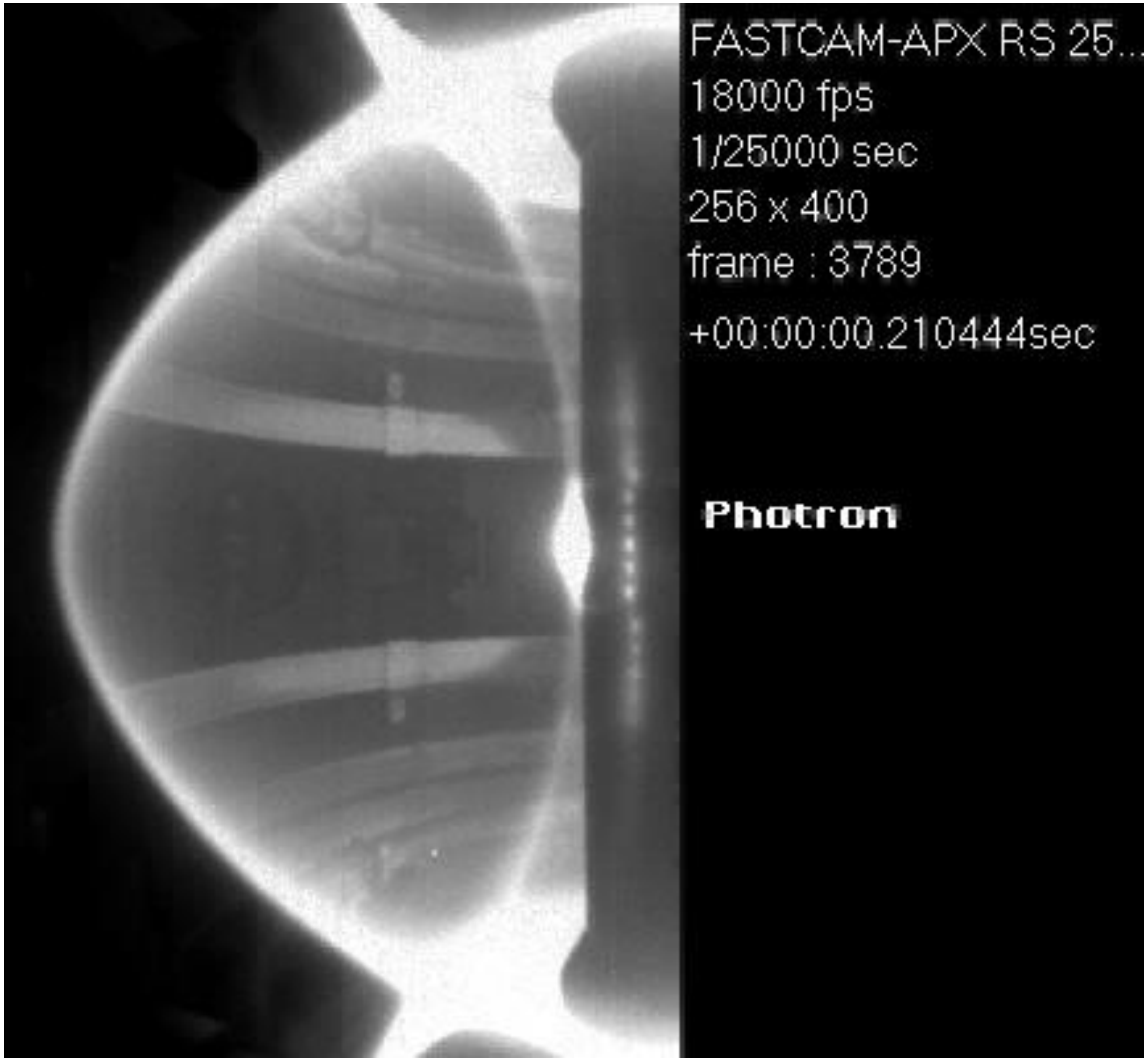

MAST [Kirk, ITPA 2010]

… are the Edge Localized Modes (ELMs) in tokamaks

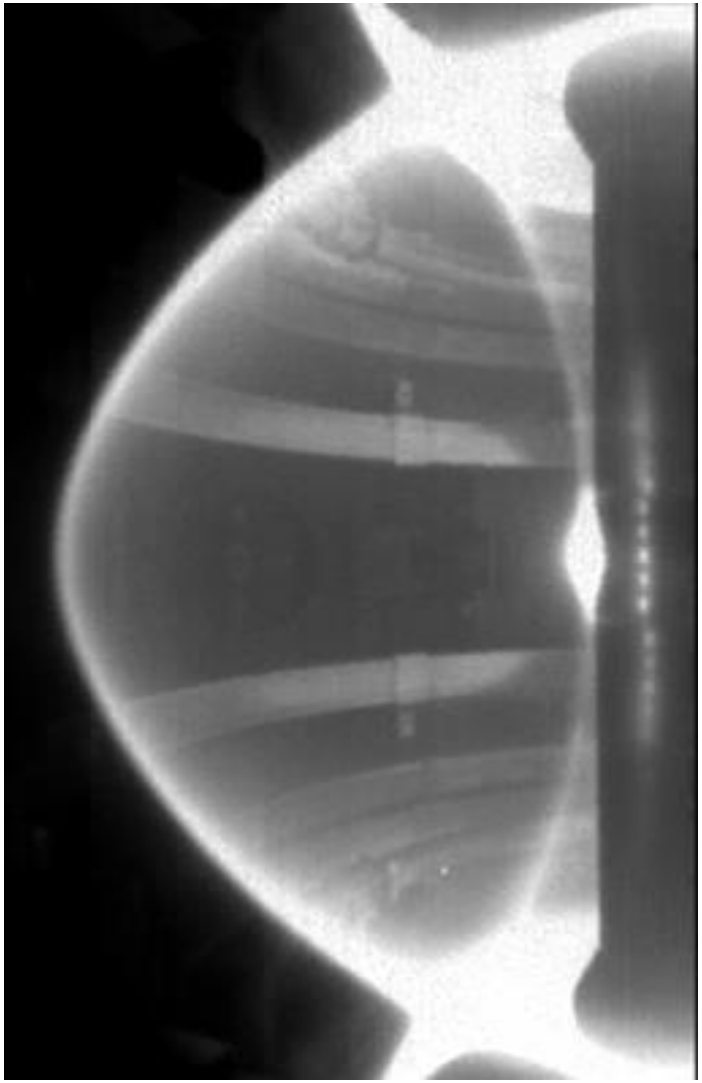

MAST [Kirk, ITPA 2010]

❖ **Type-I ELMs (or giant ELMs):**

- Most harmful ELMs:
  expel 10-15% of the plasma
- Short event ~0.1ms
- Small frequency f_{ELM} ~ 10Hz

… are the Edge Localized Modes (ELMs) in tokamaks

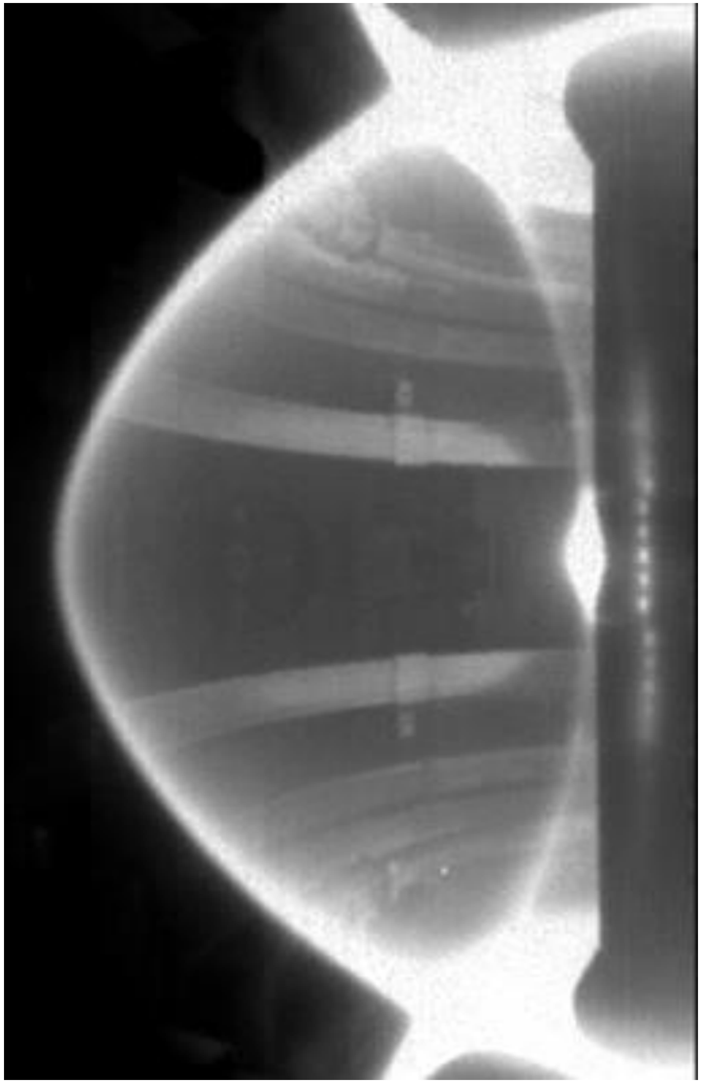

MAST [Kirk, ITPA 2010]

❖ **Type-I ELMs (or giant ELMs):**

- Most harmful ELMs:
  expel 10-15% of the plasma
- Short event ~0.1ms
- Small frequency f_{ELM} ~ 10Hz

❖ **Type-III ELMs:**

- Smaller relaxations:
  expel 1-5% of the plasma
- Larger frequency f_{ELM} ~ 100Hz – 2kHz

In ITER, TYPE-I ELM control will be mandatory

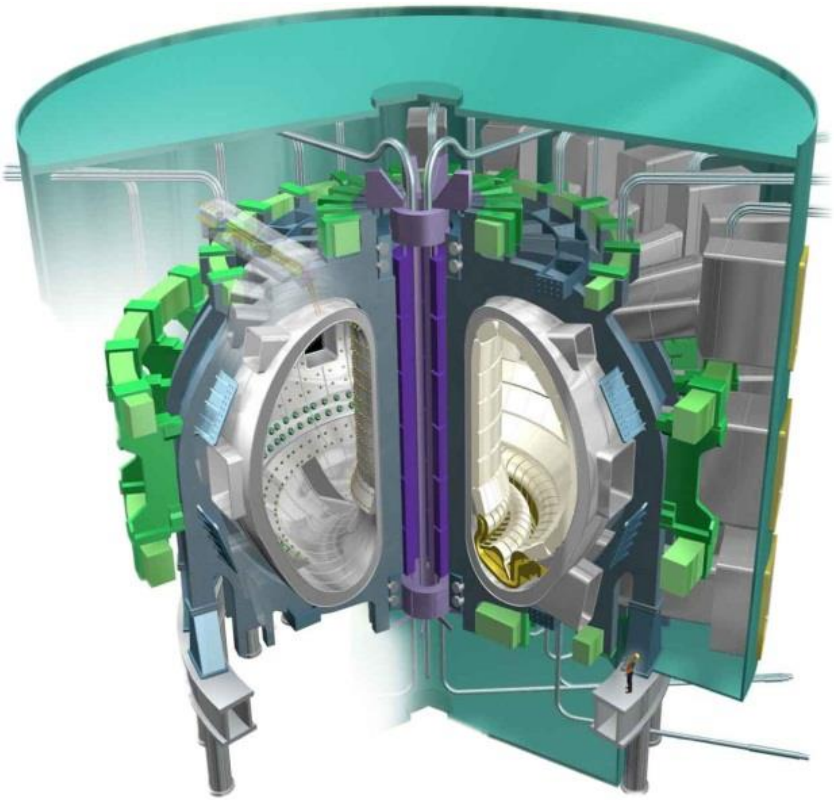

- ITER under construction: demonstrate the feasibility of an **efficient** energy production from fusion reactions
- One of the main concerns: Control of the Edge Localized Modes (ELMs)

In ITER, TYPE-I ELM control will be mandatory

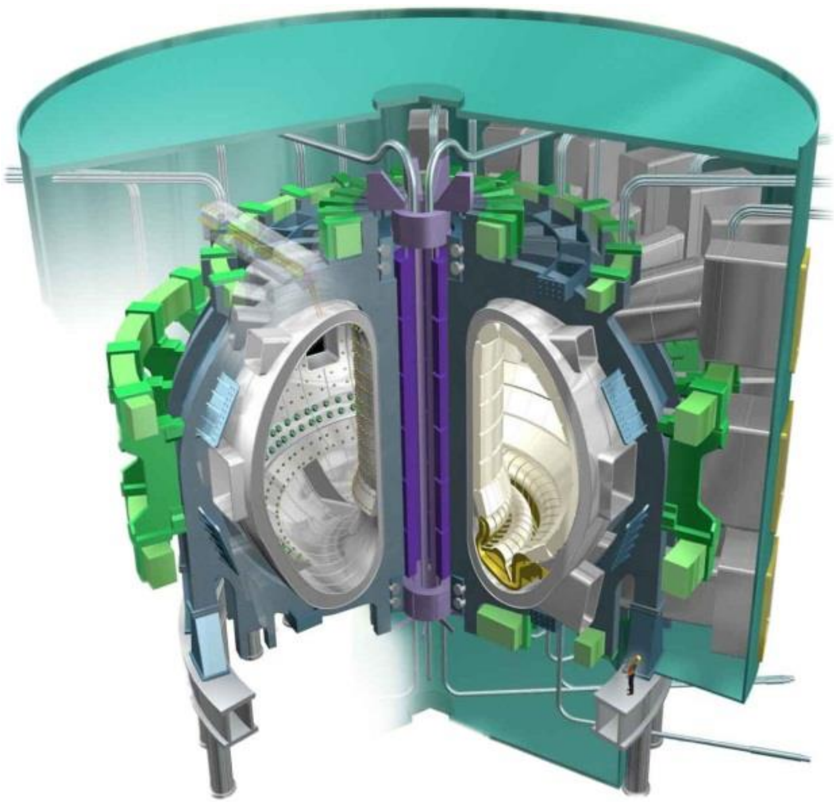

- ITER under construction: demonstrate the feasibility of an **efficient** energy production from fusion reactions
- One of the main concerns: Control of the Edge Localized Modes (ELMs)
- Tungsten sample after ELM–like power load produced by electron gun

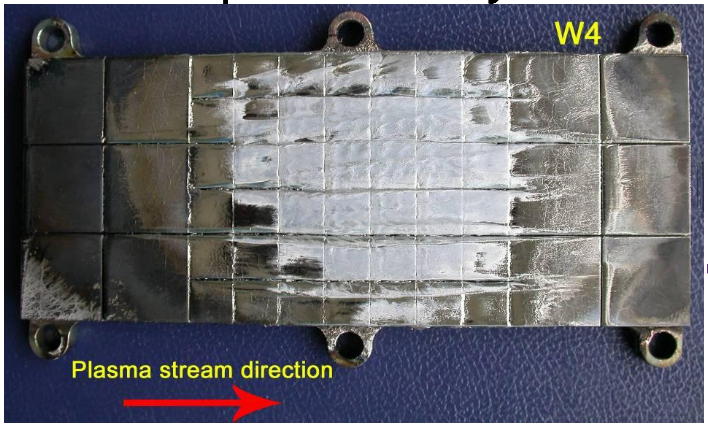

[Linke, Conf on Fusion Materials, Nice, 2007]

ITER → ELM energy~17MJ
→ Acceptable: ~1MJ

→ **ELM control is mandatory**

Theoretical understanding: ELMs = Peeling-Ballooning (MHD) instabilities

❖ Large edge current: → drives peeling/kink modes

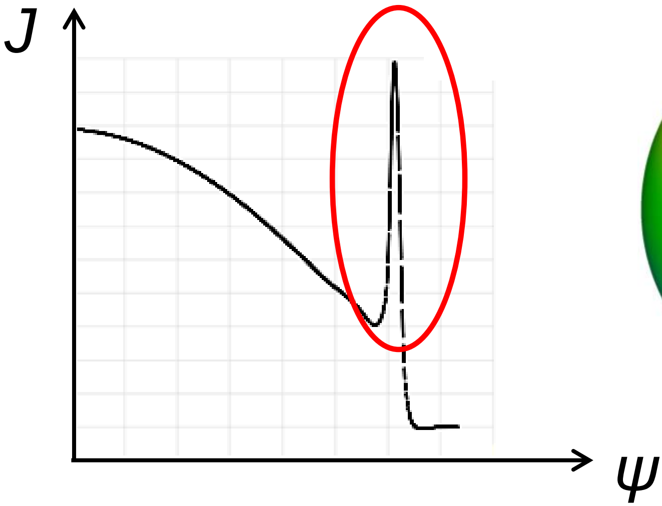

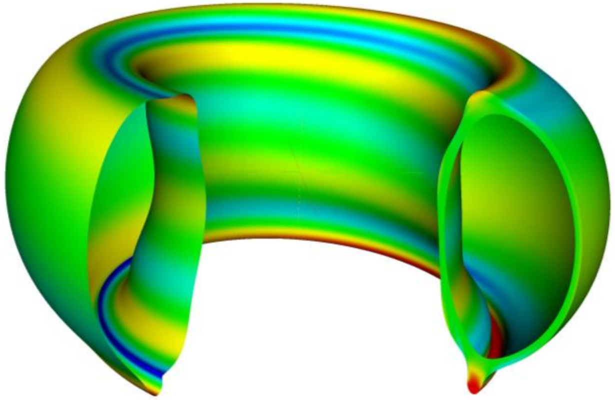

[Huysmans PPCF 2005]

Theoretical understanding:
ELMs = Peeling-Ballooning (MHD) instabilities

❖ Large edge current: → drives peeling/kink modes

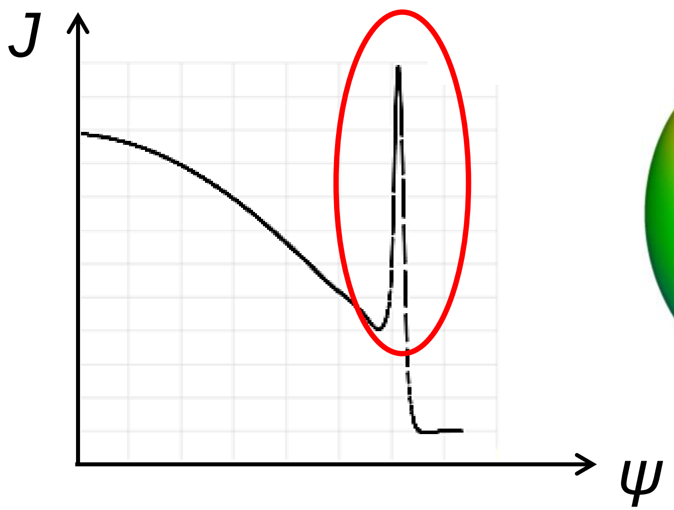

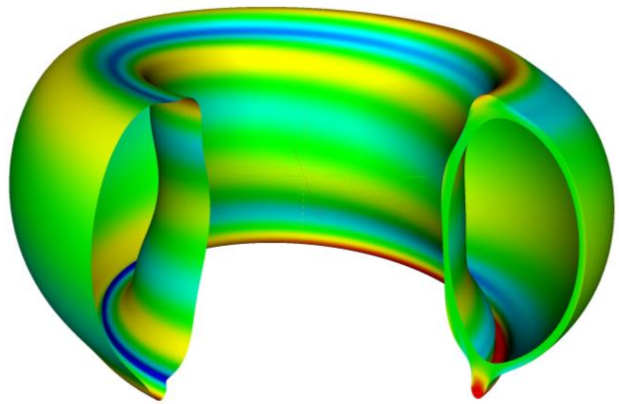

❖Large edge pressure gradient:→drives ballooning modes

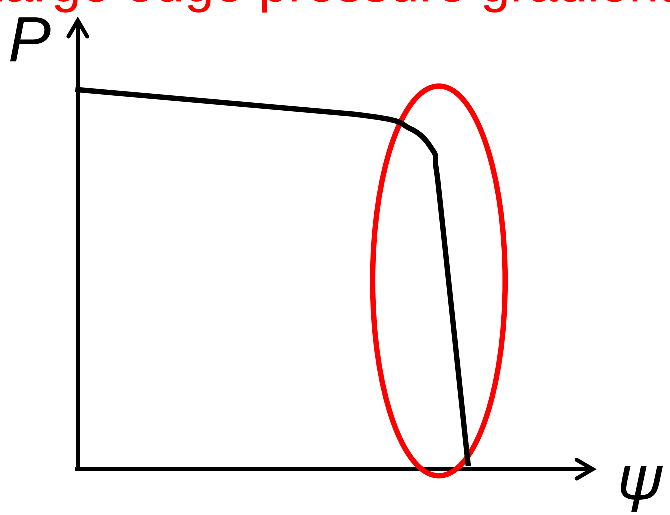

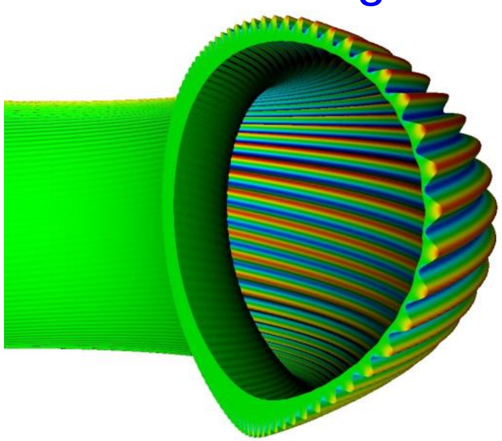

[Huysmans PPCF 2005]

Theoretical understanding: ELMs = Peeling-Ballooning (MHD) instabilities

❖ Large edge current: → drives peeling/kink modes

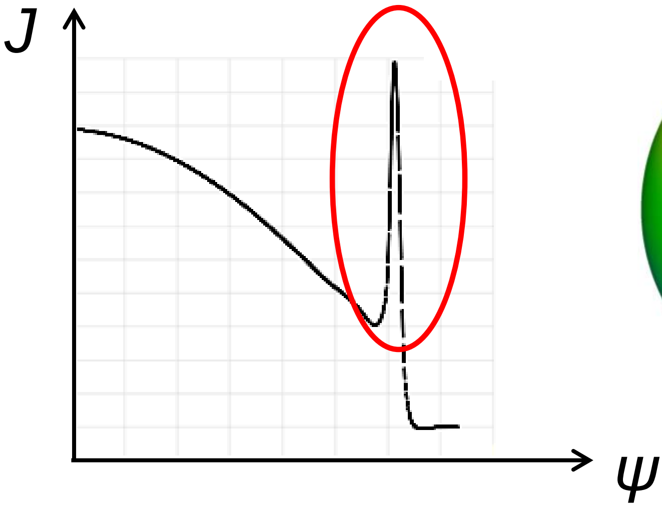

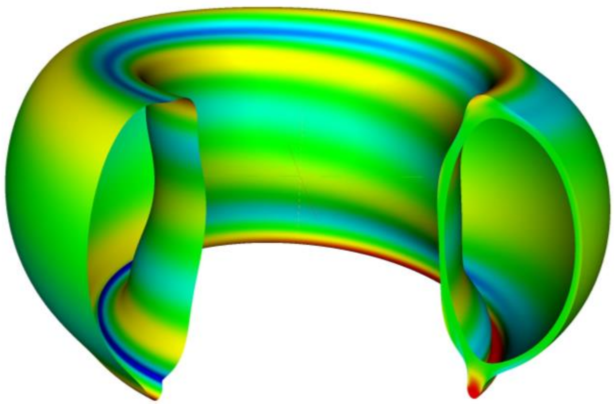

❖Large edge pressure gradient:→drives ballooning modes

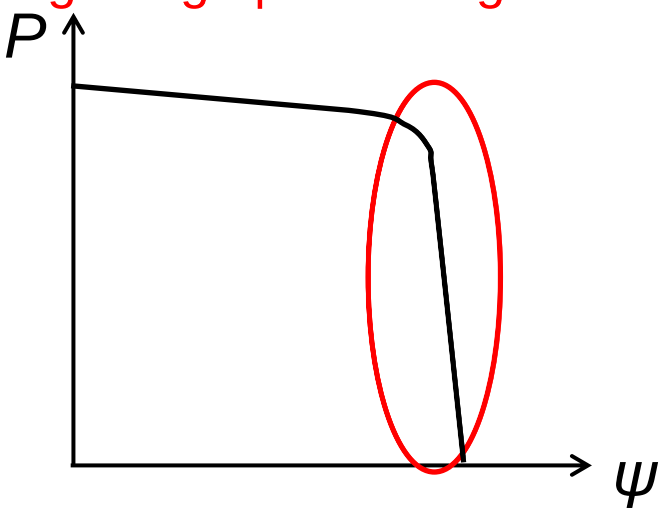

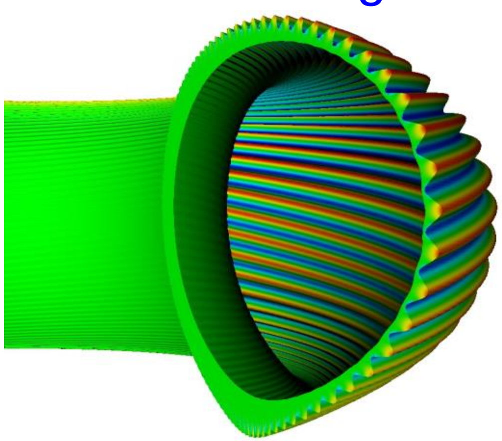

[Huysmans PPCF 2005]

- ELMs= peeling-ballooning modes
- Theoretical description: Magnetohydro-dynamics (MHD)

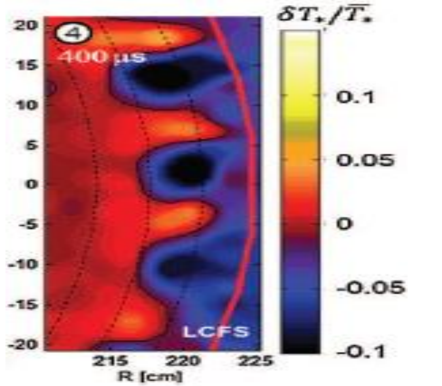

KSTAR [Yun PRL2011]

Stability diagram

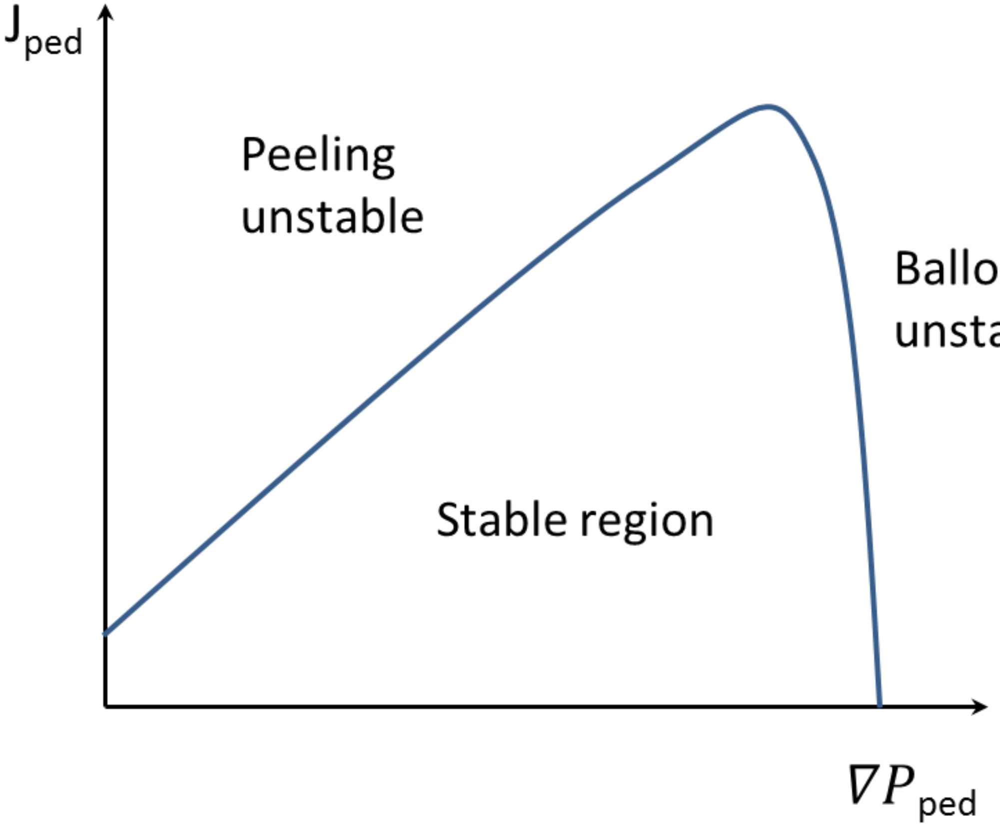

Stability diagram

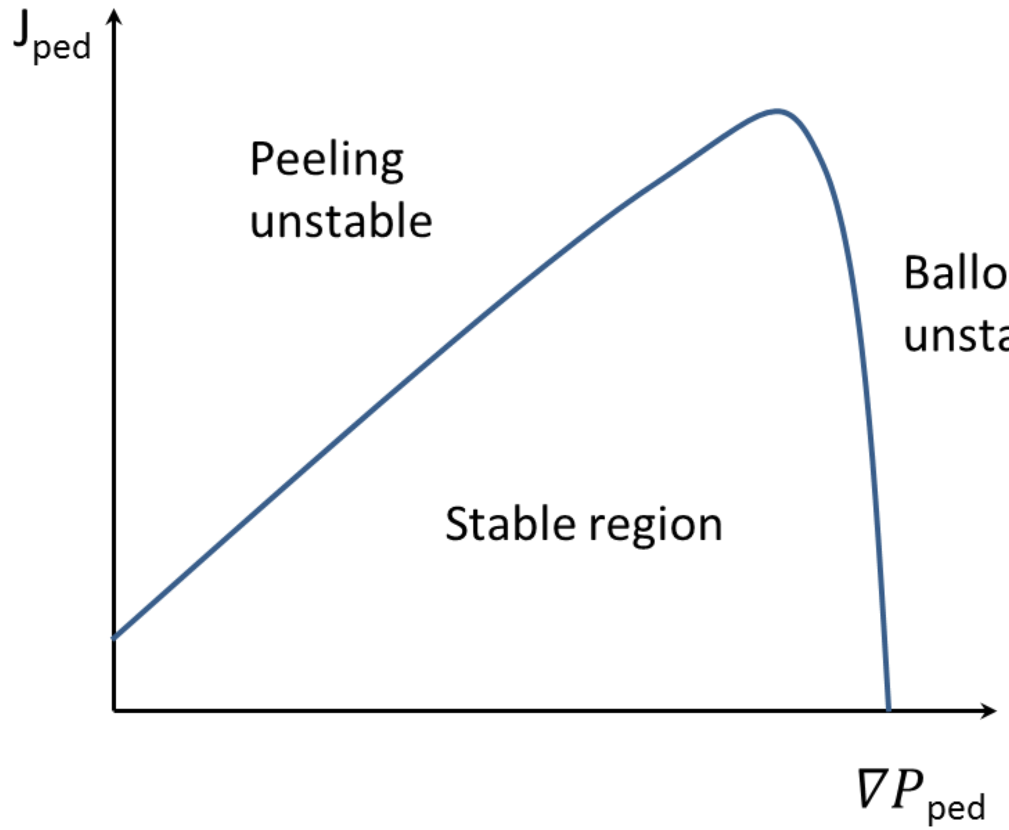

ELM-triggering threshold in ∇P_{ped} and $J_{ped} \propto \nabla P_{ped}$
$\rightarrow$ idea: maintain the plasma under ∇P_{ped} threshold

- **Aims:** ➔ Better understanding of ELM dynamics
  ➔ Accurate reproduction of experimental features
  ➔ Develop ELM control techniques

- Introduction: ELMs and RMPs
  - High-confinement regime and ELMs
  - ELM control by RMPs
- The JOREK code
- ELM dynamics
- ELM control by RMPs
- Conclusion and Outlook

Resonant Magnetic Perturbations = RMPs
RMP coils modify magnetic topology

❖ RMP coils:

Magnetic Perturbation

$\delta B/B \approx 10^{-4}$

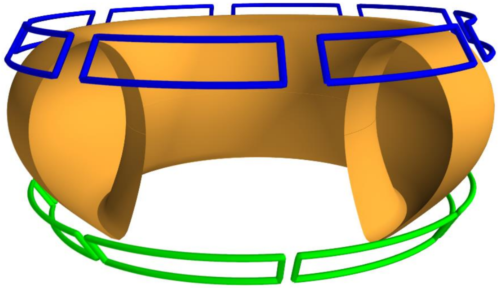

Resonant Magnetic Perturbations = RMPs
RMP coils modify magnetic topology

❖ RMP coils:
Magnetic
Perturbation
$\delta B/B \approx 10^{-4}$

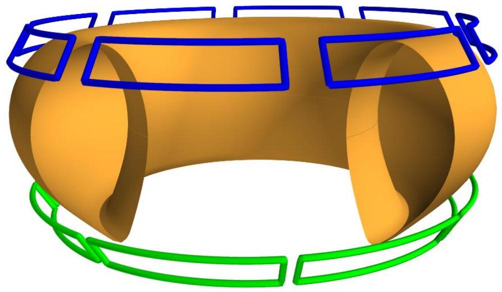

❖ Create magnetic reconnection on resonant surfaces q=m/n

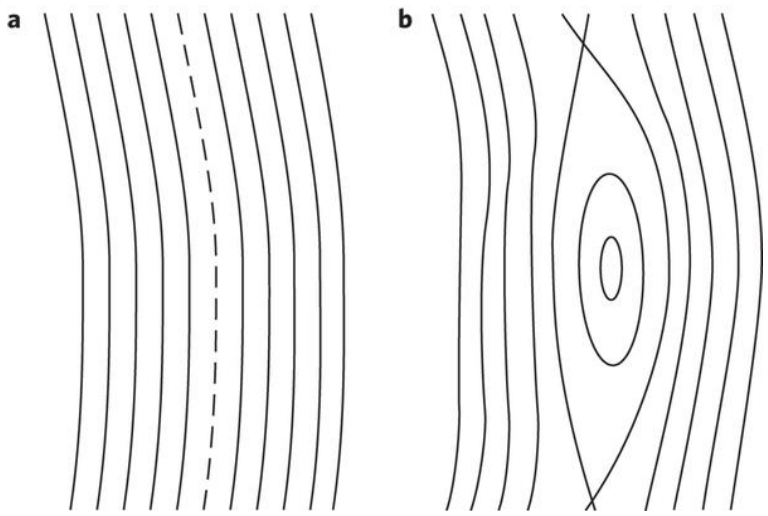

[J.Ongena, Nature16]

q = helicity of field lines
m = poloidal mode number
n = toroidal mode number

Resonant Magnetic Perturbations = RMPs
RMP coils modify magnetic topology

❖ RMP coils:
Magnetic
Perturbation
$\delta B/B \approx 10^{-4}$

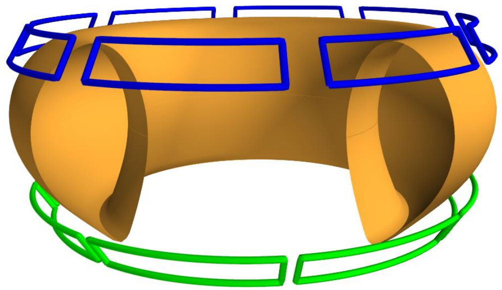

❖ Overlap of magnetic islands:
→ chaotic / ergodic magnetic field

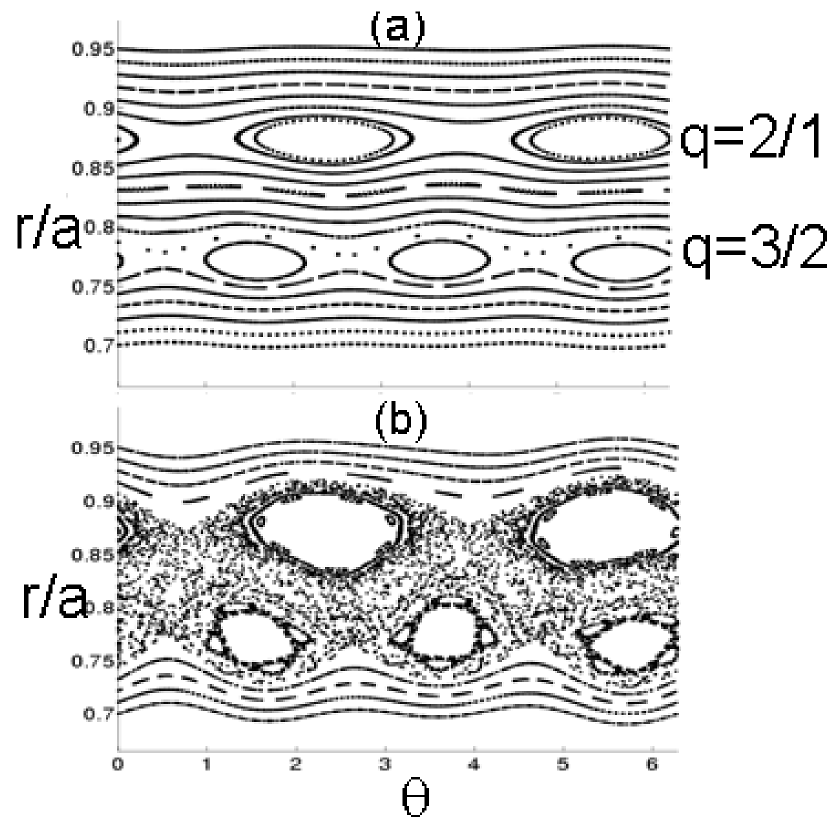

[E. Nardon, PhD thesis 2007]

❖ Create magnetic reconnection
on resonant surfaces q=m/n

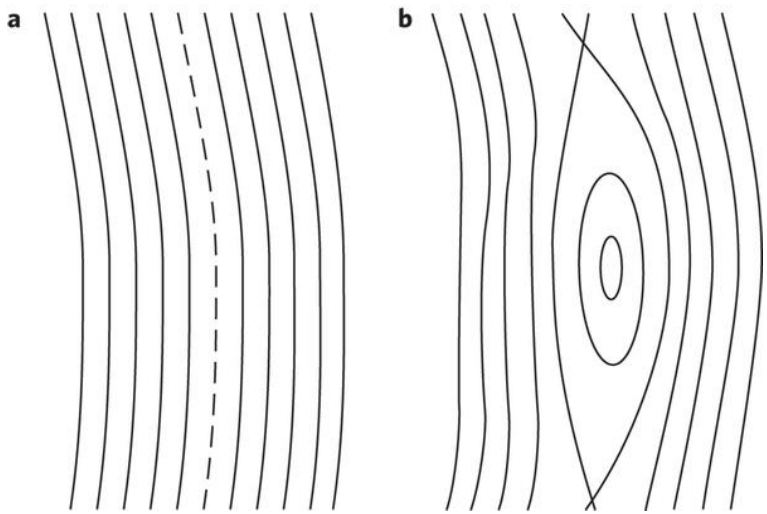

[J.Ongena, Nature16]

Original goal of RMPs:

[Original idea from Tore Supra's ergodic divertor, Ghendrih PPCF96]

Ergodic layer at the edge:

→ transport ++

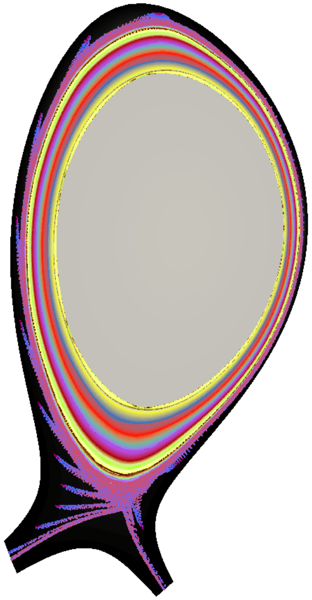

Original goal of RMPs:

[Original idea from Tore Supra's ergodic divertor, Ghendrih PPCF96]

Ergodic layer at the edge:

→ transport ++ → reduced ∇P

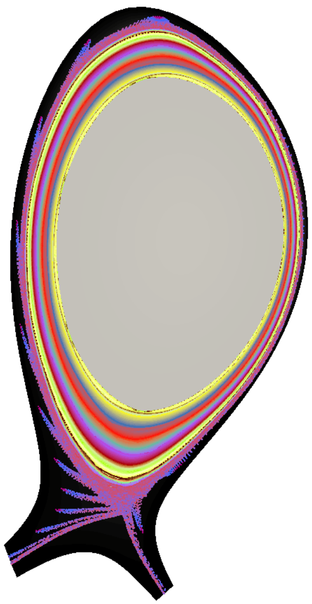

→

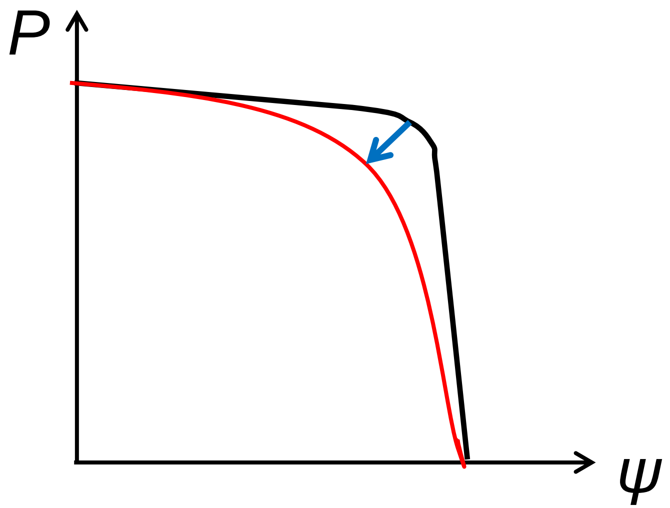

Original goal of RMPs:

[Original idea from Tore Supra's ergodic divertor, Ghendrih PPCF96]

Ergodic layer at the edge:

→ transport ++ → reduced ∇P → no ELM drive

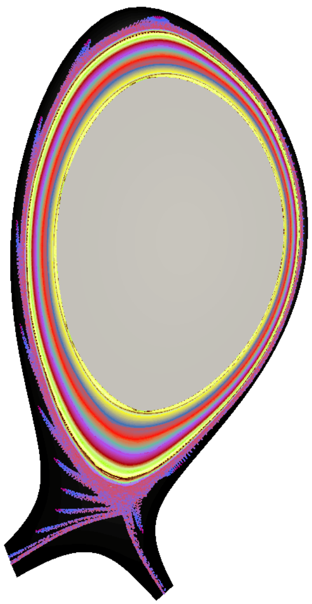

→

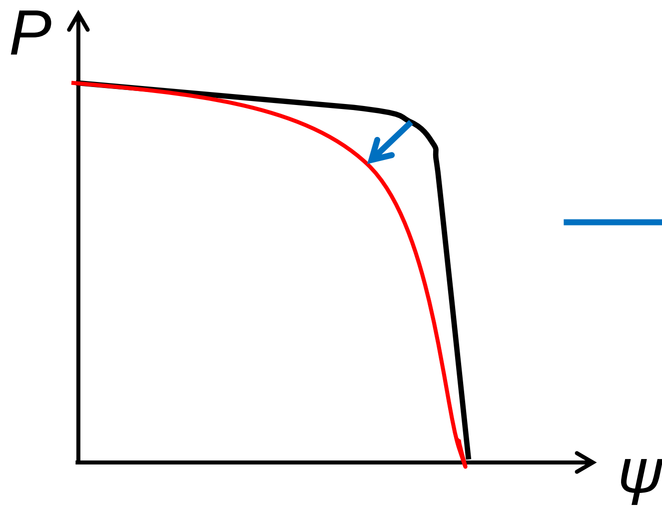

→ stable plasma

❖ For a same level of ergodization calculated in vacuum:

- DIII-D: Suppression
- AUG: Suppression
- JET: Mitigation
- MAST: Triggering

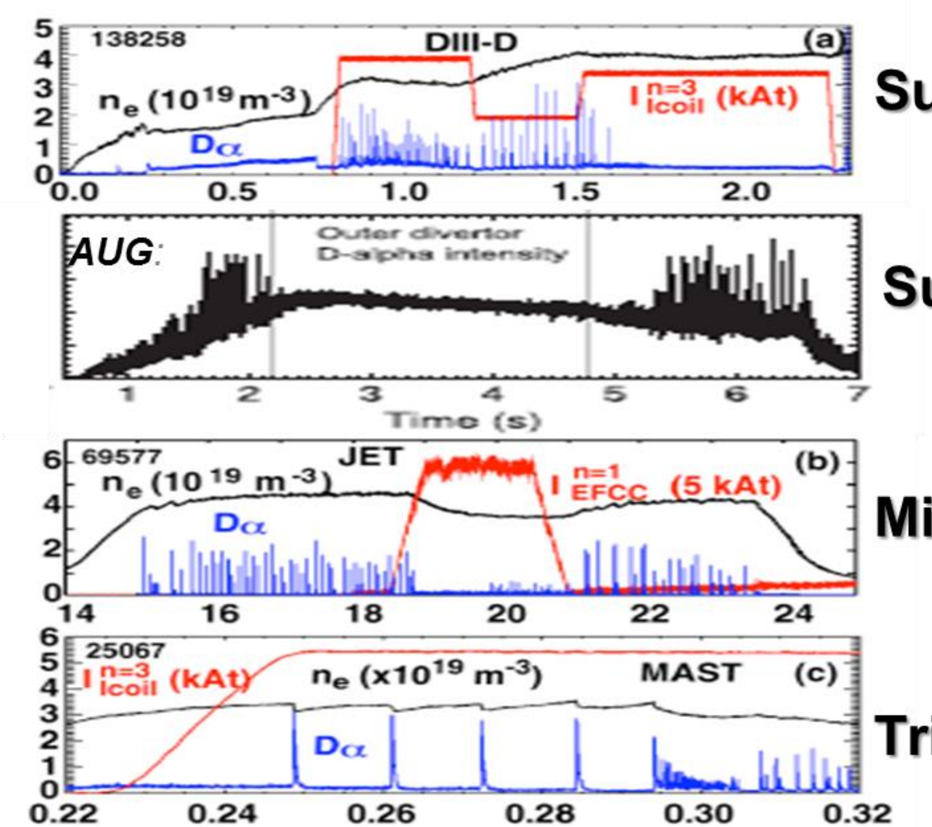

[Fenstermacher IAEA2010, Suttrop PRL 2011]

Unfortunately: more complicated picture

❖ For a same level of ergodization calculated in vacuum:

- DIII-D: **Suppression**
- AUG: **Suppression**
- JET: **Mitigation**
- MAST: **Triggering**

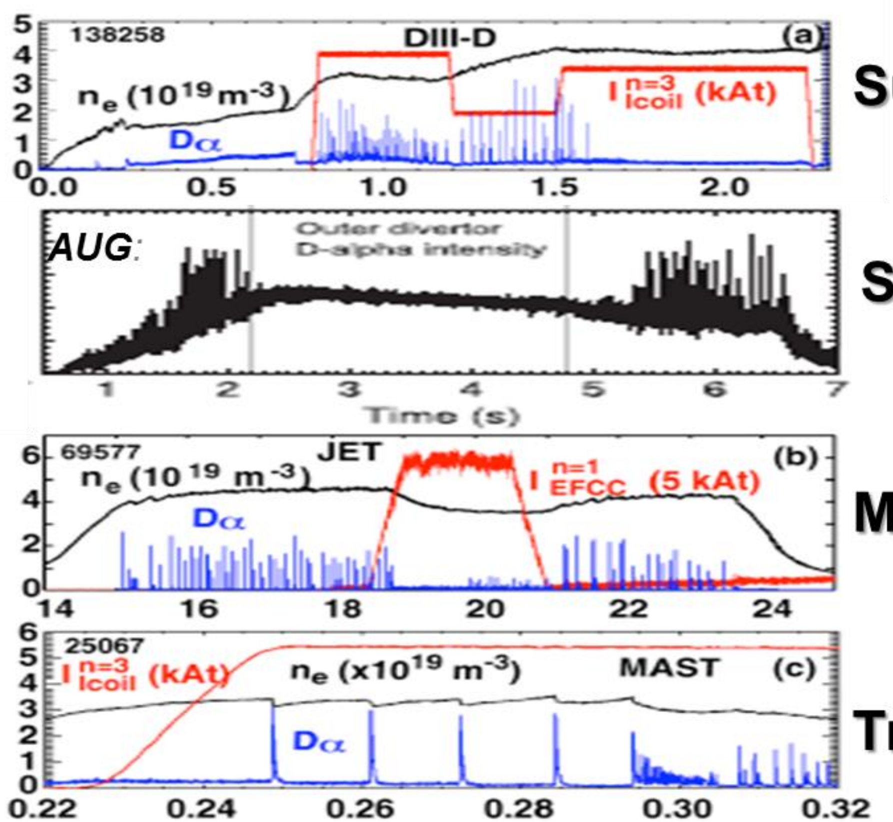

[Fenstermacher IAEA2010, Suttrop PRL 2011]

Different behaviours due to plasma response to RMPs

→ Needs better understanding

❖ **Screening of Resonant perturbation:**

Plasma (electron) rotation $\rightarrow$ induce currents in response to RMPs
$\rightarrow$ induce B field opposite to B perturbation
$\rightarrow$ screening of RMPs

Plasma response to RMPs

❖ Screening of Resonant perturbation:

Plasma (electron) rotation → induce currents in response to RMPs
→ induce B field opposite to B perturbation
→ screening of RMPs

RMPs in vacuum

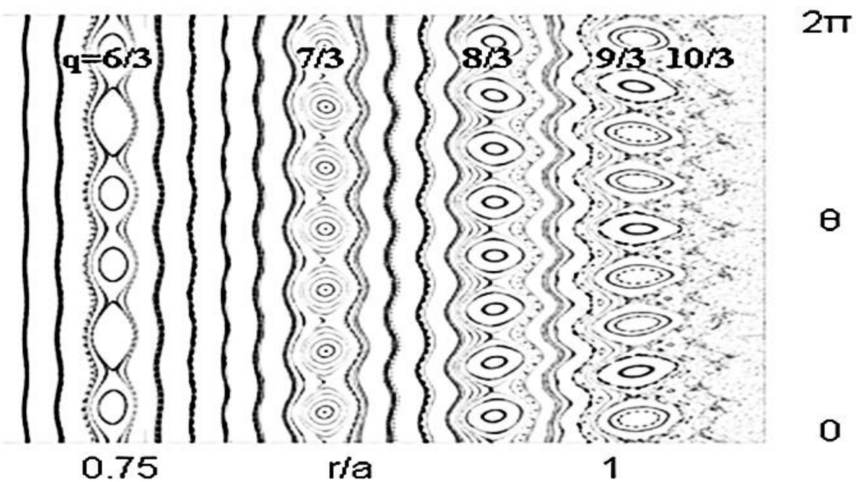

RMPs with plasma response

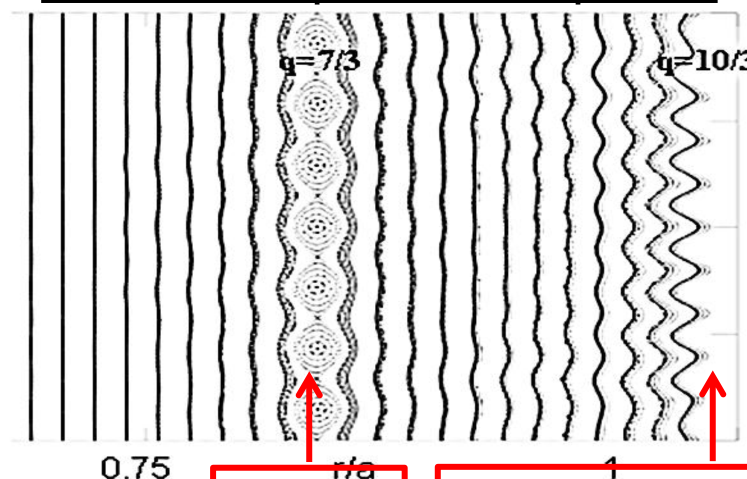

$V_{\perp e}=0$

High resistivity η

❖ **Screening of Resonant perturbation:**

Plasma (electron) rotation → induce currents in response to RMPs
→ induce B field opposite to B perturbation
→ screening of RMPs

RMPs in vacuum

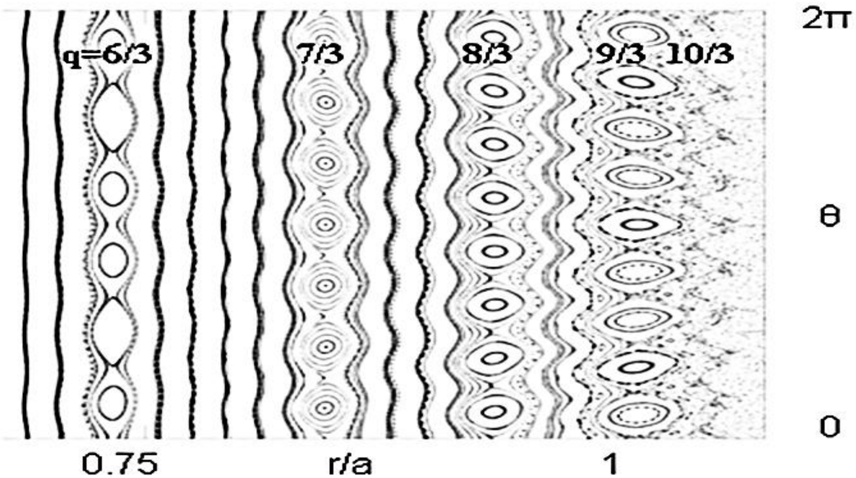

RMPs with plasma response

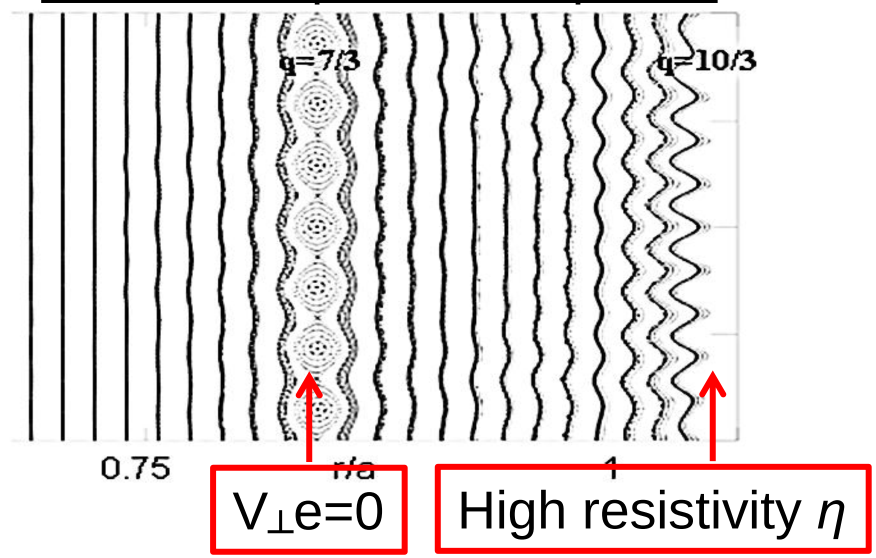

❖ **Other effect: Kink response:**

Amplification of stable peeling-kink modes by RMP

❖ Screening of Resonant perturbation:

Plasma (electron) rotation → induce currents in response to RMPs
→ induce B field opposite to B perturbation
→ screening of RMPs

RMPs in vacuum

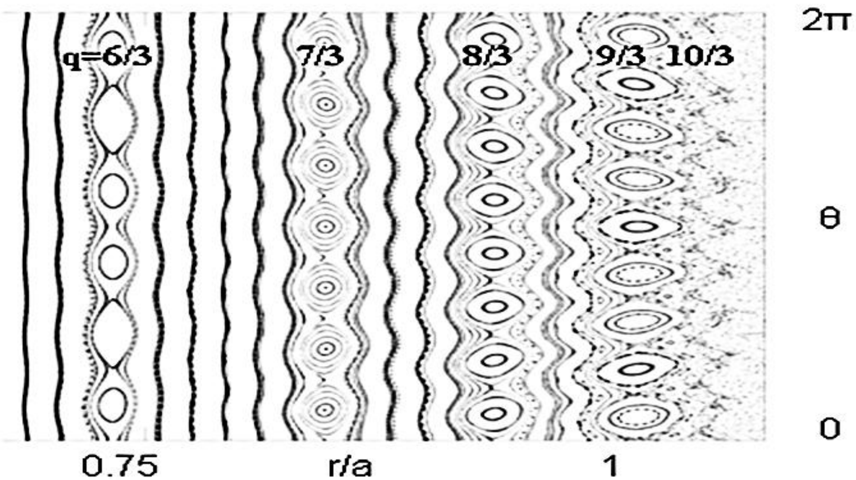

RMPs with plasma response

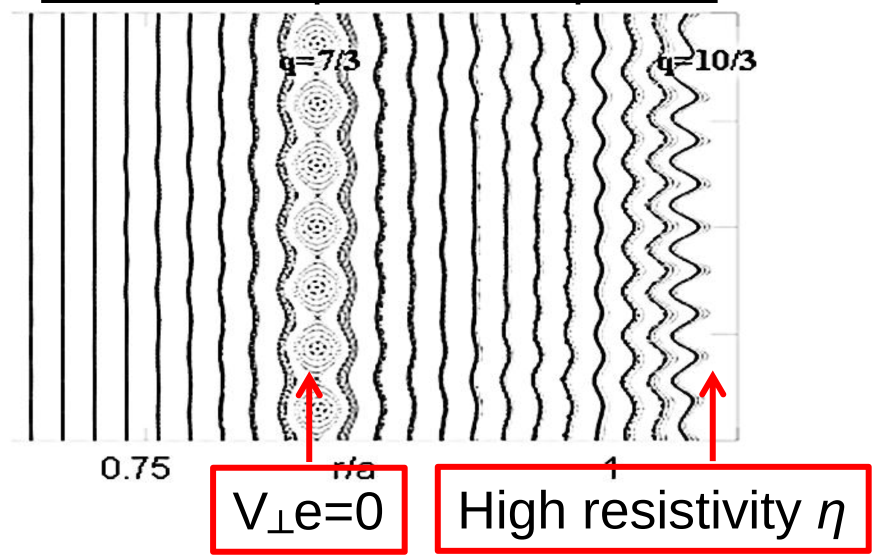

❖ Other effect: Kink response:

Amplification of stable peeling-kink modes by RMP.

❖ **Aims:** ➔ Better understanding of resonant and kink responses.
➔ Depending on plasma response, RMP effect on ELMs?

Additional effect: increased transport of density= “pumpout”

AUG#31128: best ELM mitigation obtained with n=2 RMPs, $\Delta\Phi_{coils}$= +90° :

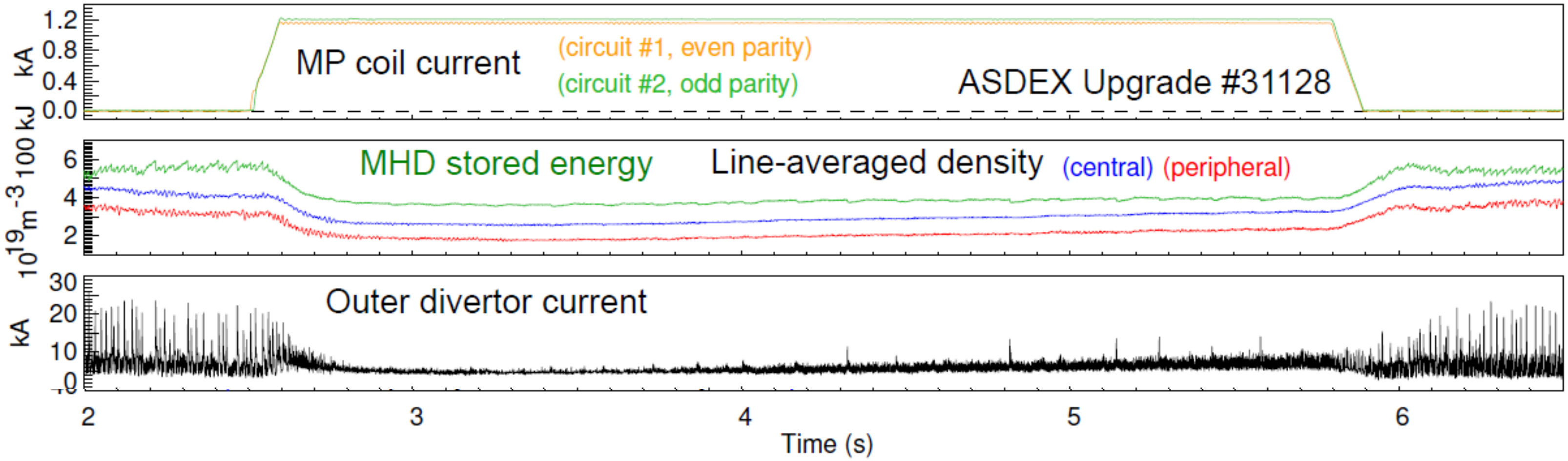

[Suttrop et al, PPCF 16]

Additional effect: increased transport of density= “pumpout”

AUG#31128: best ELM mitigation obtained with n=2 RMPs, $\Delta\Phi_{coils}$= +90° :

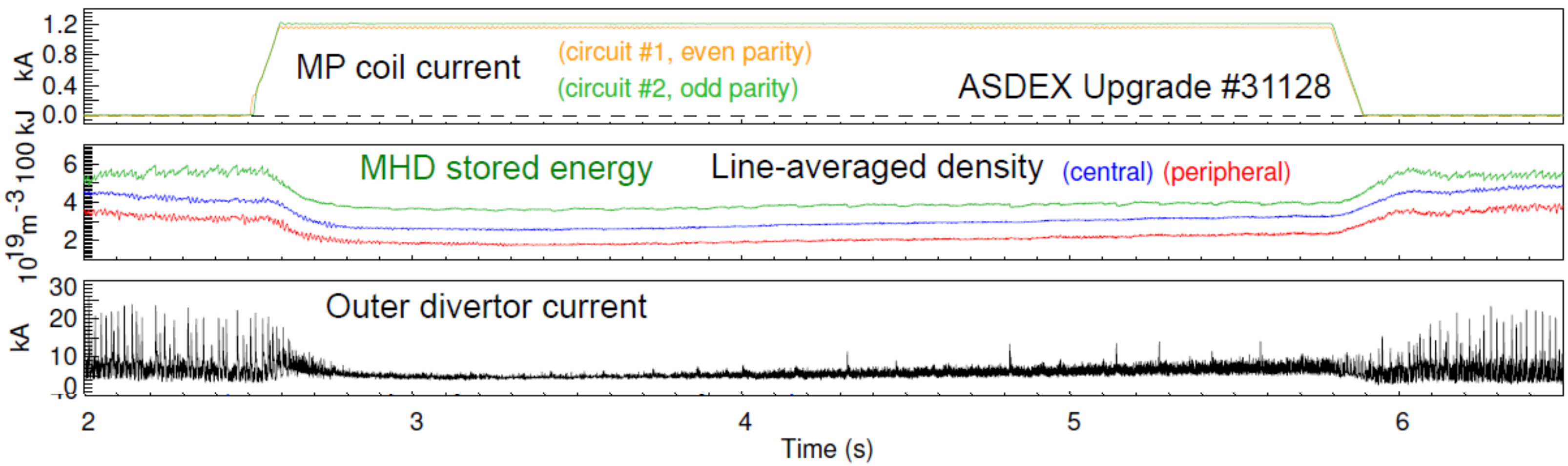

[Suttrop et al, PPCF 16]

❖ **<u>One more aim:</u>** ➔ understanding of mechanism of density pumpout

- Introduction: ELMs and RMPs
- **The JOREK code**
- ELM dynamics
- ELM control by RMPs
- Conclusion and Outlook

❖ International context:

- Developed by G. Huysmans at CEA *[G. Huysmans and O. Czarny, NF 2007]*
- World leading non-linear MHD code with BOUT++, M3D, NIMROD
- European collaboration (ITER, France, Germany, UK, Netherlands, Czech Rep.)

❖ Structure:

[O. Czarny, JCP 2008]

- Finite elements in poloidal plane → 2D cubic Bezier elements
- Toroidal direction: Fourier decomposition:
  e.g. temperature $T = \sum T_n \exp(i\, n\, \varphi)$

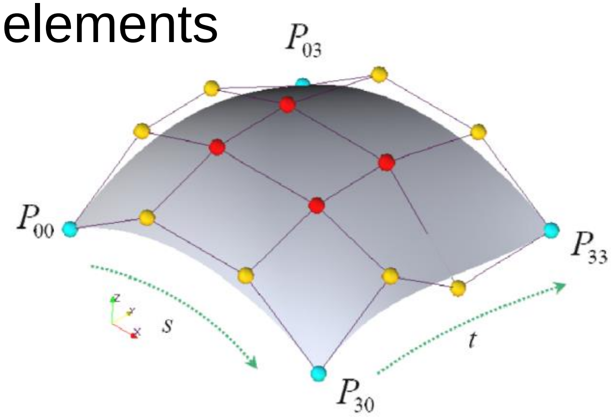

❖ Computations:

- Fully implicit time stepping
- Large sparse matrices (PastiX, *[INRIA Team Bacchus, Hénon Parall. Comp 2002]*)
- Massively parallelized (MPI / OpenMP) → 256 – 1500 processors
- **Typical run: 10.000-200.000 cpuh**

JOREK challenges

❖ Main physics applications:

- **ELMs** and control by RMPs, pellets, kicks, ELM-free regimes
- **Disruptions**: mitigation by massive gas injection, runaway electrons

❖ Challenges in physical description:

- Realistic geometry (X-point, SOL…)
- Non-linear MHD over long time scales ($\mu s \rightarrow s$)
- Realistic plasma parameters (resistivity)
- Large number of toroidal harmonics

❖ Computing issues:

- Need refined mesh with large number of harmonics:

→ resolution depends on linear solver performance (PASTIX)

→ parallelization / memory consumption

Reduced MHD model implemented in JOREK:

Ohm's law:

$$\frac{1}{R^2}\frac{\partial \psi}{\partial t} = \eta \frac{J}{R^2} - \vec{B}\cdot(\nabla_{\parallel} u + \frac{\tau_{IC}}{\rho}\nabla_{\parallel} p)$$

Mass density:

$$\frac{\partial \rho}{\partial t} = -\nabla\cdot\left(\rho\vec{V}\right) + \nabla\cdot\left(D_{\perp}\nabla_{\perp}\rho\right) + S_{\rho}$$

Parallel momentum:

$$\vec{B}\left\{\begin{array}{l}\left[\rho(\frac{\partial}{\partial t}+\vec{V}\cdot\nabla)\vec{V}_E + (\frac{\partial}{\partial t}+\vec{V}\cdot\nabla)\vec{V}_{\parallel,i})\right] + \\ +\nabla(\rho T) + \nabla\cdot\Pi_i^{neo} - \vec{J}\times\vec{B} + \vec{S}_V - \vec{V}S_{\rho} - \nu_{\parallel}\Delta\vec{V}\end{array}\right\} = 0$$

Poloidal momentum (vorticity):

$$\nabla\varphi\cdot\nabla\times\left\{\begin{array}{l}\left[\rho(\frac{\partial}{\partial t}+\vec{V}\cdot\nabla)\vec{V}_E + (\frac{\partial}{\partial t}+\vec{V}\cdot\nabla)\vec{V}_{\parallel,i})\right] + \\ +\nabla(\rho T) + \nabla\cdot\Pi_i^{neo} - \vec{J}\times\vec{B} + \vec{S}_V - \vec{V}S_{\rho} - \nu_{\parallel}\Delta\vec{V}\end{array}\right\} = 0$$

Tempe-rature:

$$\frac{\partial(\rho T)}{\partial t} = -(\vec{V}_E + \vec{V}_{\parallel,i})\cdot\nabla(\rho T) - \gamma\rho T\nabla\cdot(\vec{V}_E + \vec{V}_{\parallel,i}) + \nabla\cdot\left(K_{\perp}\nabla_{\perp}T + K_{\parallel}\nabla_{\parallel}T\right) + (1-\gamma)S_T + 0.5V^2 S_{\rho}$$

[Huysmans PPCF 2009, Orain PoP 2013]

Reduced MHD model implemented in JOREK:

Ohm's law: $$\frac{1}{R^2}\frac{\partial \psi}{\partial t} = \eta \frac{J}{R^2} - \vec{B}\cdot(\nabla_{\parallel} u + \frac{\tau_{IC}}{\rho}\nabla_{\parallel} p)$$

Mass density: $$\frac{\partial \rho}{\partial t} = -\nabla\cdot\left(\rho\vec{V}\right) + \nabla\cdot\left(D_{\perp}\nabla_{\perp}\rho\right) + S_{\rho}$$

Parallel momentum: $$\vec{B}\left\{\begin{array}{l}\left[\rho(\frac{\partial}{\partial t}+\vec{V}\cdot\nabla)\vec{V}_E + (\frac{\partial}{\partial t}+\vec{V}\cdot\nabla)\vec{V}_{\parallel,i})\right] + \\ +\nabla(\rho T) + \nabla\cdot\Pi_i^{neo} - \vec{J}\times\vec{B} + \vec{S}_V - \vec{V}S_{\rho} - \nu_{\parallel}\Delta\vec{V}\end{array}\right\} = 0$$

Poloidal momentum (vorticity): $$\nabla\varphi\cdot\nabla\times\left\{\begin{array}{l}\left[\rho(\frac{\partial}{\partial t}+\vec{V}\cdot\nabla)\vec{V}_E + (\frac{\partial}{\partial t}+\vec{V}\cdot\nabla)\vec{V}_{\parallel,i})\right] + \\ +\nabla(\rho T) + \nabla\cdot\Pi_i^{neo} - \vec{J}\times\vec{B} + \vec{S}_V - \vec{V}S_{\rho} - \nu_{\parallel}\Delta\vec{V}\end{array}\right\} = 0$$

Tempe-rature: $$\frac{\partial(\rho T)}{\partial t} = -(\vec{V}_E + \vec{V}_{\parallel,i})\cdot\nabla(\rho T) - \gamma\rho T\nabla\cdot(\vec{V}_E + \vec{V}_{\parallel,i}) + \nabla\cdot\left(K_{\perp}\nabla_{\perp}T + K_{\parallel}\nabla_{\parallel}T\right) + (1-\gamma)S_T + 0.5V^2 S_{\rho}$$

Flows included in the model:

- ExB and diamagnetic drifts:

$$\vec{V}_s = V_{\parallel,s}\vec{B} \underbrace{- R^2\nabla u\times\nabla\varphi}_{\vec{V}_{E\times B}} \underbrace{- Z_s\tau_{IC}\frac{R^2}{\rho}\nabla p\times\nabla\varphi}_{\vec{V}_s^* = diamagnetic}$$

[Huysmans PPCF 2009, Orain PoP 2013]

Reduced MHD model implemented in JOREK:

Ohm's law:

$$\frac{1}{R^2}\frac{\partial \psi}{\partial t} = \eta \frac{J}{R^2} - \vec{B}\cdot(\nabla_{\parallel} u + \frac{\tau_{IC}}{\rho}\nabla_{\parallel} p)$$

Mass density:

$$\frac{\partial \rho}{\partial t} = -\nabla\cdot\left(\rho\vec{V}\right) + \nabla\cdot\left(D_{\perp}\nabla_{\perp}\rho\right) + S_{\rho}$$

Parallel momentum:

$$\vec{B}\left\{\left[\rho(\frac{\partial}{\partial t} + \vec{V}\cdot\nabla)\vec{V}_E + (\frac{\partial}{\partial t} + \vec{V}\cdot\nabla)\vec{V}_{\parallel,i})\right] + \nabla(\rho T) + \nabla\cdot\Pi_i^{neo} - \vec{J}\times\vec{B} + \vec{S}_V - \vec{V}S_{\rho} - \nu_{\parallel}\Delta\vec{V}\right\} = 0$$

Poloidal momentum (vorticity):

$$\nabla\varphi\cdot\nabla\times\left\{\left[\rho(\frac{\partial}{\partial t} + \vec{V}\cdot\nabla)\vec{V}_E + (\frac{\partial}{\partial t} + \vec{V}\cdot\nabla)\vec{V}_{\parallel,i})\right] + \nabla(\rho T) + \nabla\cdot\Pi_i^{neo} - \vec{J}\times\vec{B} + \vec{S}_V - \vec{V}S_{\rho} - \nu_{\parallel}\Delta\vec{V}\right\} = 0$$

Temperature:

$$\frac{\partial(\rho T)}{\partial t} = -(\vec{V}_E + \vec{V}_{\parallel,i})\cdot\nabla(\rho T) - \gamma\rho T\nabla\cdot(\vec{V}_E + \vec{V}_{\parallel,i}) + \nabla\cdot\left(K_{\perp}\nabla_{\perp}T + K_{\parallel}\nabla_{\parallel}T\right) + (1-\gamma)S_T + 0.5V^2 S_{\rho}$$

Flows included in the model:

- ExB and diamagnetic drifts:

$$\vec{V}_s = V_{\parallel,s}\vec{B} \underbrace{- R^2\nabla u\times\nabla\varphi}_{\vec{V}_{E\times B}} \underbrace{- Z_s\tau_{IC}\frac{R^2}{\rho}\nabla p\times\nabla\varphi}_{\vec{V}_s^* = diamagnetic}$$

- A source of toroidal rotation S_V

[Huysmans PPCF 2009, Orain PoP 2013]

Reduced MHD model implemented in JOREK:

Ohm's law: $$\frac{1}{R^2}\frac{\partial \psi}{\partial t} = \eta \frac{J}{R^2} - \vec{B}\cdot\left(\nabla_{\|} u + \frac{\tau_{IC}}{\rho}\nabla_{\|} p\right)$$

Mass density: $$\frac{\partial \rho}{\partial t} = -\nabla\cdot\left(\rho\vec{V}\right) + \nabla\cdot\left(D_{\perp}\nabla_{\perp}\rho\right) + S_{\rho}$$

Parallel momentum: $$\vec{B}\left\{\begin{array}{l}\left[\rho\left(\frac{\partial}{\partial t}+\vec{V}\cdot\nabla\right)\vec{V}_E + \left(\frac{\partial}{\partial t}+\vec{V}\cdot\nabla\right)\vec{V}_{\|,i}\right) \Big] + \\ +\nabla(\rho T) + \nabla\cdot\Pi_i^{neo} - \vec{J}\times\vec{B} + \vec{S}_V - \vec{V}S_{\rho} - \nu_{\|}\Delta\vec{V}\end{array}\right\} = 0$$

Poloidal momentum (vorticity): $$\nabla\varphi\cdot\nabla\times\left\{\begin{array}{l}\left[\rho\left(\frac{\partial}{\partial t}+\vec{V}\cdot\nabla\right)\vec{V}_E + \left(\frac{\partial}{\partial t}+\vec{V}\cdot\nabla\right)\vec{V}_{\|,i}\right) \Big] + \\ +\nabla(\rho T) + \nabla\cdot\Pi_i^{neo} - \vec{J}\times\vec{B} + \vec{S}_V - \vec{V}S_{\rho} - \nu_{\|}\Delta\vec{V}\end{array}\right\} = 0$$

Tempe-rature: $$\frac{\partial(\rho T)}{\partial t} = -(\vec{V}_E + \vec{V}_{\|,i})\cdot\nabla(\rho T) - \gamma\rho T\nabla\cdot(\vec{V}_E + \vec{V}_{\|,i}) + \nabla\cdot\left(K_{\perp}\nabla_{\perp}T + K_{\|}\nabla_{\|}T\right) + (1-\gamma)S_T + 0.5V^2 S_{\rho}$$

Flows included in the model:

- ExB and diamagnetic drifts:

$$\vec{V}_s = V_{\|,s}\vec{B} \underbrace{- R^2\nabla u\times\nabla\varphi}_{\vec{V}_{E\times B}} \underbrace{- Z_s\tau_{IC}\frac{R^2}{\rho}\nabla p\times\nabla\varphi}_{\vec{V}_s^* = diamagnetic}$$

- A source of toroidal rotation S_V

[Huysmans PPCF 2009, Orain PoP 2013]

- Neoclassical tensor: *[Gianakon PoP2002]*

$$\nabla\cdot\Pi_i^{neo} \approx \mu_{i,neo}\rho(B^2/B_\theta^2)(V_{\theta,i} - V_{\theta,neo})\vec{e}_\theta$$

$$V_{\theta,i} \rightarrow V_{\theta,neo} = -k_{i,neo}\tau_{IC}(\nabla_\perp\psi\cdot\nabla_\perp T)/B_\theta$$

Equilibrium flows affect ELM dynamics & RMP penetration: Source of toroidal rotation, sheath conditions, neoclassical effects and diamagnetic rotation

❖ **Parallel flow:**

❑ **Central plasma**: source of toroidal rotation keeps initial experimental profile

❑ **SOL**: sheath conditions on targets: $V_{||, div} = \pm C_s$

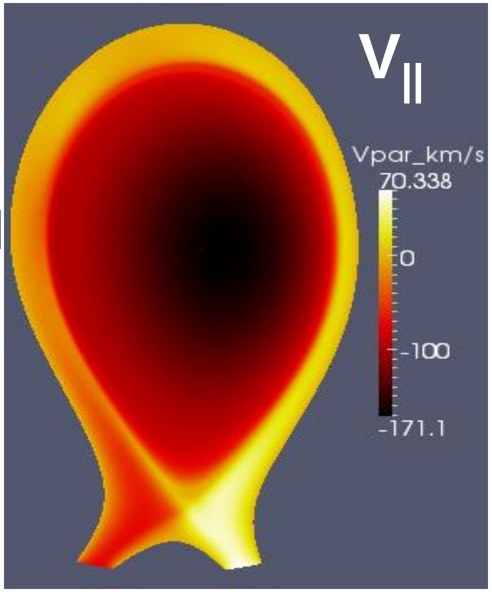

Equilibrium flows affect ELM dynamics & RMP penetration: Source of toroidal rotation, sheath conditions, neoclassical effects and diamagnetic rotation

❖ **Parallel flow:**

❑ **Central plasma**: source of toroidal rotation keeps initial experimental profile

❑ **SOL**: sheath conditions on targets: $V_{\|, div} = \pm C_s$

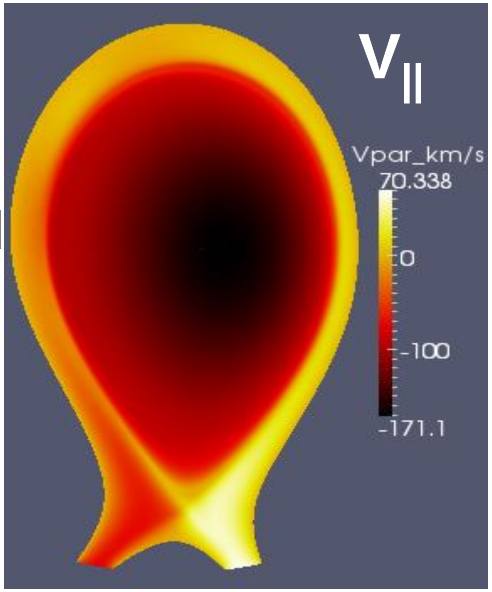

❖ **Poloidal flow:**

❑ **Pedestal**: neoclassical friction

$V_{\theta,i} \rightarrow V_{\theta,neo} \propto \nabla_{\perp} T_i$

❑ **SOL:**

$V_{\theta,i} \approx V_{\|} B_{\theta}$

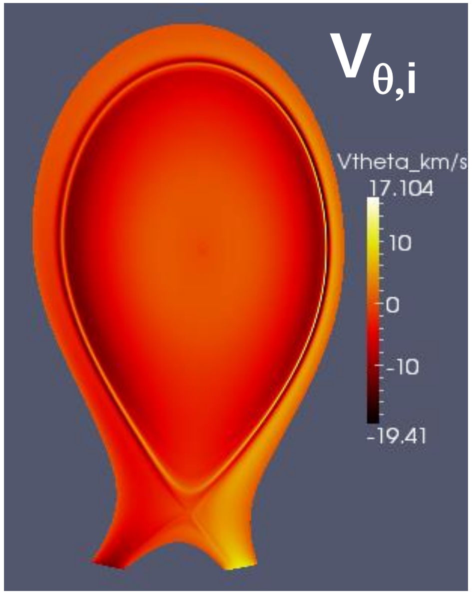

Equilibrium flows affect ELM dynamics & RMP penetration: Source of toroidal rotation, sheath conditions, neoclassical effects and diamagnetic rotation

❖ **Parallel flow:**

❑ **Central plasma**: source of toroidal rotation keeps initial experimental profile

❑ **SOL**: sheath conditions on targets: $V_{\parallel,div} = \pm C_s$

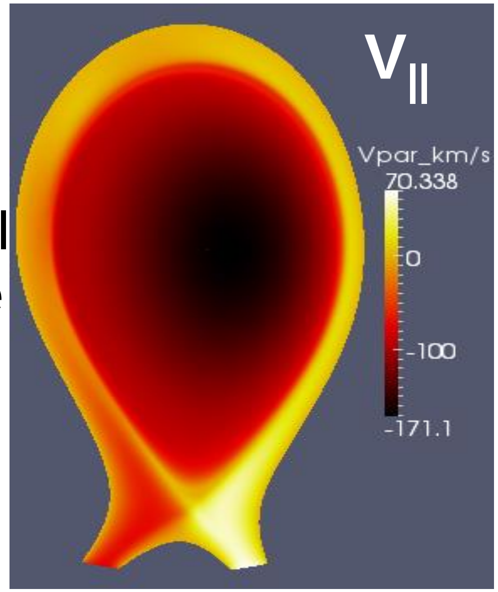

❖ **Poloidal flow:**

❑ **Pedestal**: neoclassical friction

$$V_{\theta,i} \rightarrow V_{\theta,neo} \propto \nabla_\perp T_i$$

❑ **SOL:**

$$V_{\theta,i} \approx V_\parallel B_\theta$$

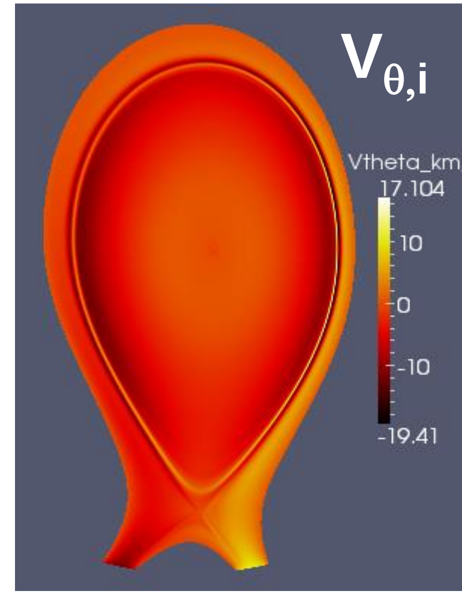

❖ ***Radial electric field:***

$$E_r = \nabla p/n\,e + (V_\varphi B_\theta - V_\theta B_\varphi)$$

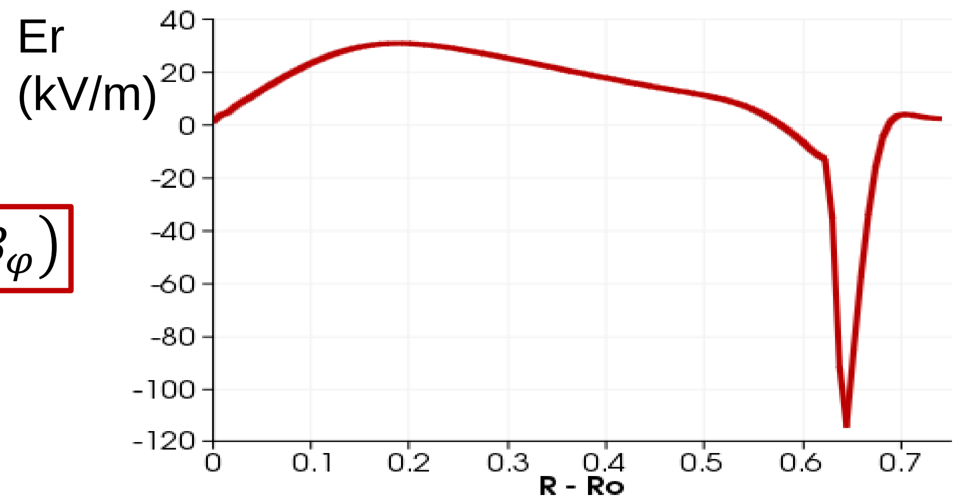

Modeling choices and limitations

Mass density:

$$\frac{d\rho}{dt} = \nabla \cdot \left(D_\perp \nabla_\perp \rho \right) + S_\rho$$

Temperature:

$$\frac{d(\rho T)}{dt} = \nabla \cdot \left(K_\perp \nabla_\perp T + K_{||} \nabla_{||} T \right) + S_T$$

- Heat and particle sources:

→ key to rebuild pedestal after ELM crash

Modeling choices and limitations

Mass density:

$$\frac{d\rho}{dt} = \nabla \cdot \left(D_\perp \nabla_\perp \rho \right) + S_\rho$$

Temperature:

$$\frac{d(\rho T)}{dt} = \nabla \cdot \left(K_\perp \nabla_\perp T + K_{||} \nabla_{||} T \right) + S_T$$

- Heat and particle sources:

→ key to rebuild pedestal after ELM crash

- Perpendicular (turbulent) transport mimicked by diffusive terms:

→ Reduced in pedestal: transport barrier:

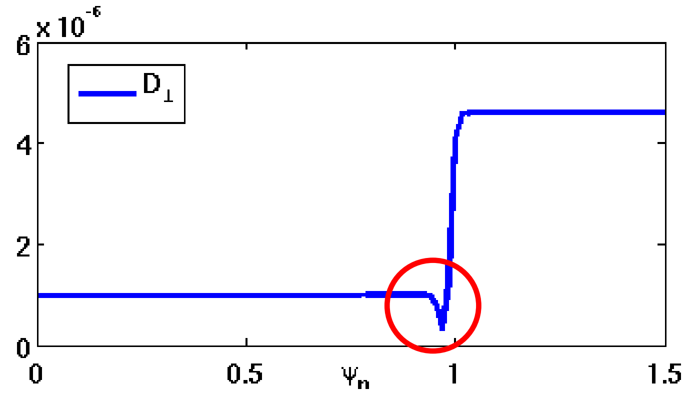

Modeling choices and limitations

Mass density: $$\frac{d\rho}{dt} = \nabla \cdot \left(D_\perp \nabla_\perp \rho \right) + S_\rho$$

Temperature: $$\frac{d(\rho T)}{dt} = \nabla \cdot \left(K_\perp \nabla_\perp T + K_{||} \nabla_{||} T \right) + S_T$$

- Heat and particle sources:

→ key to rebuild pedestal after ELM crash

- Perpendicular (turbulent) transport mimicked by diffusive terms:

→ Reduced in pedestal: transport barrier:

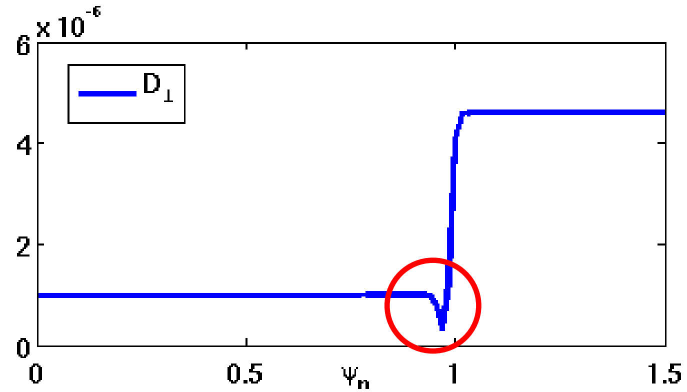

- $\eta \propto T^{-3/2}$, $K_{||} \propto T^{5/2}$, $\nu_{||} \propto T^{-3/2}$: temperature-dependent, $K_{||} / K_\perp = 2 \times 10^8$
- Main numerical limit: central η_0 10-100 times larger than experiment

A typical JOREK run: e.g. in ITER geometry

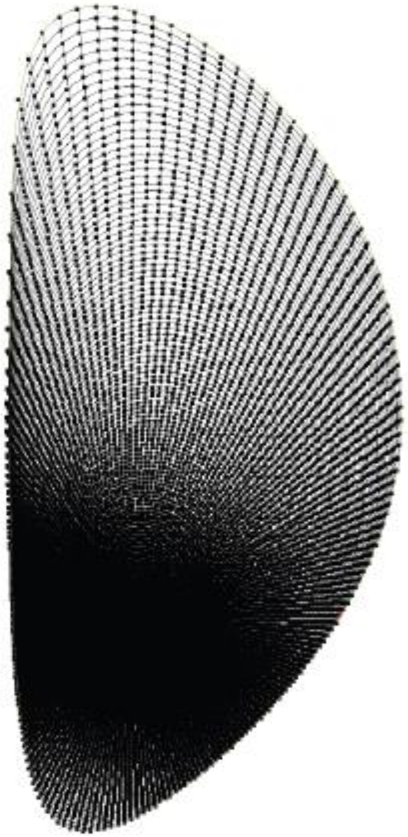

1) **Initial grid: polar grid for Bézier elements**
2) Flux-aligned grid including X-point and BC
3) Equilibrium *(n=0)* flows
4) Time integration for all *n* harmonics

A typical JOREK run: e.g. in ITER geometry

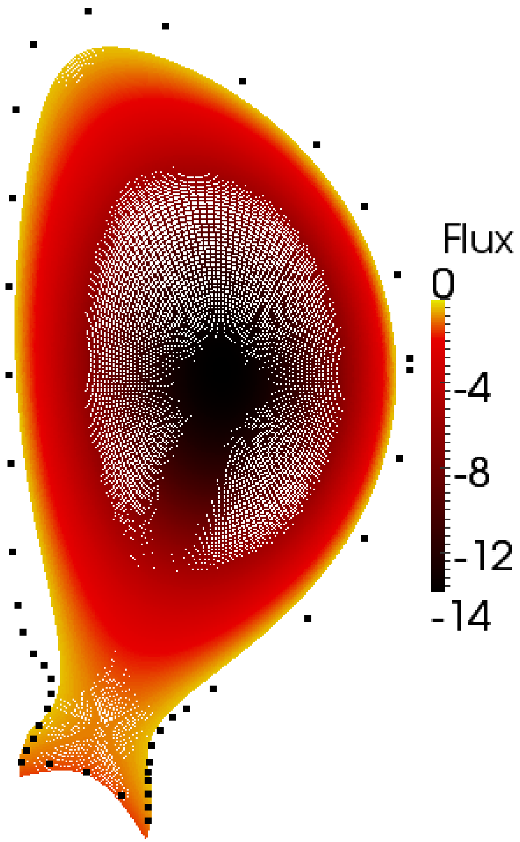

1) Initial grid: polar grid for Bézier elements

2) Flux-aligned grid including X-point and BC

3) Equilibrium *(n=0)* flows

4) Time integration for all *n* harmonics

A typical JOREK run: e.g. in ITER geometry

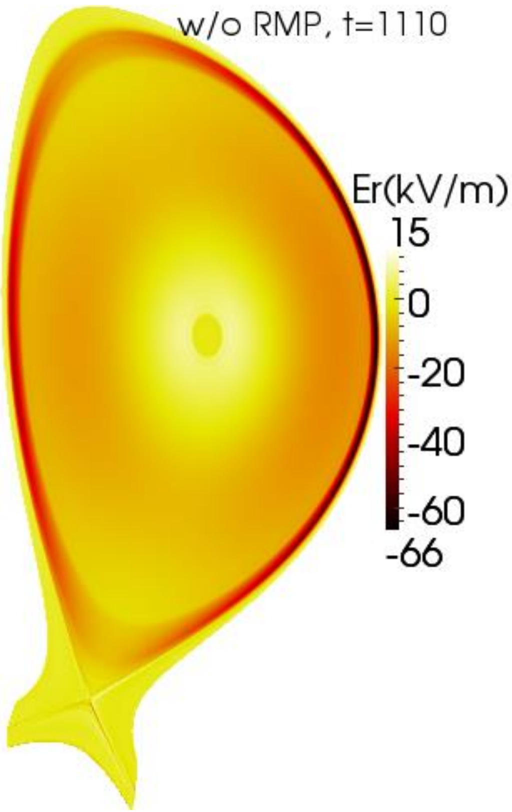

1) Initial grid: polar grid for Bézier elements

2) Flux-aligned grid including X-point and BC

3) **Equilibrium *(n=0)* flows**

4) Time integration for all *n* harmonics

A typical JOREK run: e.g. in ITER geometry

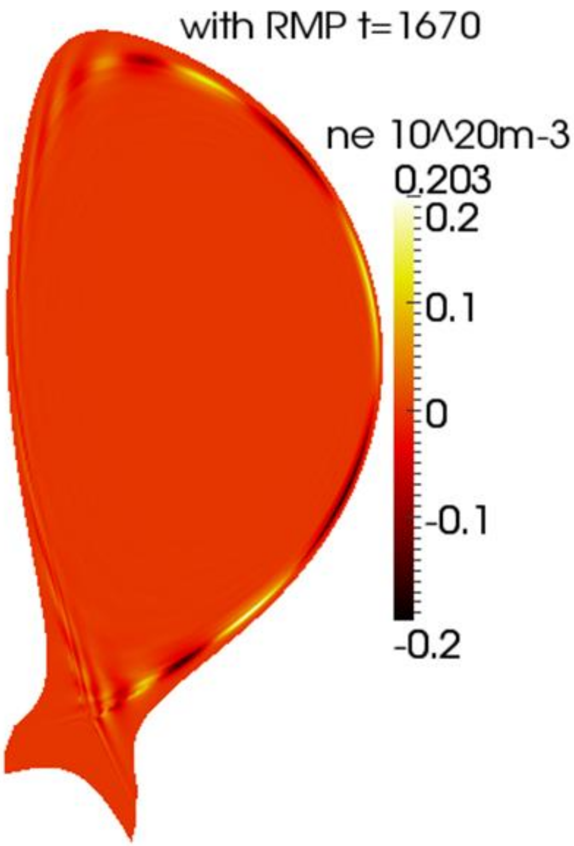

1) Initial grid: polar grid for Bézier elements

2) Flux-aligned grid including X-point and BC

3) Equilibrium *(n=0)* flows

4) **Time integration for all *n* harmonics**
→ e.g. *(n=3)* RMPs

A typical JOREK run: e.g. in ITER geometry

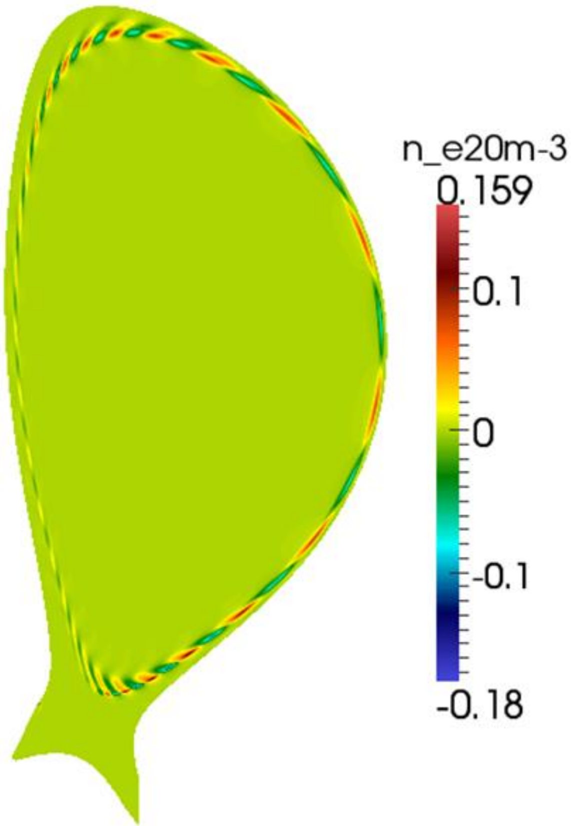

1) Initial grid: polar grid for Bézier elements

2) Flux-aligned grid including X-point and BC

3) Equilibrium *(n=0)* flows

4) **Time integration for all *n* harmonics**
→ e.g. *(n=9)* ELM

- Introduction: ELMs and RMPs
- The JOREK code
- **ELM dynamics**
  - ➔ **Main exp. features of ELMs reproduced in simulations**
  - ➔ **Cyclic ELM dynamics**
- ELM control by RMPs
- Conclusion and Outlook

Single ELM crash simulation (w/o diamagnetic drifts)

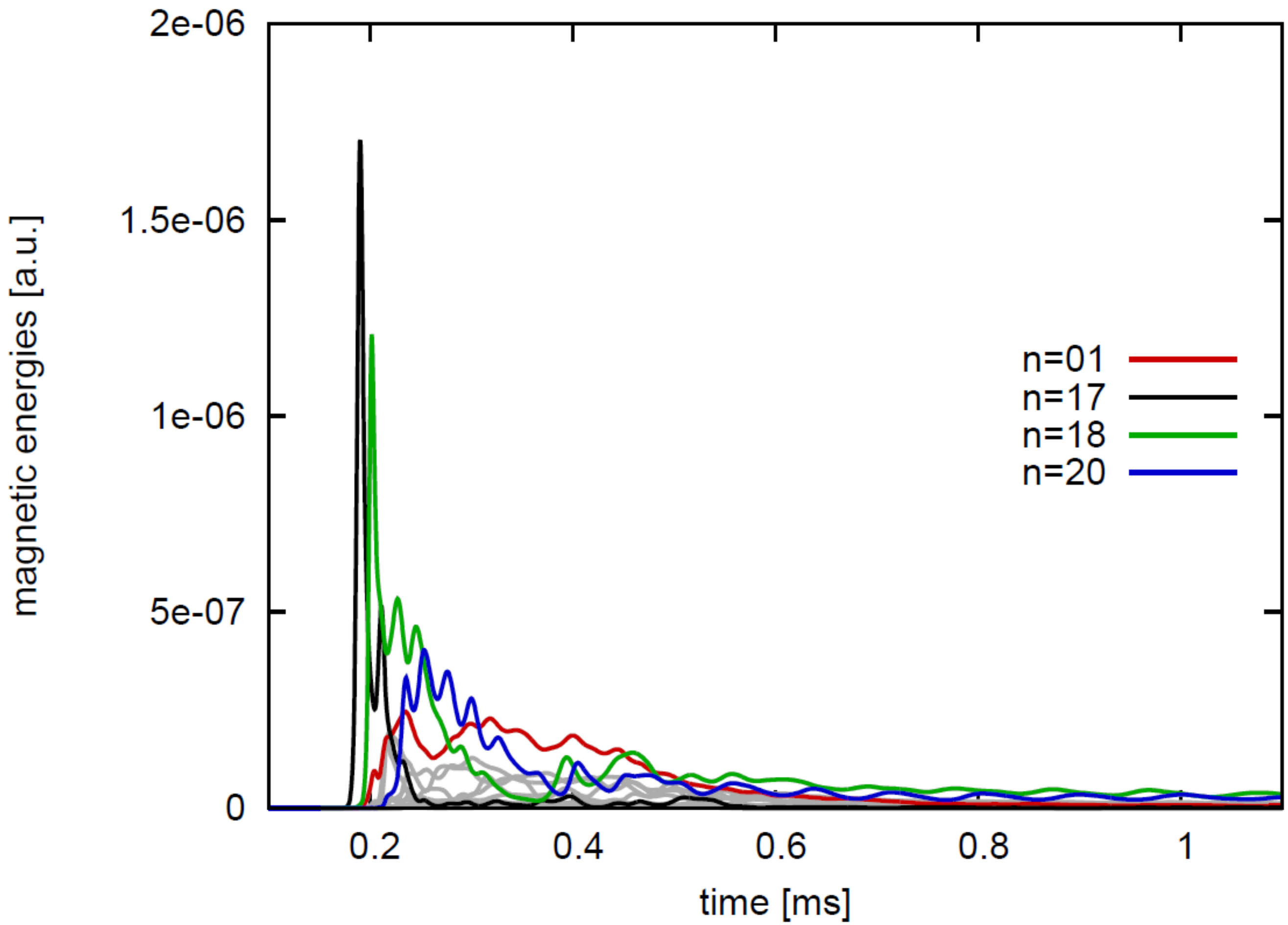

- ❖ Harmonics 0. . . 22 included
- ❖ No diamagnetic flow → single ELM crash
- ❖ Resistivity in simulation: $5 \times 10^{-6}\ \Omega.m$ = 10 x experimental value

Collapse of the edge pressure profile

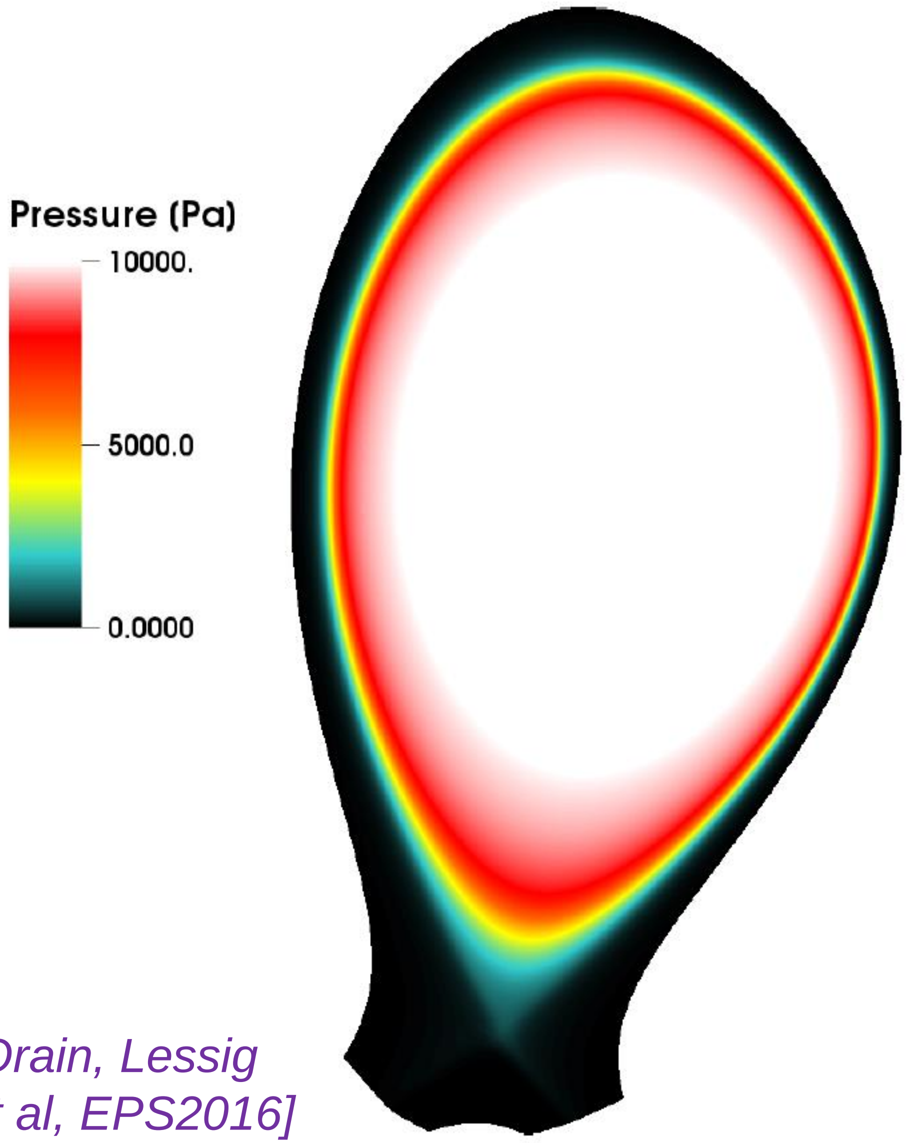

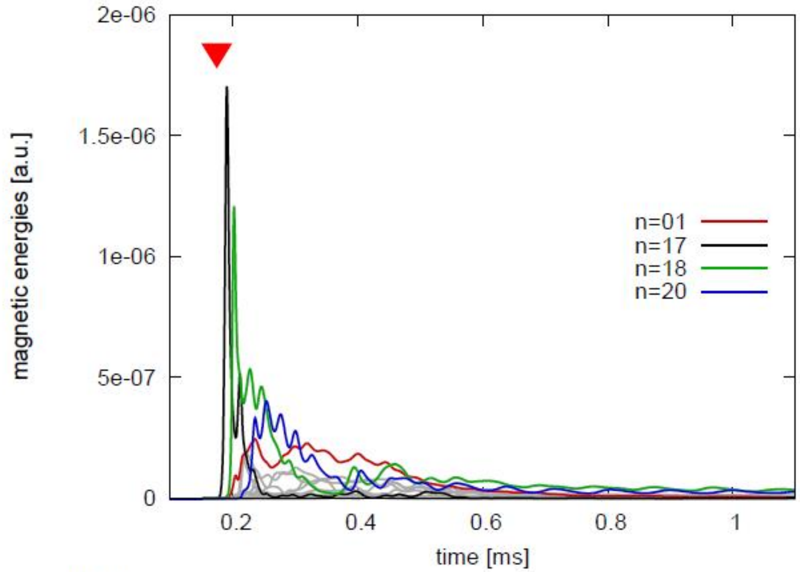

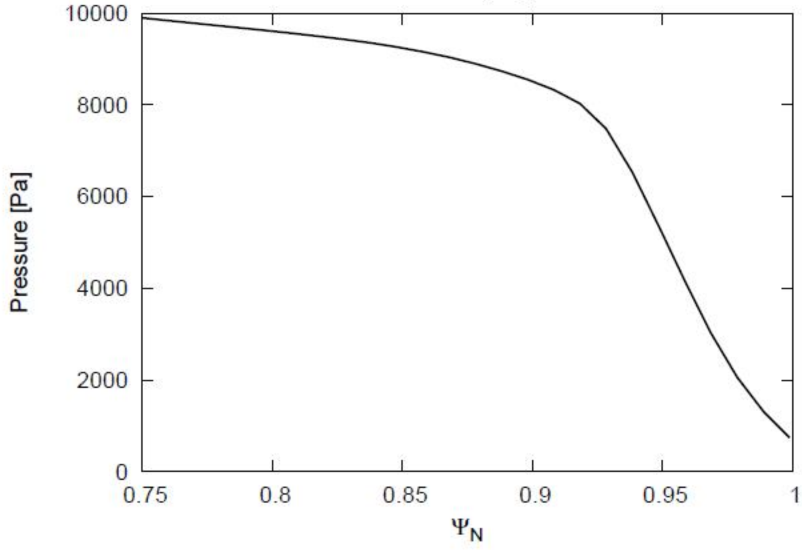

[Orain, Lessig et al, EPS2016]

Collapse of the edge pressure profile

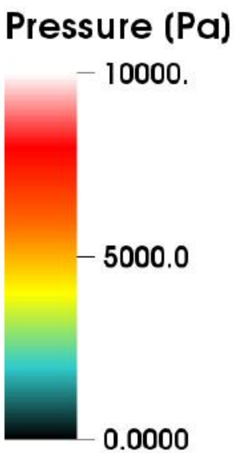

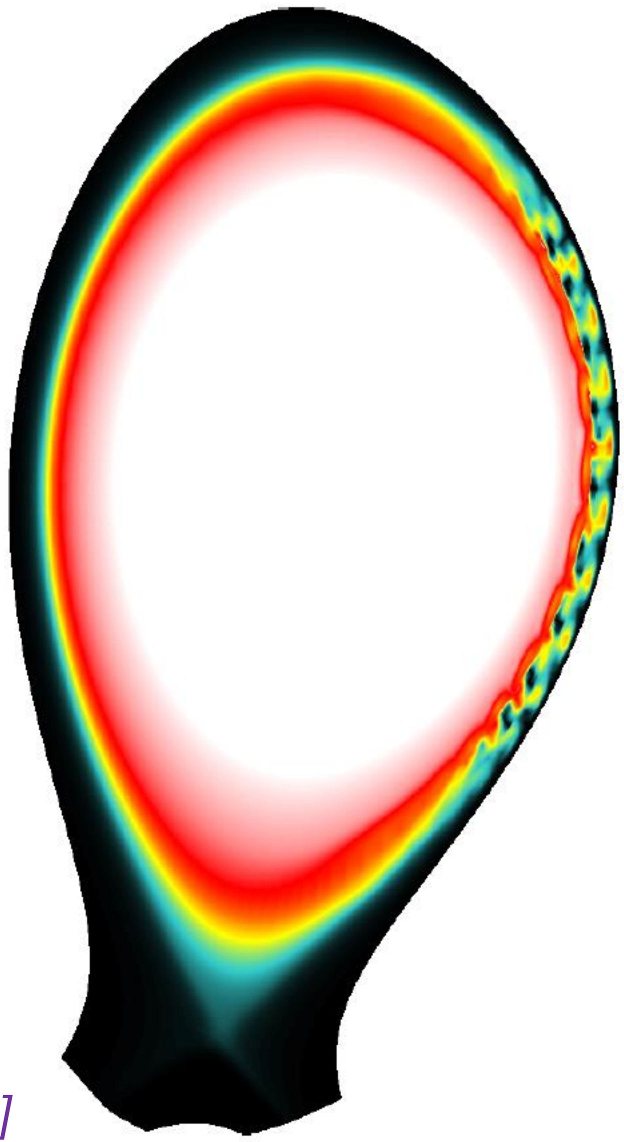

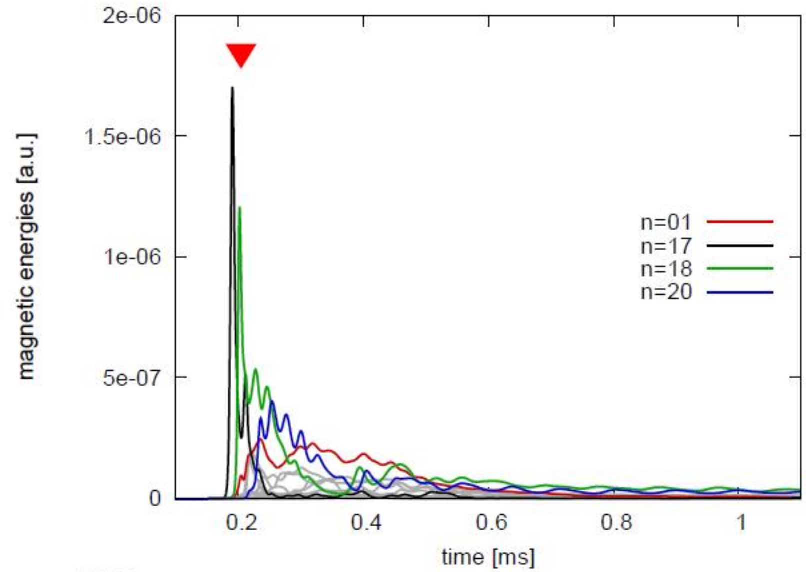

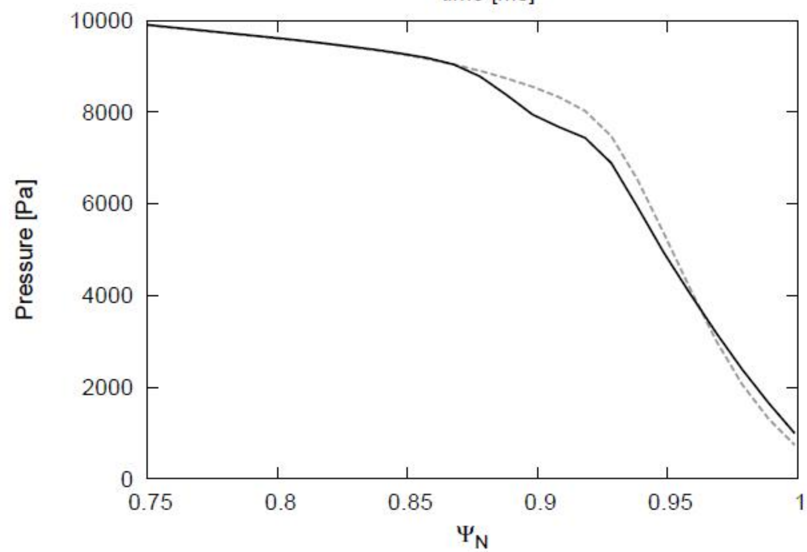

[Orain, Lessig et al, EPS2016]

Collapse of the edge pressure profile

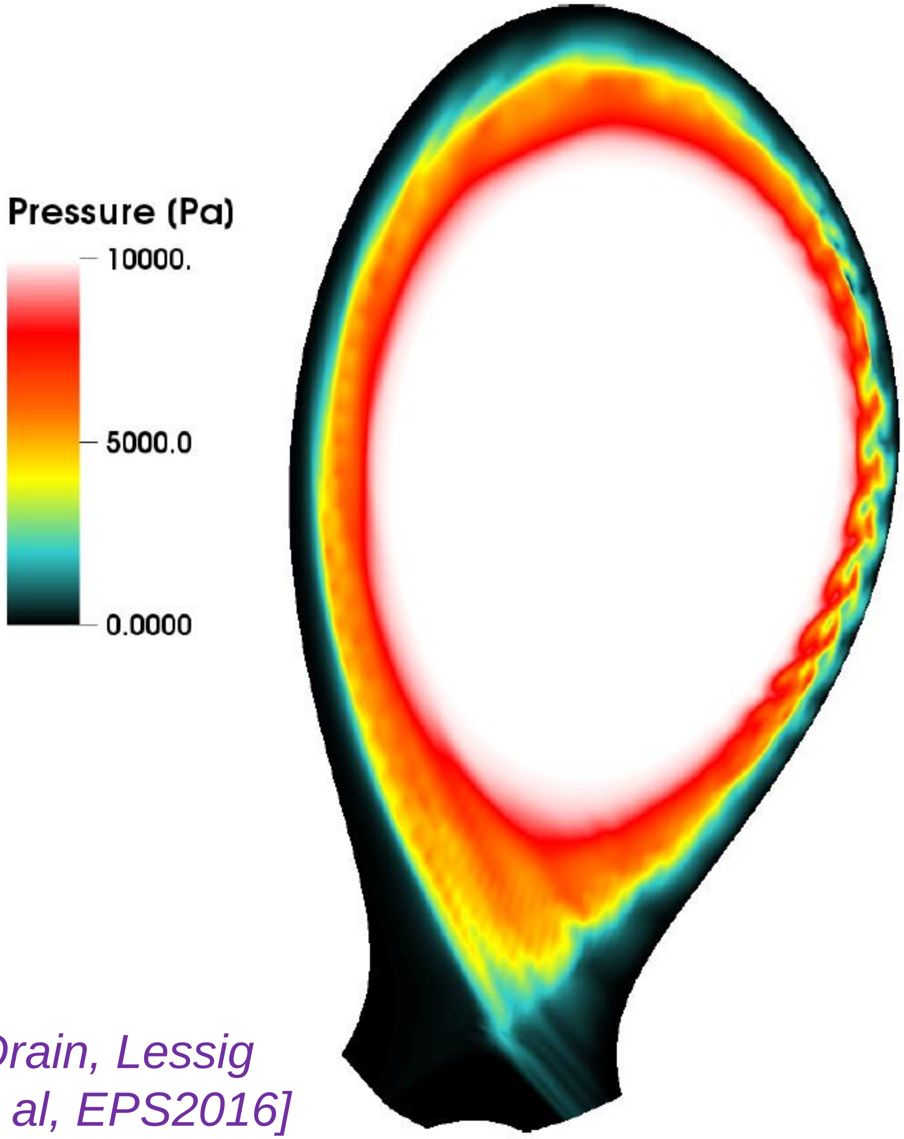

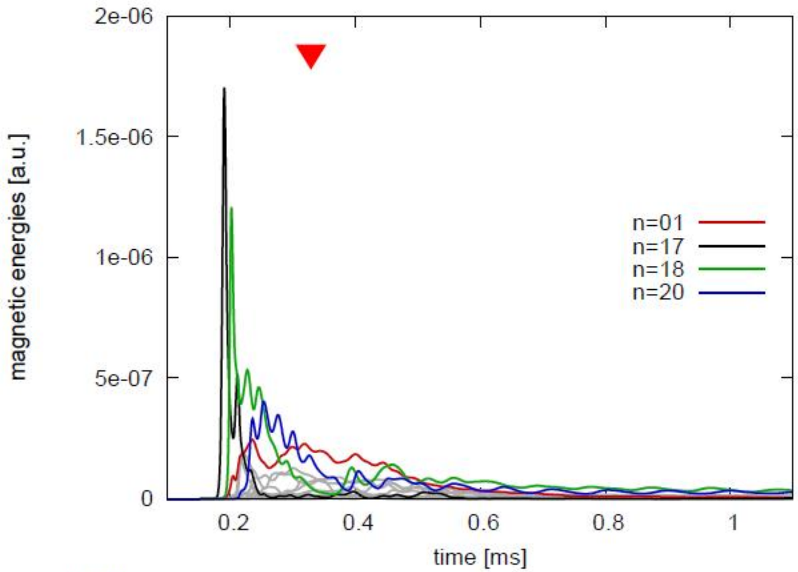

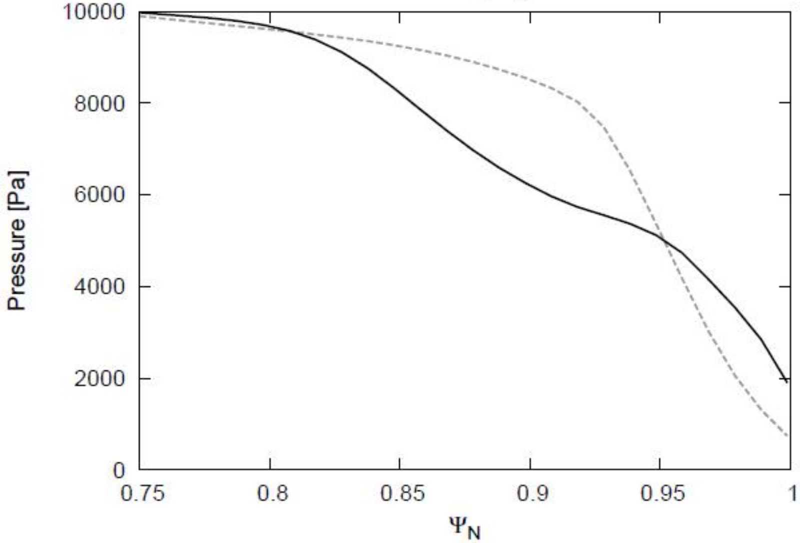

[Orain, Lessig et al, EPS2016]

Collapse of the edge pressure profile

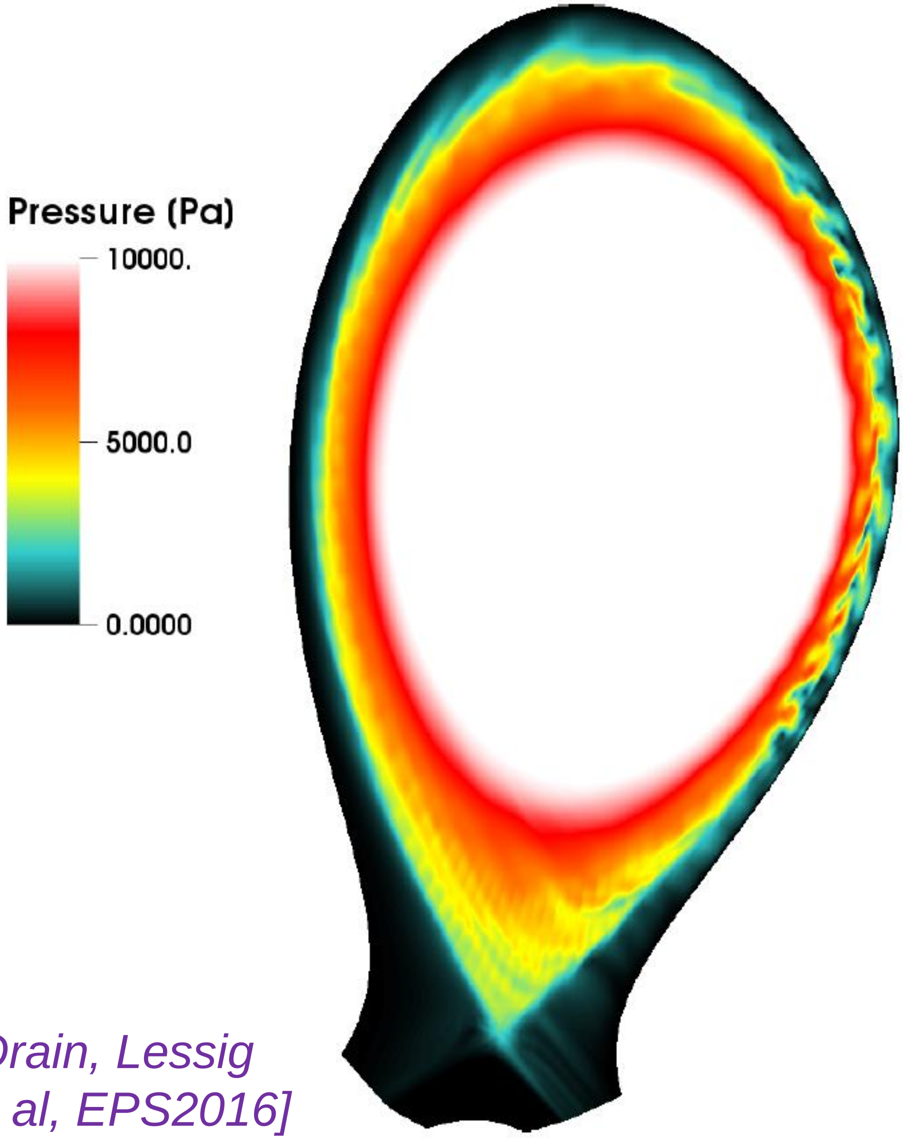

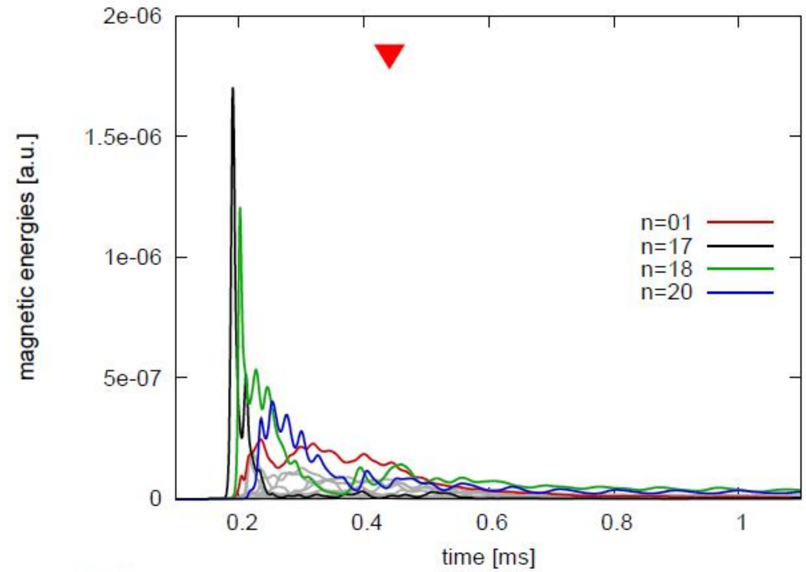

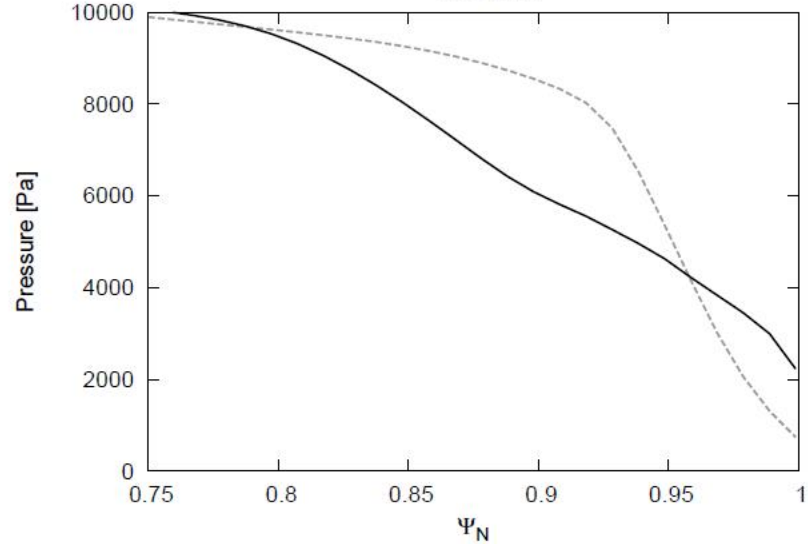

[Orain, Lessig et al, EPS2016]

Collapse of the edge pressure profile

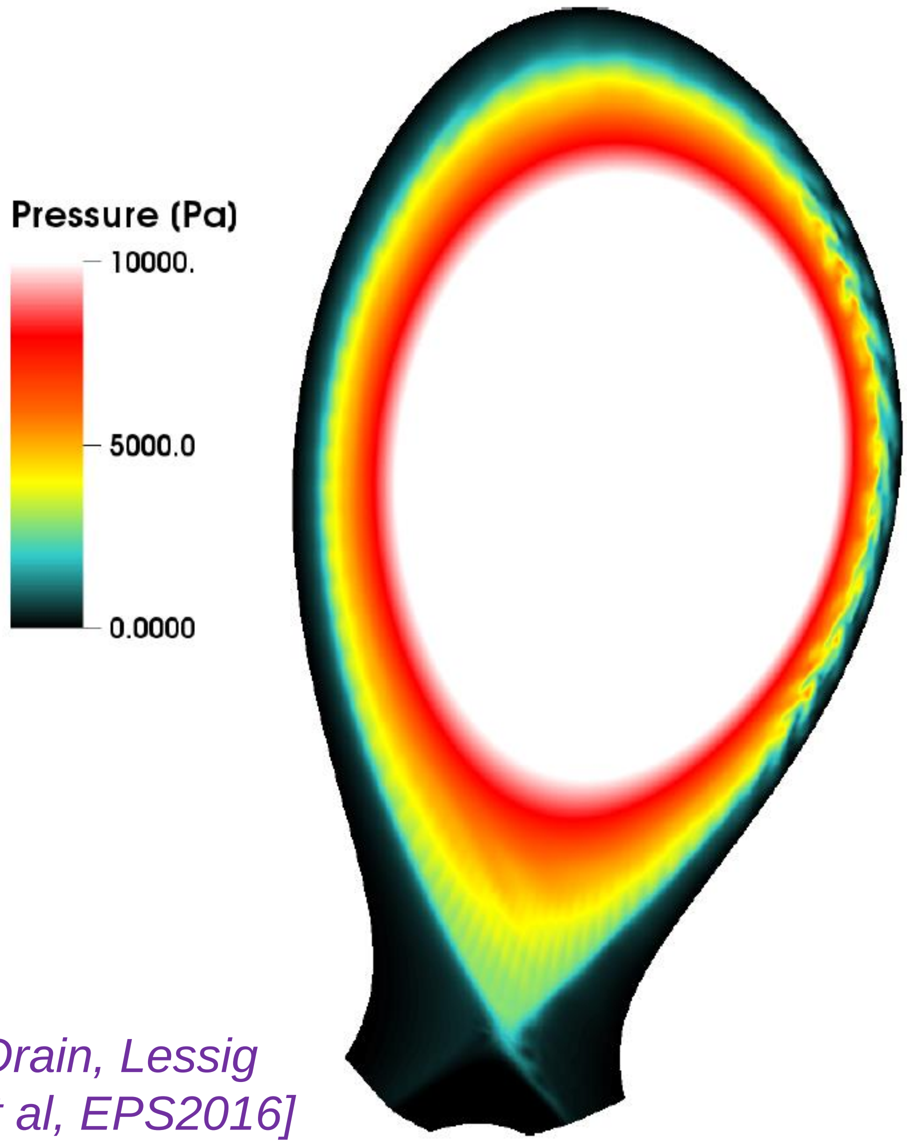

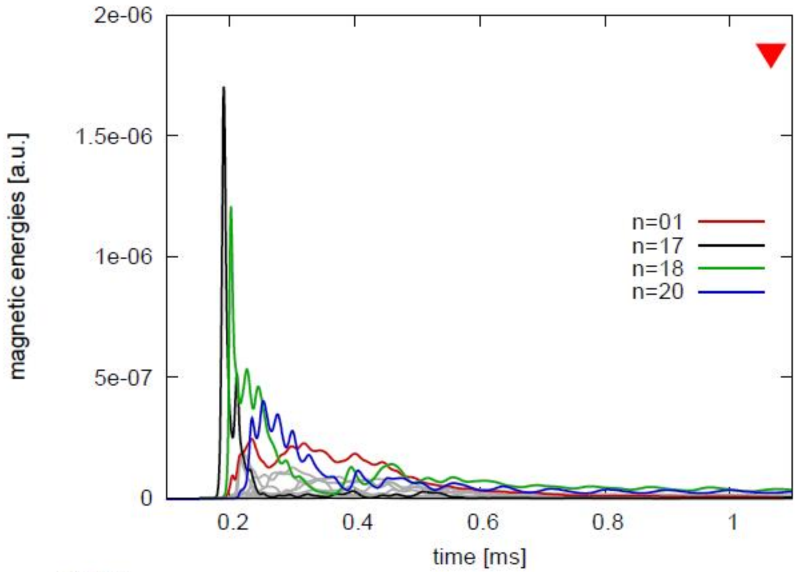

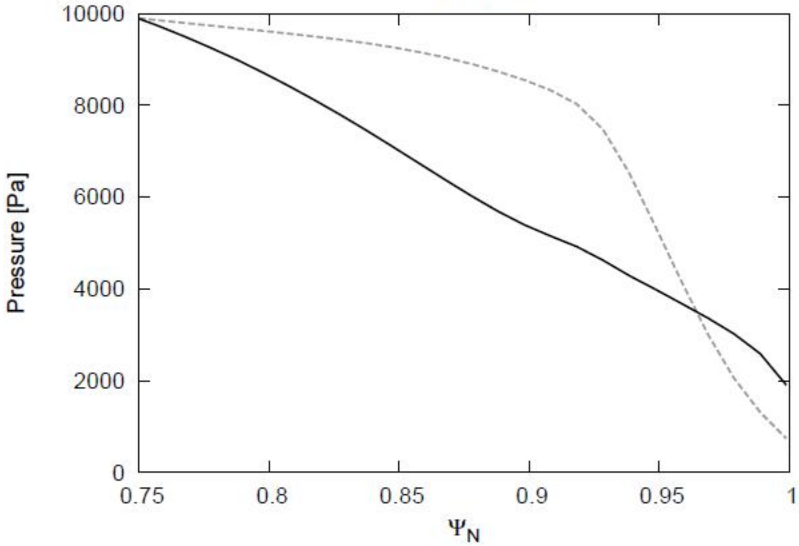

[Orain, Lessig et al, EPS2016]

Low-n structure observed in experiments : explained in modeling by non-linear coupling

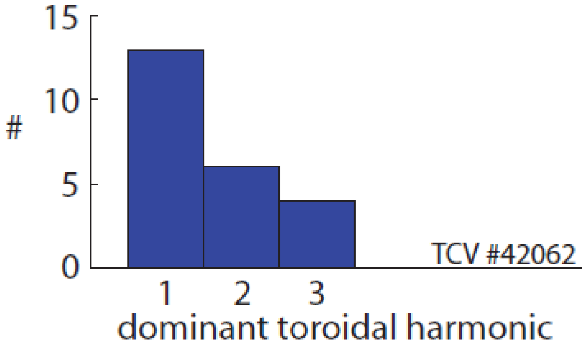

- ❖ Dominant magnetic components in TCV discharges = **low n modes**

[Wenninger NF 2013]

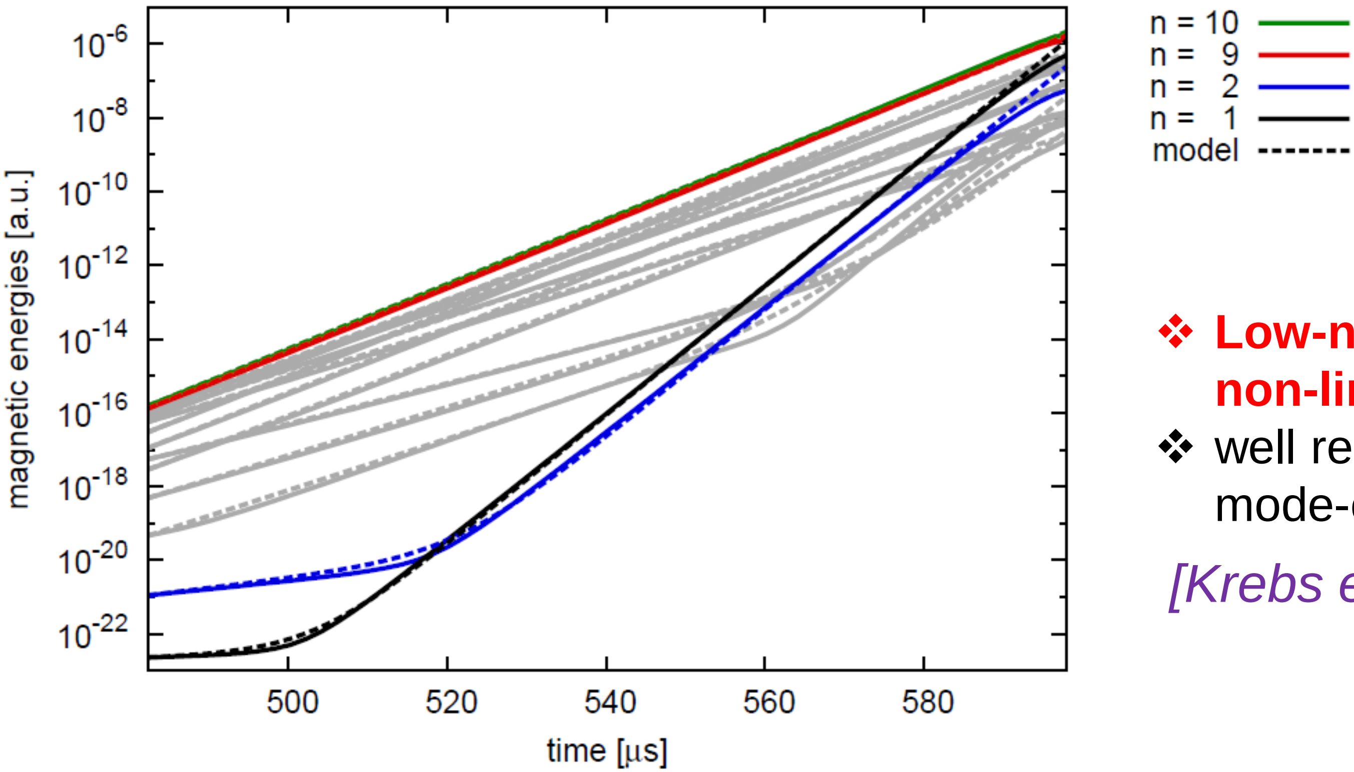

- ❖ **Low-n numbers driven by non-linear coupling**
- ❖ well reproduced in simple mode-coupling model

[Krebs et al, PoP 2013]

- Introduction: ELMs and RMPs
- The JOREK code
- **ELM dynamics**
  - ➔ Main exp. features of ELMs reproduced in simulations
  - ➔ **Cyclic ELM dynamics**
- ELM control by RMPs
- Conclusion and Outlook

Diamagnetic rotation ω* instrumental to get ELM cycle
Without diamagnetic rotation: single ELM

ω*=0: single ELM:

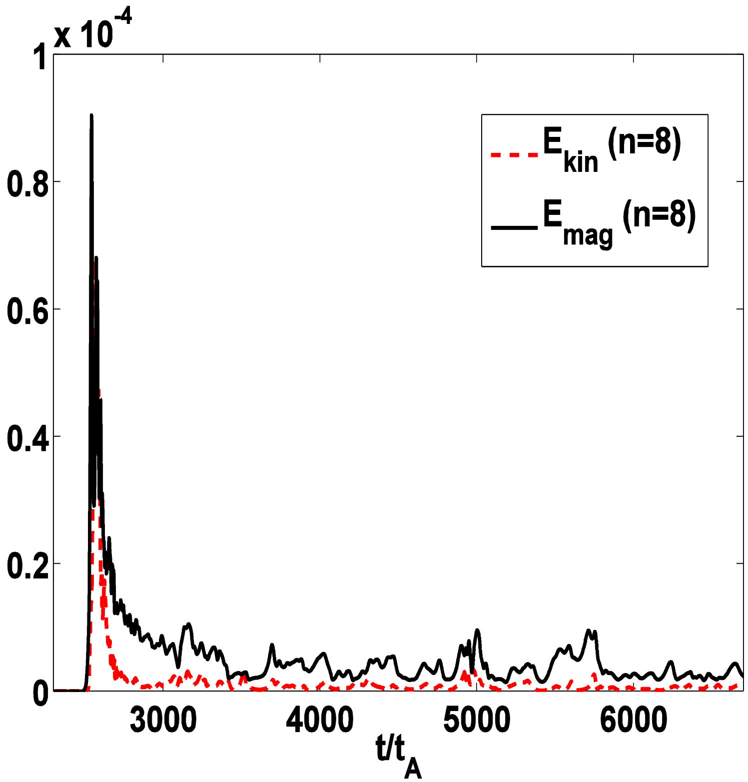

Diamagnetic rotation ω* instrumental to get ELM cycle

Without diamagnetic rotation: single ELM

ω*=0: single ELM:

-crash: large ergodic layer

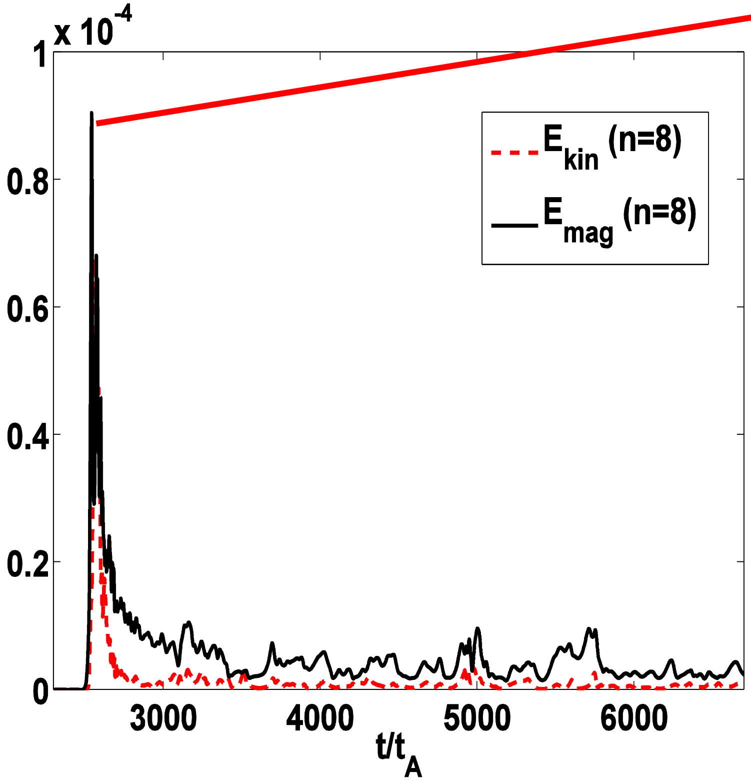

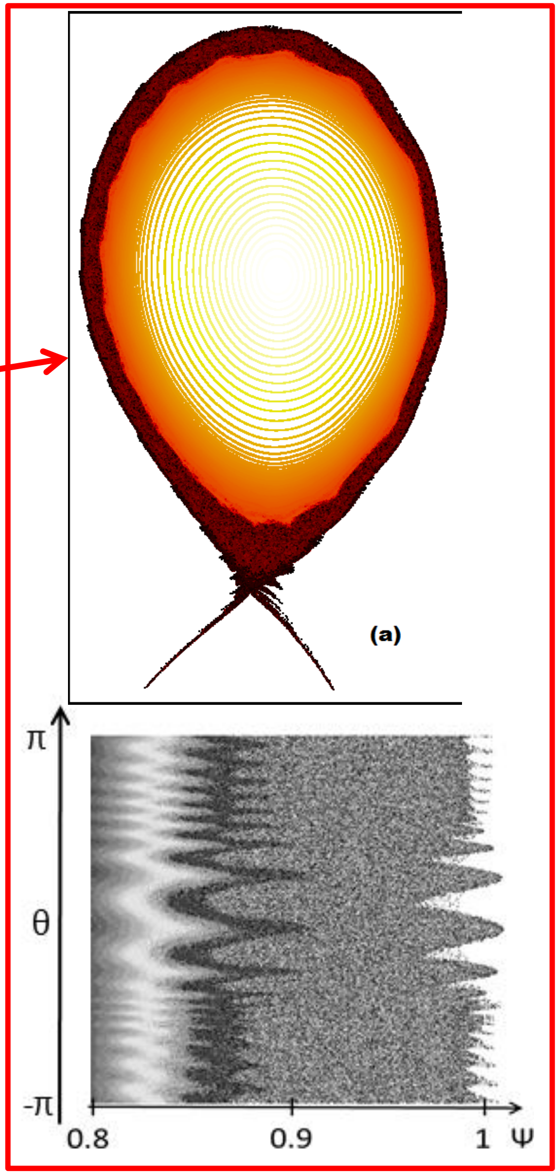

Diamagnetic rotation ω* instrumental to get ELM cycle

Without diamagnetic rotation: single ELM

ω*=0: single ELM:
- crash: large ergodic layer
- modes keep unstable after ELM

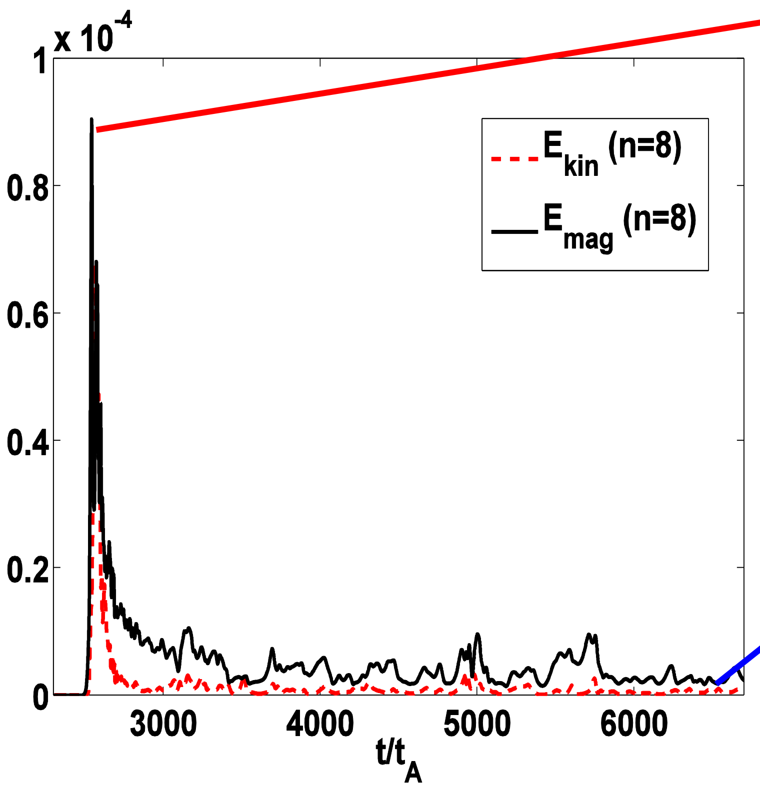

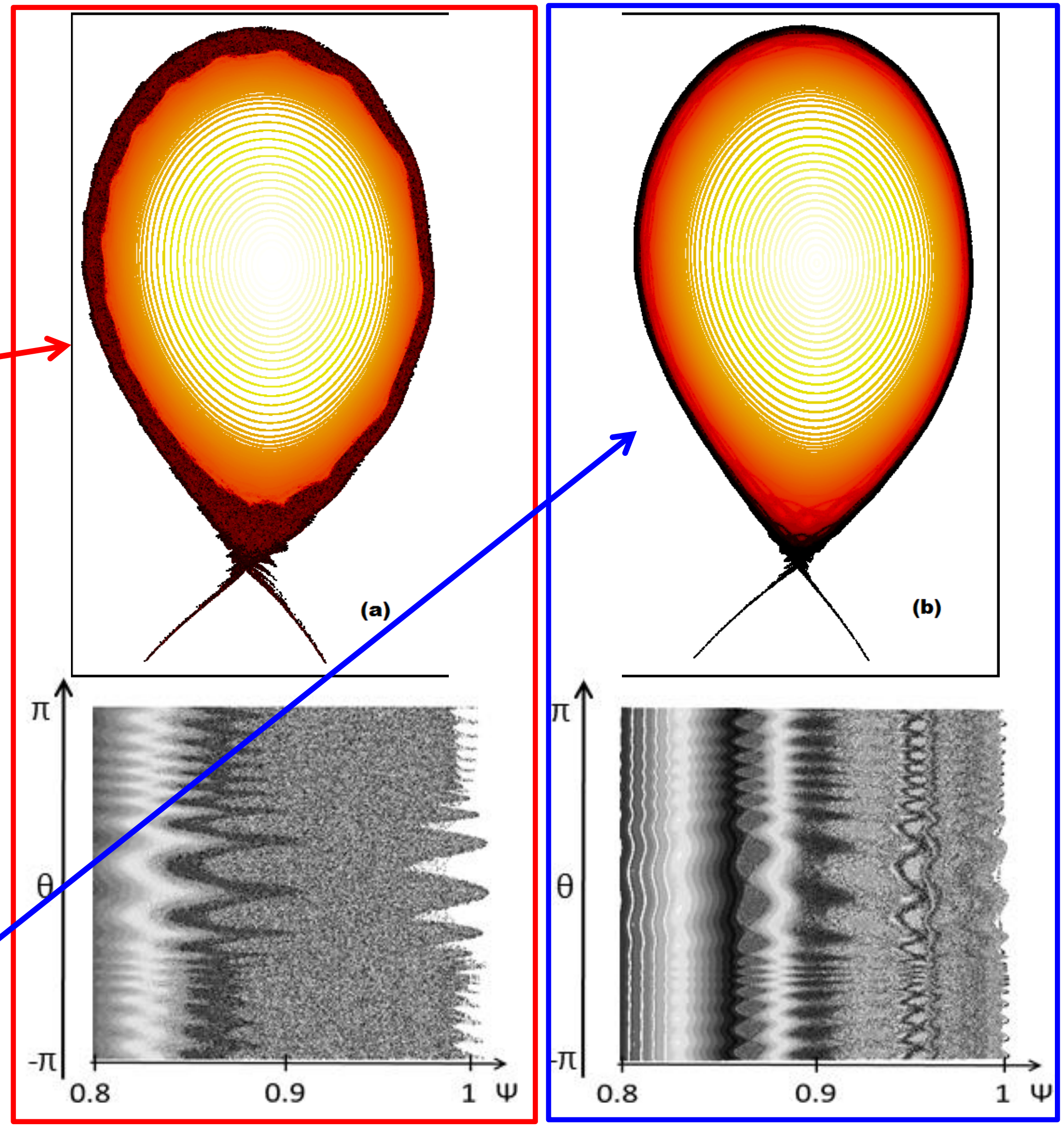

Diamagnetic rotation ω* instrumental to get ELM cycle

∇P

- Destabilize Ballooning modes
- Stabilizing through $\omega^* \propto \nabla P$

} Ambivalent role

Diamagnetic rotation ω* instrumental to get ELM cycle

∇P → Destabilize Ballooning modes

∇P → Stabilizing through $\omega^* \propto \nabla P$

} Ambivalent role

Just after ELM crash:
reduced ∇P
→ ω* stabilization dominant

Later after crash:
heat source ↑↑∇P
→ destabilization dominant

Diamagnetic rotation ω* instrumental to get ELM cycle

∇P → Destabilize Ballooning modes
∇P → Stabilizing through $\omega^* \propto \nabla P$

} Ambivalent role

Just after ELM crash:
reduced ∇P
→ ω* stabilization dominant

Later after crash:
heat source ↑↑∇P
→ destabilization dominant

Competition between stabilization and destabilization
→ cyclic dynamics

JET case with ω*: ELM cycle: Transient ELMs before quasiperiodic ELMy regime

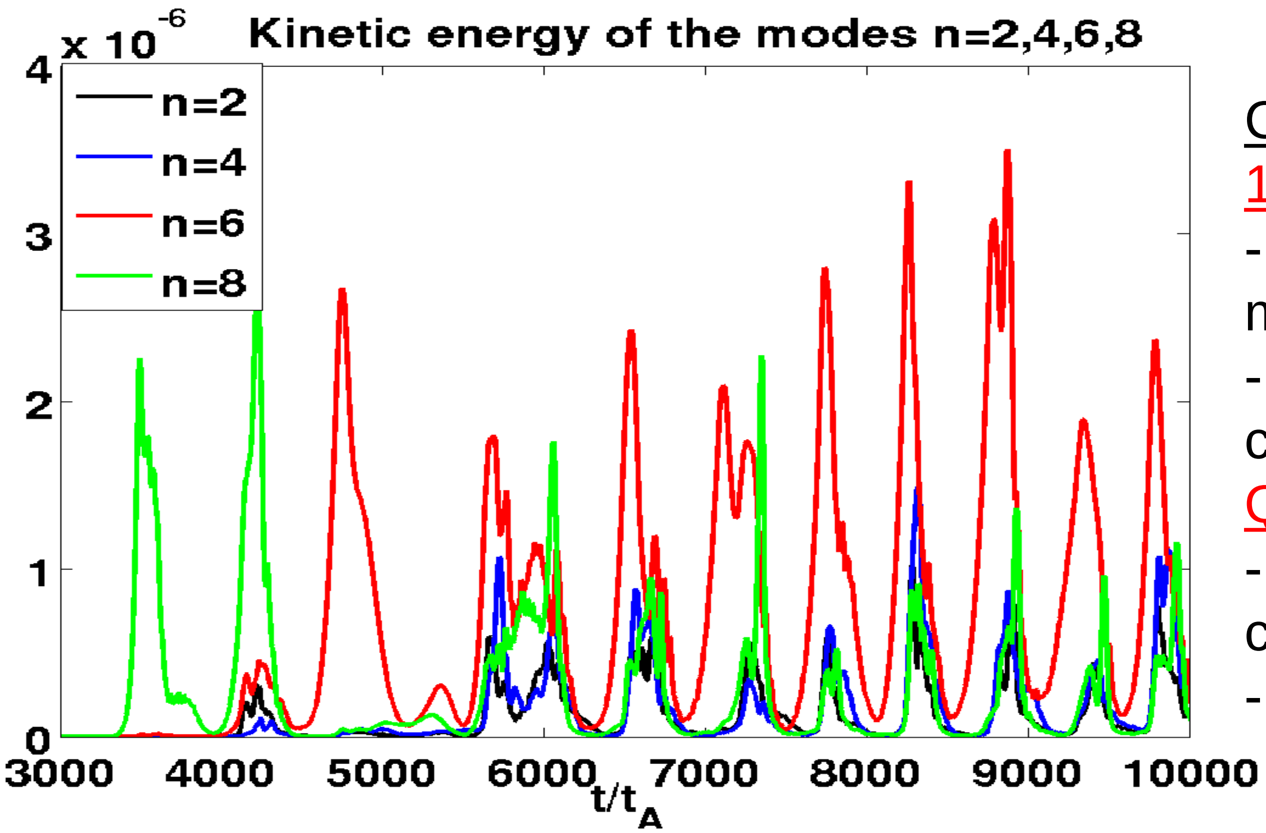

CYCLE:

1st transient ELMs:

- most unstable high-n mode dominate
- depends on initial conditions

Quasiperiodic ELMy regime

- modes non-linearly coupled
- self-organized

[Orain et al, PPCF2015, PRL 2015]

Quasiperiodic regime: ELM crashes occur at ~same ∇P_{limit} + ~same power deposition

- Each ELM: relaxation of the pressure profile
- Peeling-Ballooning diagram:

ELM crashes occur at same ∇P_{limit}

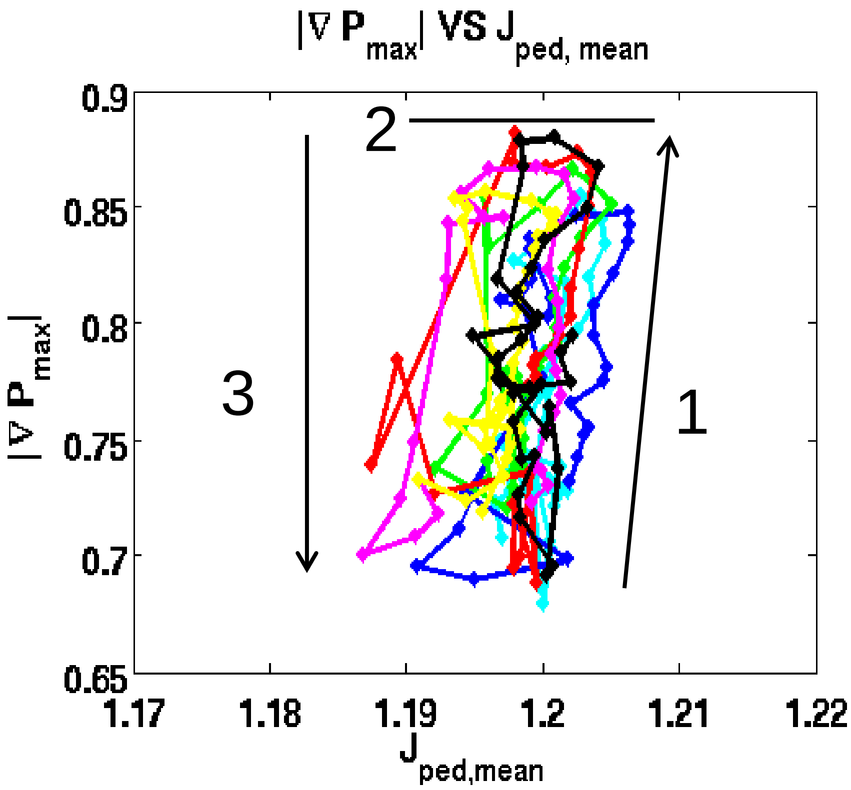

Quasiperiodic regime: ELM crashes occur at ~same ∇P_{limit} + ~same power deposition

- Each ELM: relaxation of the pressure profile
- Peeling-Ballooning diagram:

ELM crashes occur at same ∇P_{limit}

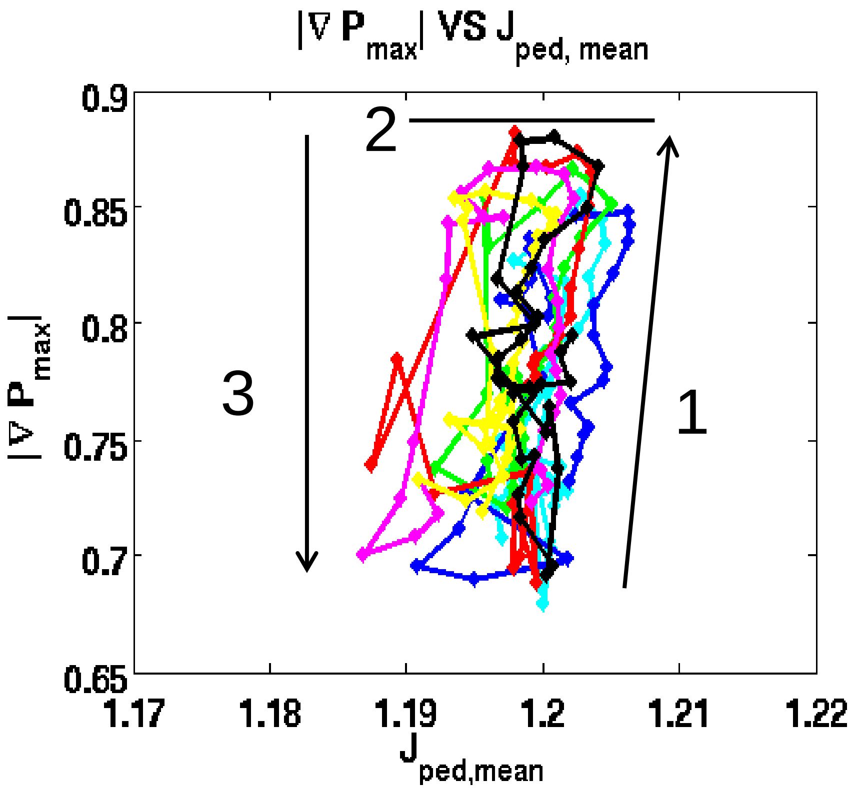

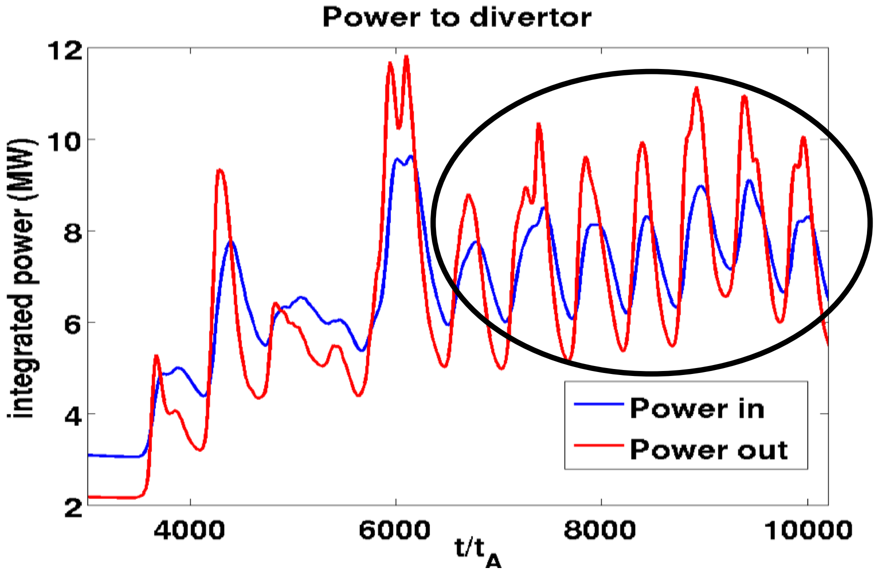

- ~Same power deposition for all ELMs in quasiperiodic regime

Discussion: simulation on ELM dynamics

→ Improved validation against experiment: exponential growth of instabilities, filamentation, non-linear coupling → low-n structures, heat power deposition on divertor targets, qualitatively similar as experiments

→ Cyclic ELM dynamics: first time modeled.

→ Two-fluid diamagnetic rotation: key ingredient

→ Results from competition between stabilization and destabilization by pressure gradient

→ Similar behaviour for all ELMs in quasiperiodic ELMy regime

→ Determined by intrinsic parameters rather than initial conditions

→ Limitations: small ELMs, high frequency, large resistivity

→ Directions to overcome limitations:

- more realistic sources
- more realistic bootstrap current
- improvement of numerical scheme needed to reduce resistivity
- simulations with turbulence → model self-consistent transport barrier *(long term)*

- Introduction: ELMs and RMPs
- The JOREK code
- ELM dynamics
- **ELM control by RMPs**
  - ➔ **Plasma response to RMPs (without ELMs)**
  - ➔ **ELM/RMP interaction**
- Conclusion and Outlook

Boundary conditions for RMPs

❖ RMP spectrum applied as boundary condition

1/ RMP field calculated in vacuum
(VACFIELD code *[Strumberger 05]*)

AUG:
RMP ***n=2,***
I_{coil} = *5-6 kAt*

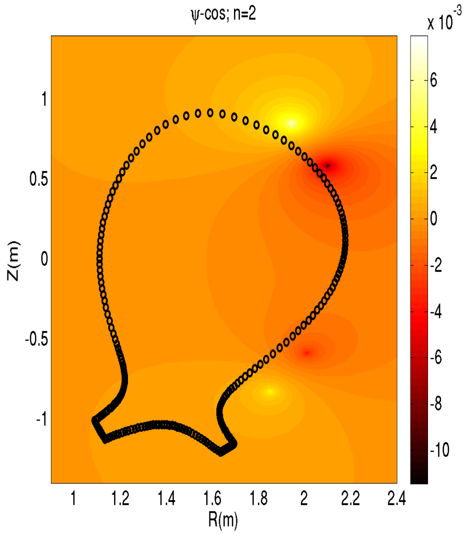

2/ Applied at the boundary of JOREK domain
and increased in 1000 t_A
→ penetration takes into account plasma response

JET case: RMP *ON* → *n=2 driven mode* → current perturbations on resonant surfaces

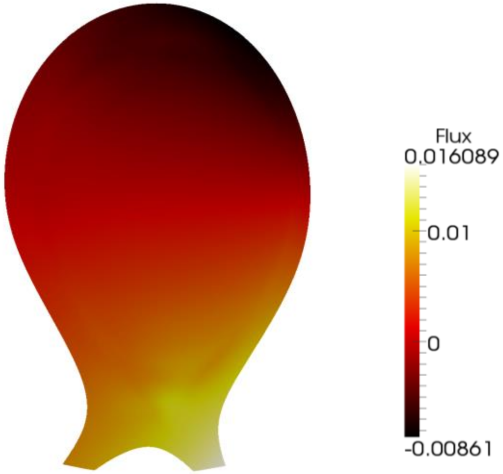

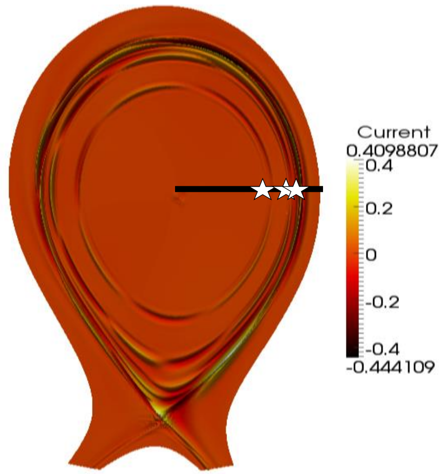

Penetration of the magn. flux perturbation

Response currents J_{mn} on $q=m/n$

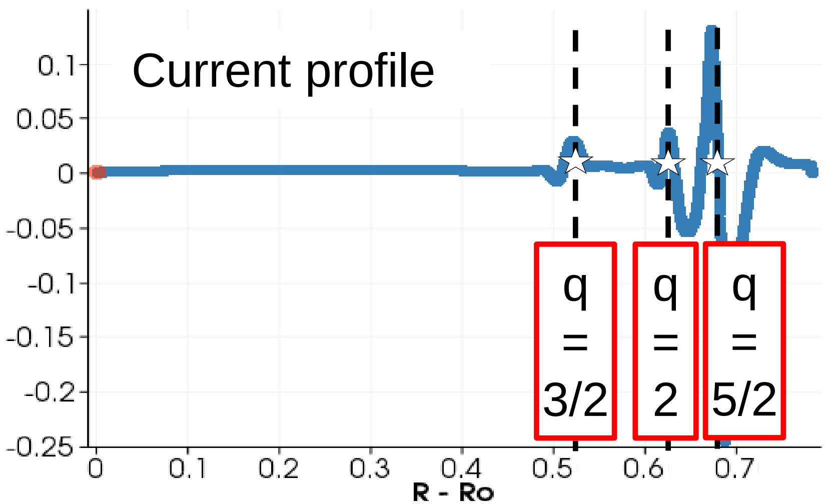

JET case: RMP *ON* → *n=2 driven mode* → current perturbations on resonant surfaces

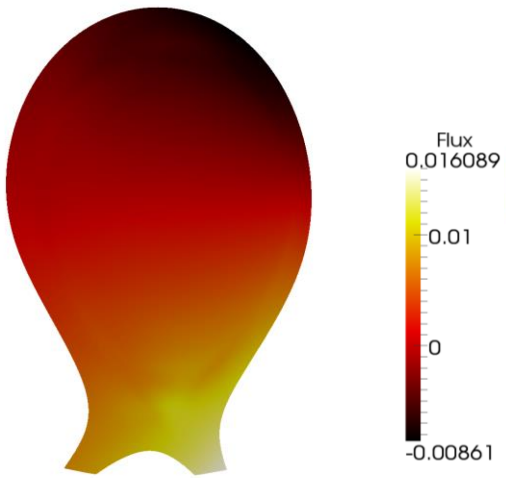

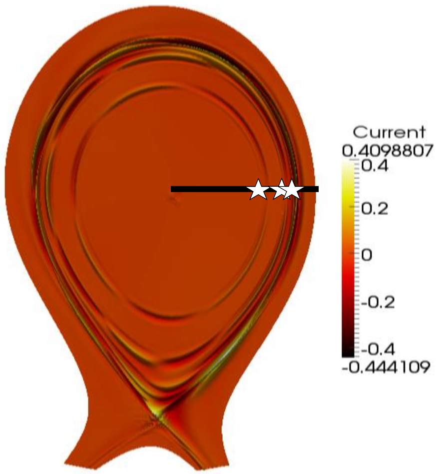

Penetration of the magn. flux perturbation

Response currents J_{mn} on *q=m/n*

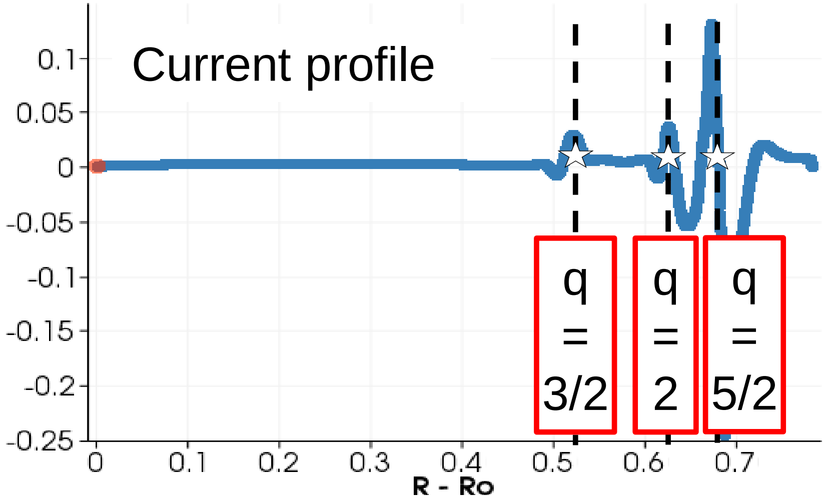

- Without RMPs: *n=2* mode → stable
- With RMPs: growth of the *n=2* mode driven by RMPs

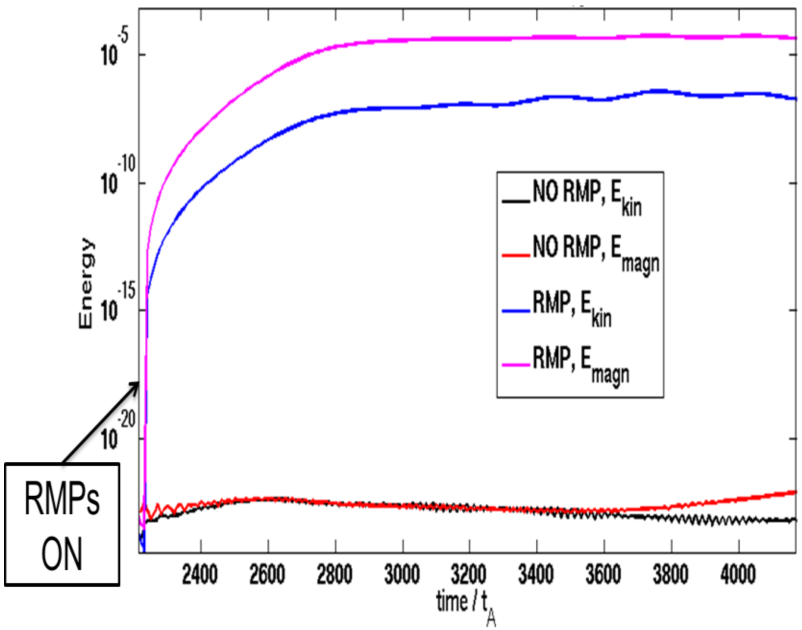

RMP screening by plasma perpendicular rotation (ExB + diamagnetic)

<u>No flows:</u> RMP generate magnetic islands on rational surfaces q= m/n
→ large ergodic layer
→ lobe structure near X-point

<u>With flows: RMP screening:</u>
→ Smaller islands in the bulk plasma
→ Smaller edge ergodic layer (r/a>0.95)
→ Shorter lobes near the X-point

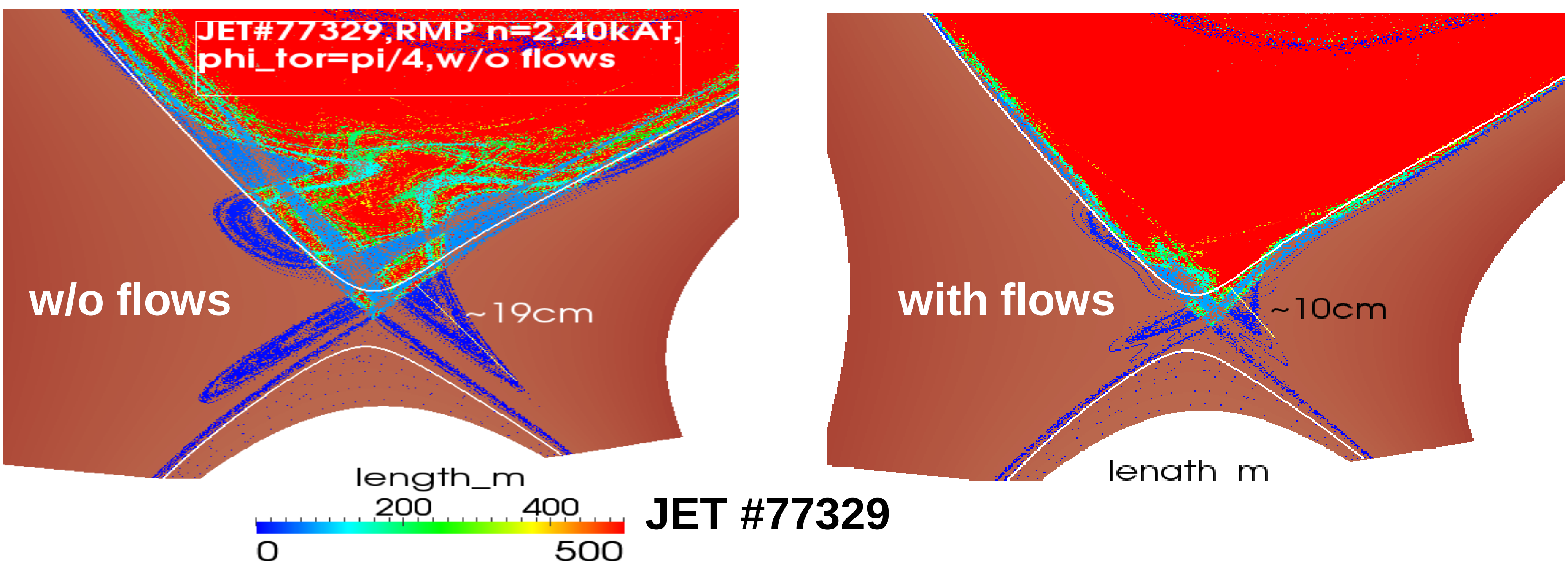

JET #77329

[Orain PoP 2013]

Other effects of RMPs:
❖ 3D-corrugation of plasma profiles
❖ Edge ergodization → enhanced transport

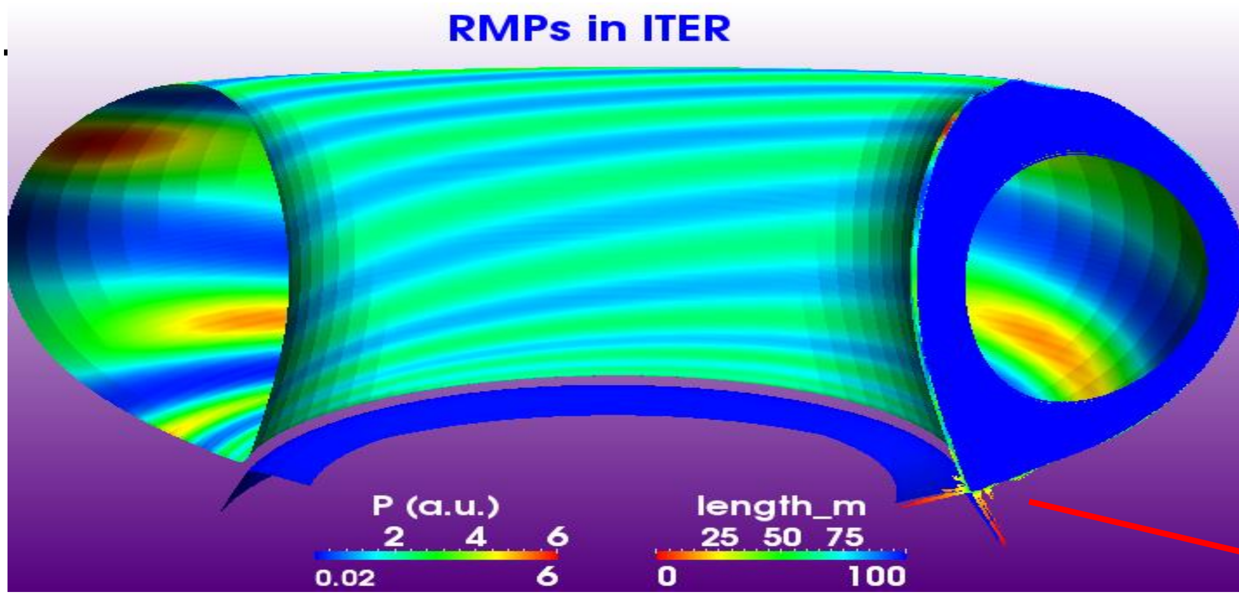

→ 3D-displacement of the separatrix

→ Maximal distortion near the X-point: **lobes**

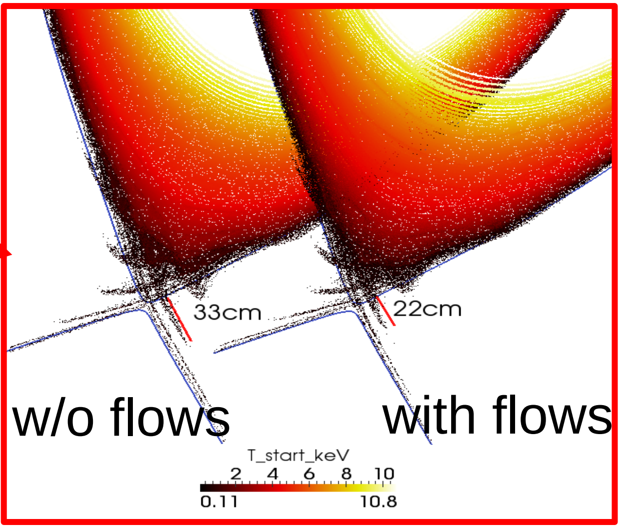

Other effects of RMPs:

❖ 3D-corrugation of plasma profiles

❖ Edge ergodization → enhanced transport

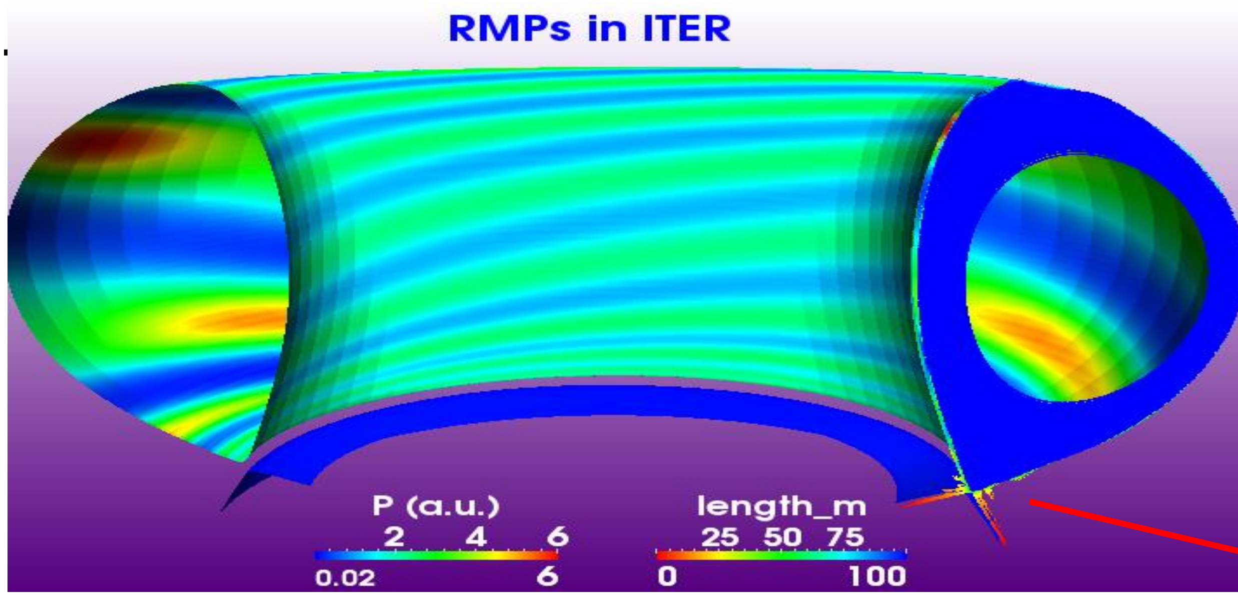

→ 3D-displacement of the separatrix

→ Maximal distortion near the X-point: **lobes**

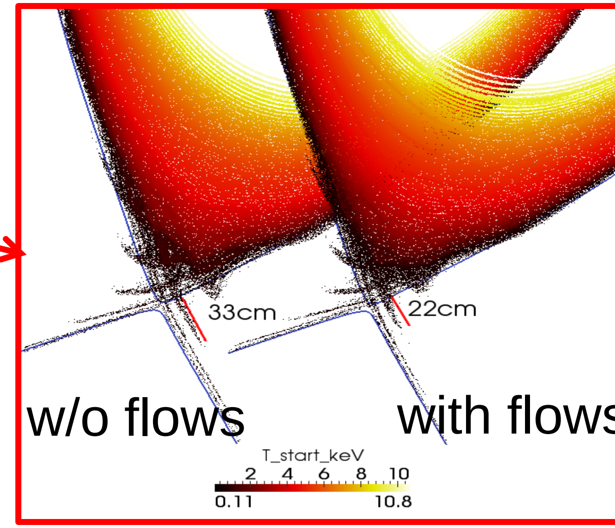

Edge ergodization by RMPs **→ increased particle and heat transport** near the X-point + strike-point splitting

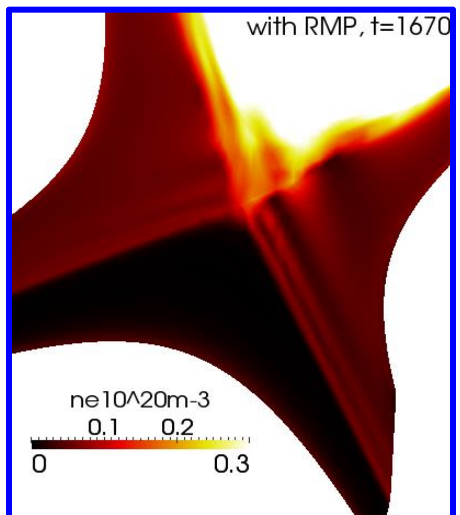

[Orain PoP2013]

Close comparison to experimental results in AUG

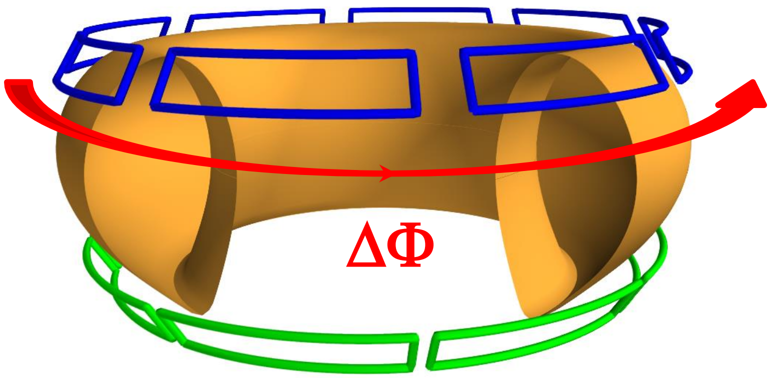

Rotation of differential phase ΔΦ
between upper and lower coil currents
→ change applied RMP spectrum
→ change plasma response to RMP

❖ Input from exp:
- H-mode plasma at low collisionality
- n=2 RMPs applied

❖ In this part, only n=2 and n=0 modes included in modeling.

Typical plasma response: RMP screening except at very edge

❖ RMP-induced magnetic topology:

- Edge ergodic layer
- Lobe structures near X-point

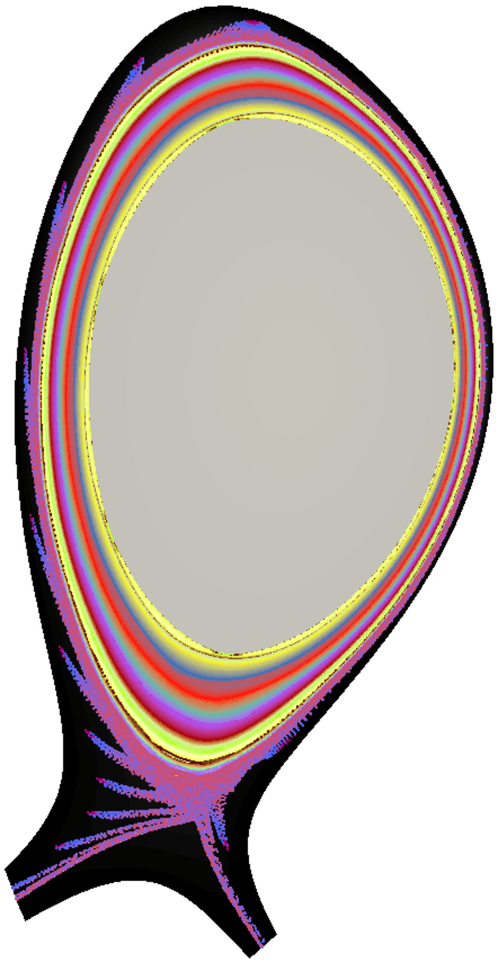

Typical plasma response: RMP screening except at very edge

❖ RMP-induced magnetic topology:
- Edge ergodic layer
- Lobe structures near X-point

Perpendicular electron velocity

❖ Magnetic islands on resonant surfaces

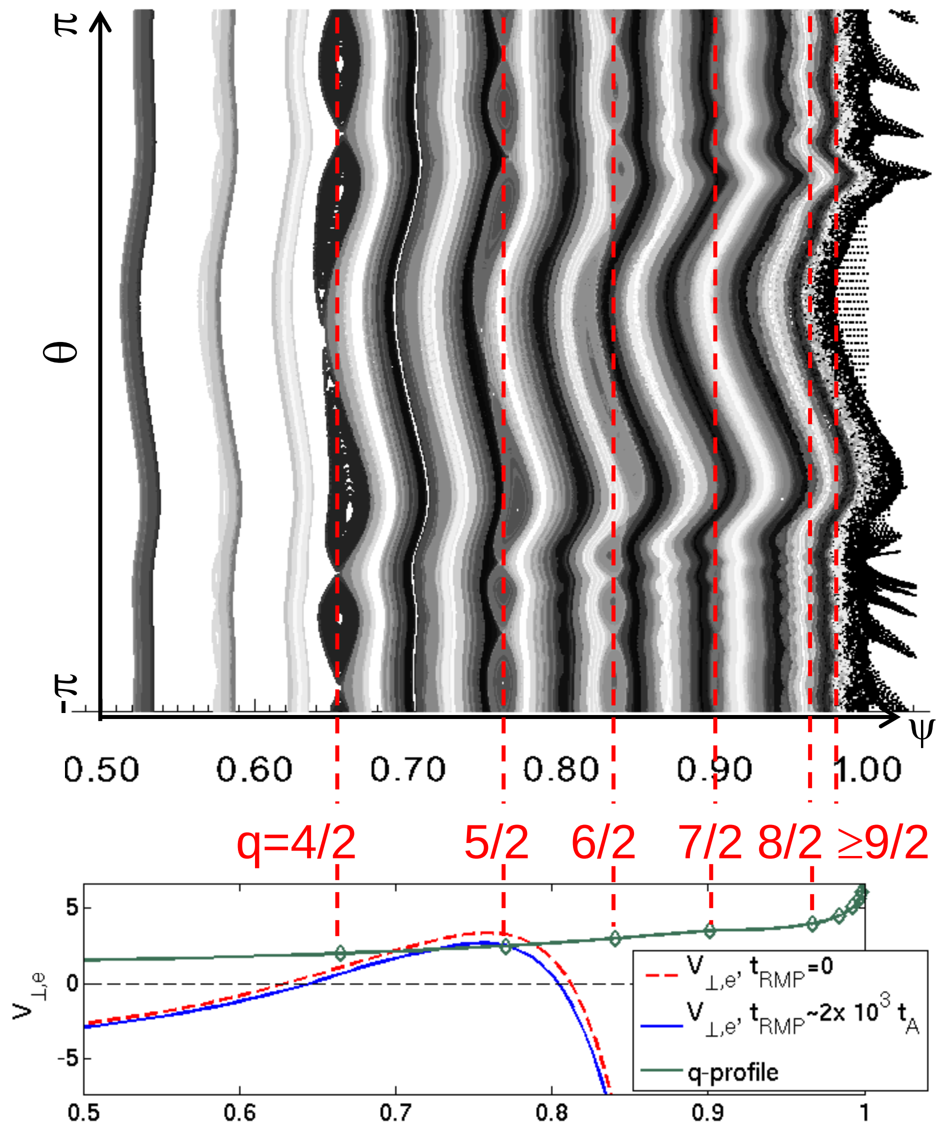

Magnetic topology at the edge depends on applied spectrum

Exp: strongest ELM mitig. $\Delta\Phi = +90°$ | smaller ELM mitig. Even ($\Delta\Phi = 0°$) | No mitigation $\Delta\Phi = -90°$

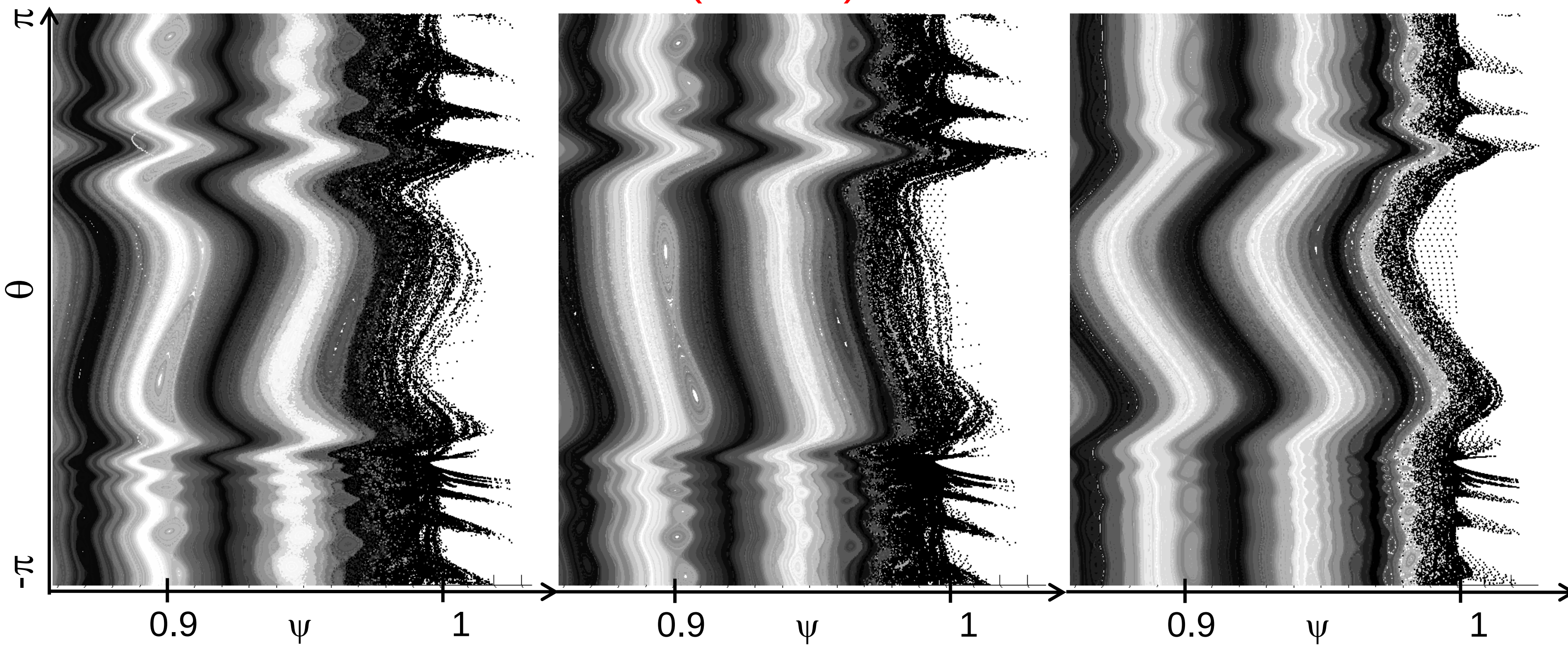

- Larger ergodic layer for strong mitigation case $\Delta\Phi = +90°$
- $\Delta\Phi = +90°$: kinking max near X-point ; $\Delta\Phi = -90°$: kinking max at midplane

[F.Orain, NF2016]

Resonant component very similar at pedestal top (q≈7/2). config ΔΦ =60 to 90° most resonant at very edge (ψ>0.97)

➢Magnetic flux perturbation on resonant surfaces

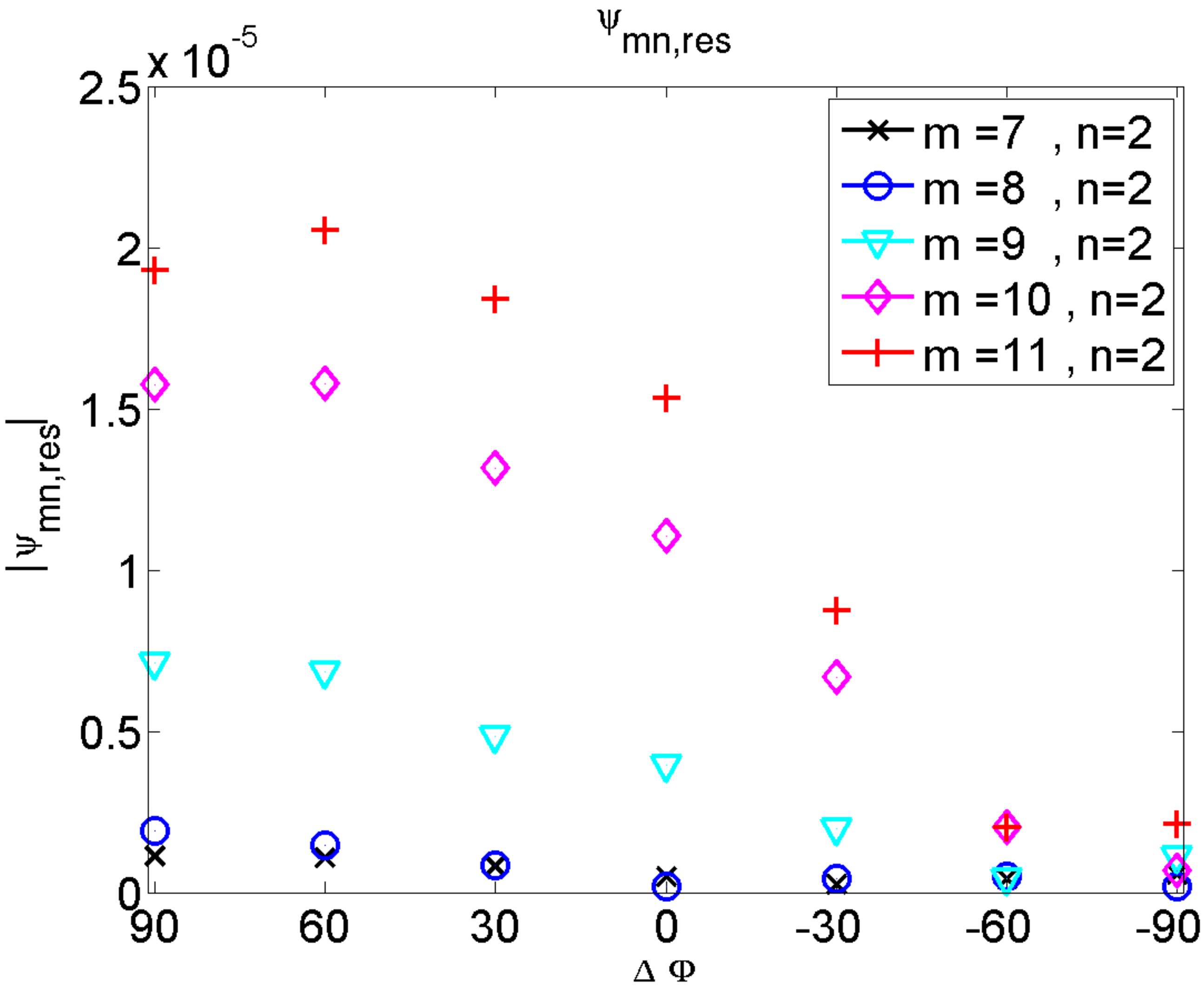

Footprints on divertor largest for strong mitigation case

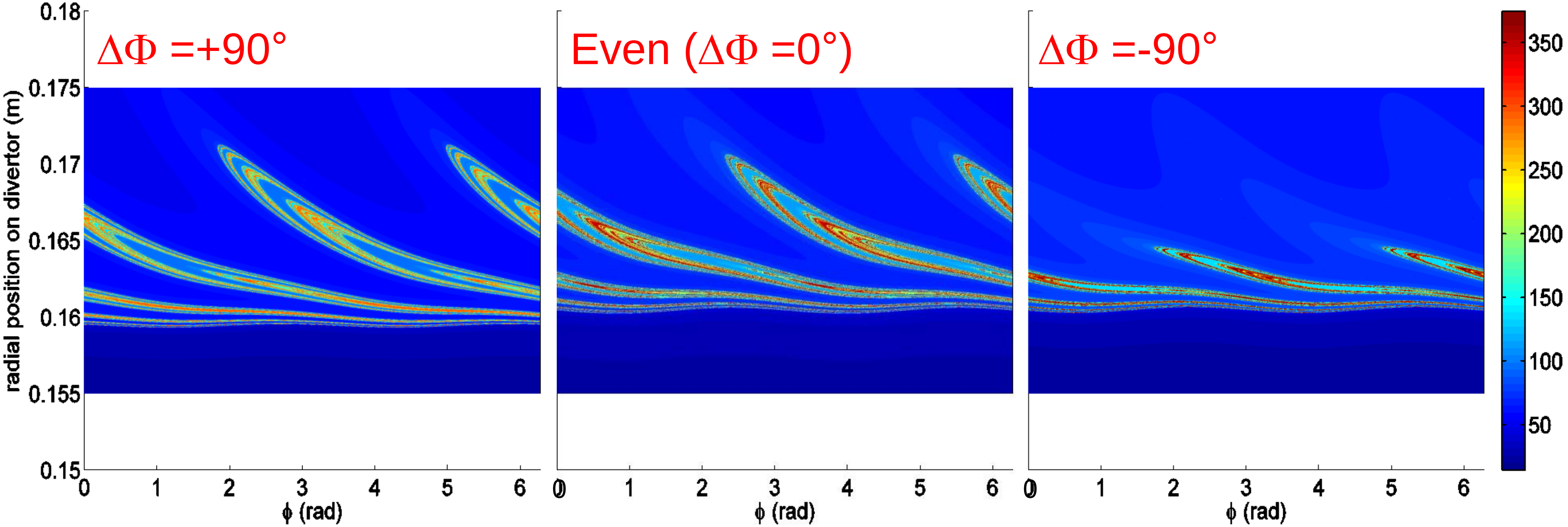

Density profile displacement around X-point

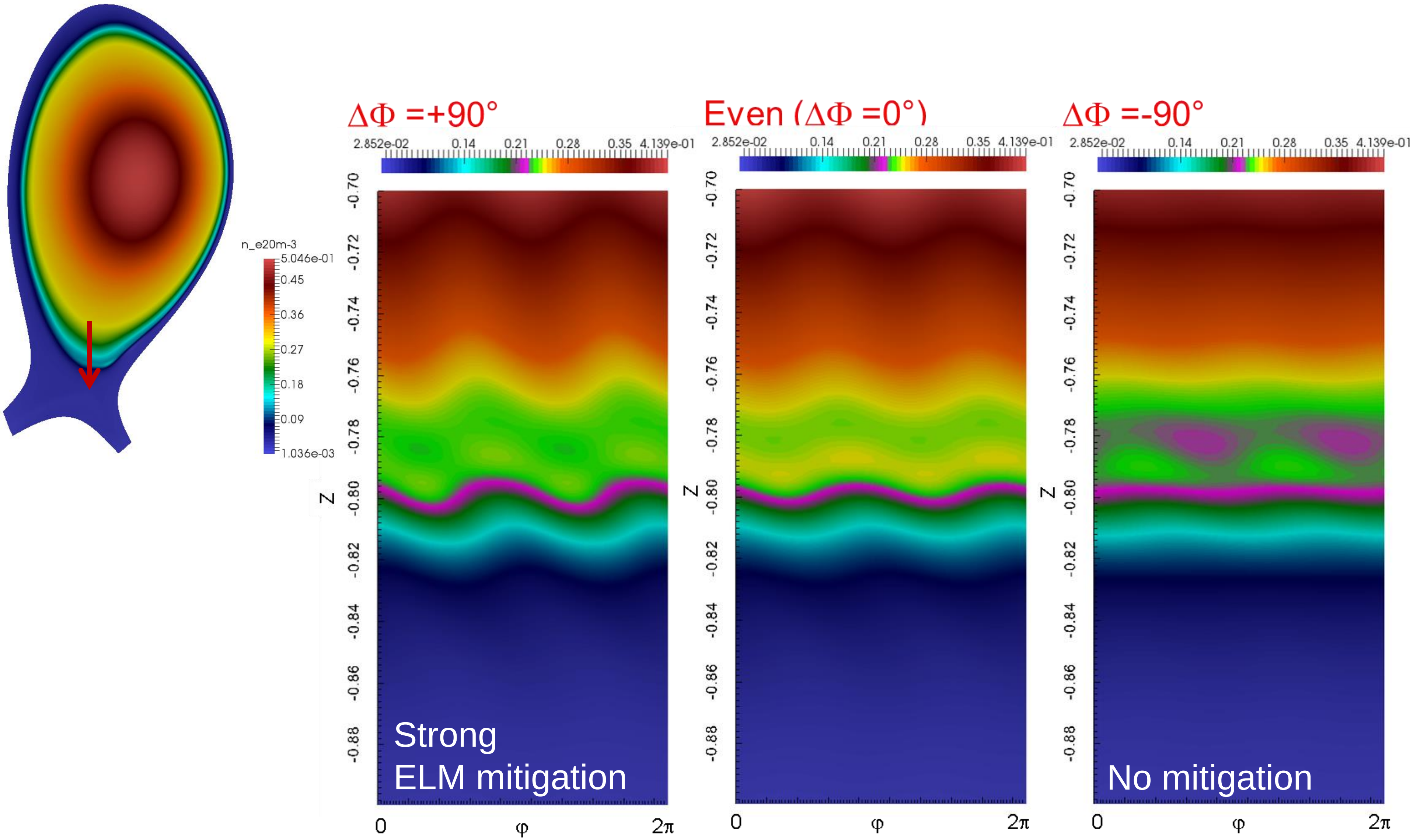

Largest edge kink response for strong mitigation case

Radial perturbation of magnetic field

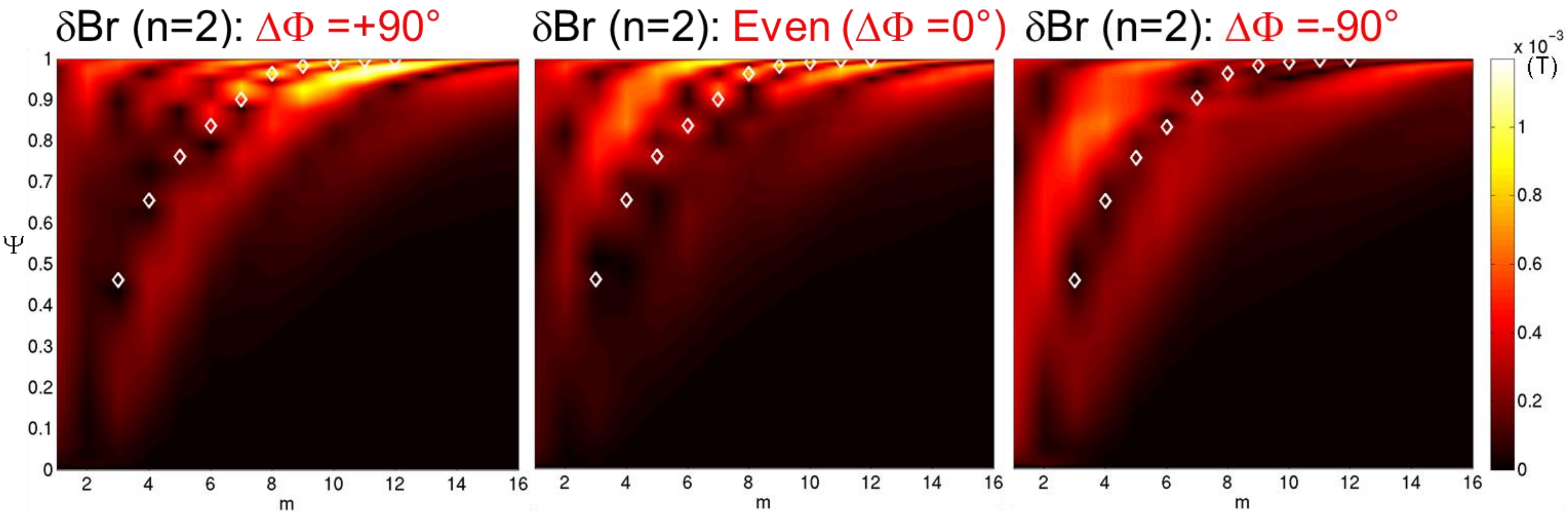

Largest edge kink response for strong mitigation case

Radial perturbation of magnetic field

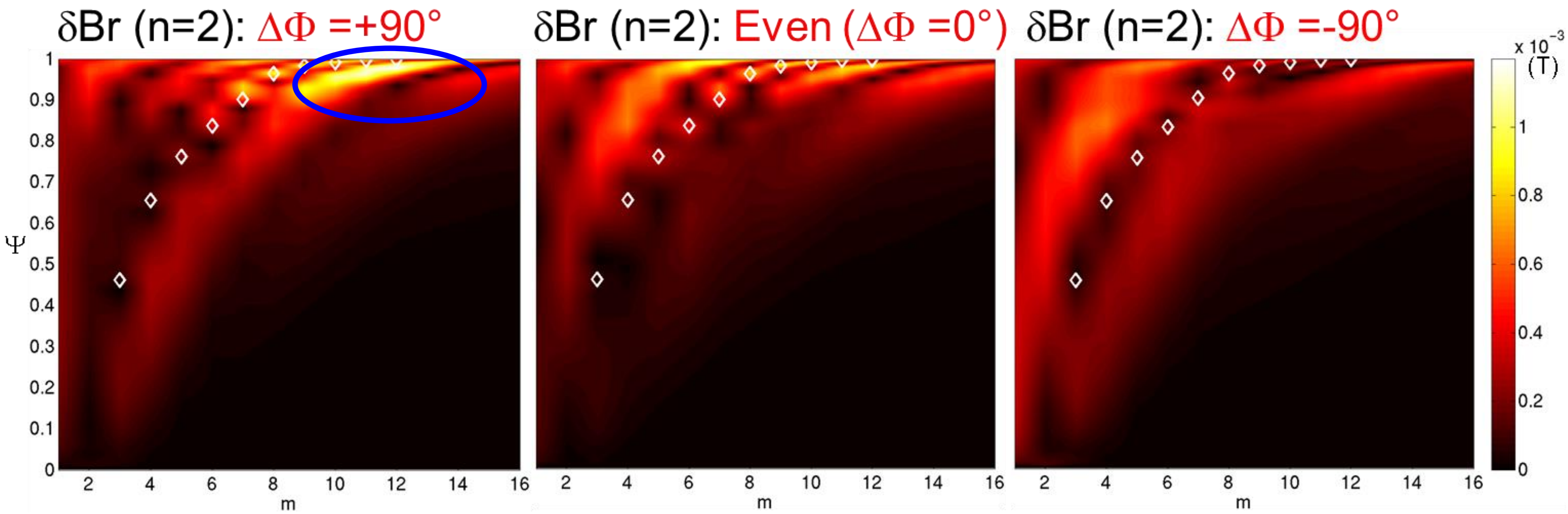

- Edge kink response: modes *m* > *nq* amplified by RMPs
- **Poloidal coupling of *m>nq* kink modes with *m* resonant component**
  → amplification of resonant response

[Orain et al, NF2016]

- Introduction: ELMs and RMPs
- The JOREK code
- ELM dynamics
- ELM control by RMPs
  - → Plasma response to RMPs (without ELMs)
  - → ELM/RMP interaction
- Conclusion and Outlook

Without RMP → large crash due to n=8.

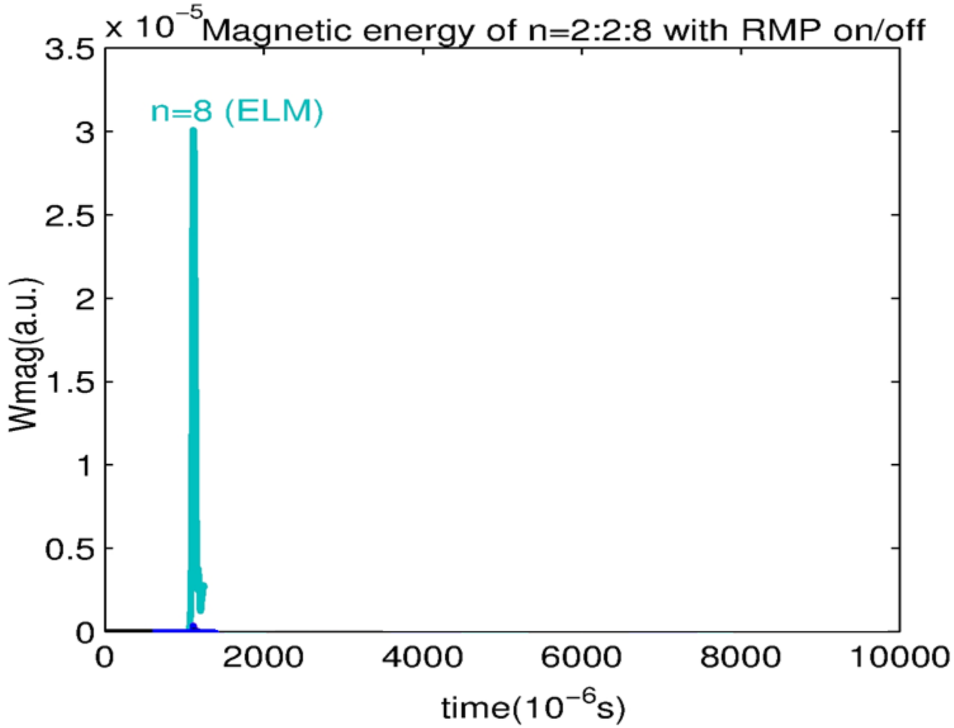

ELM mitigation by RMPs (n=2). Harmonics n=2,4,6,8.

Without RMP → large crash due to n=8.

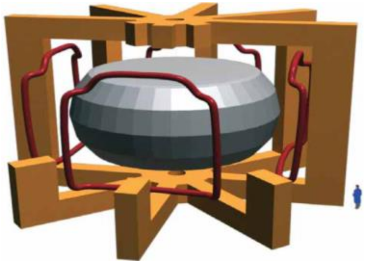

JET: ***n=2*** RMP

I_{coil}=20-80kAt

With RMP→ small relaxations due to n=2,4,6,8.

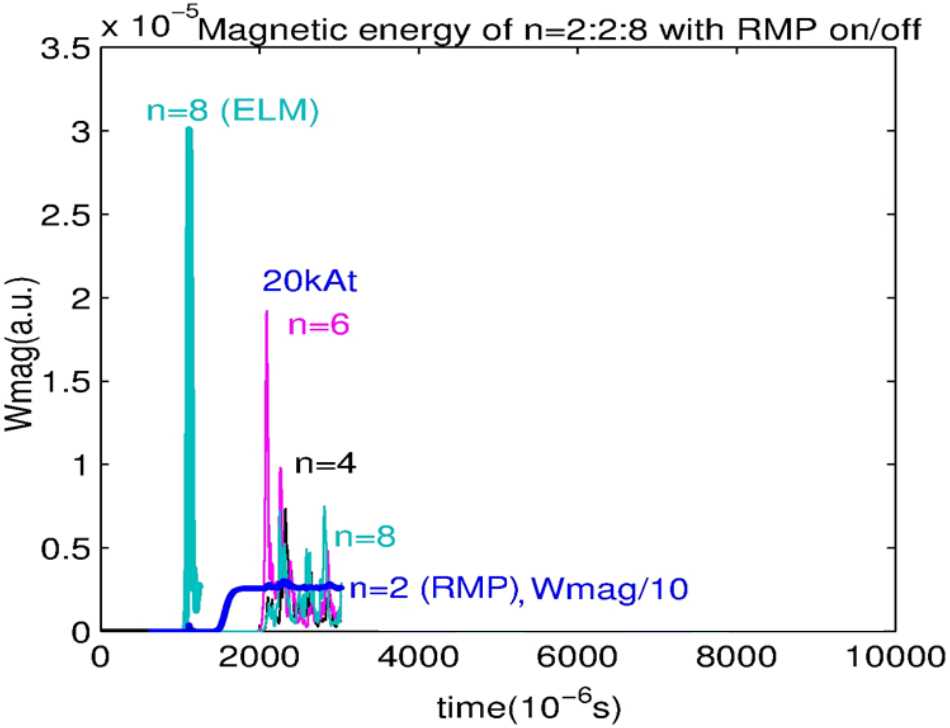

Without RMP → large crash due to n=8.

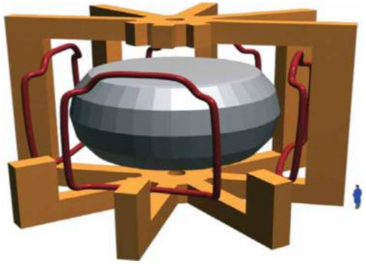

JET: ***n=2*** RMP

I_{coil}=20-80kAt

With RMP→ small relaxations due to n=2,4,6,8.

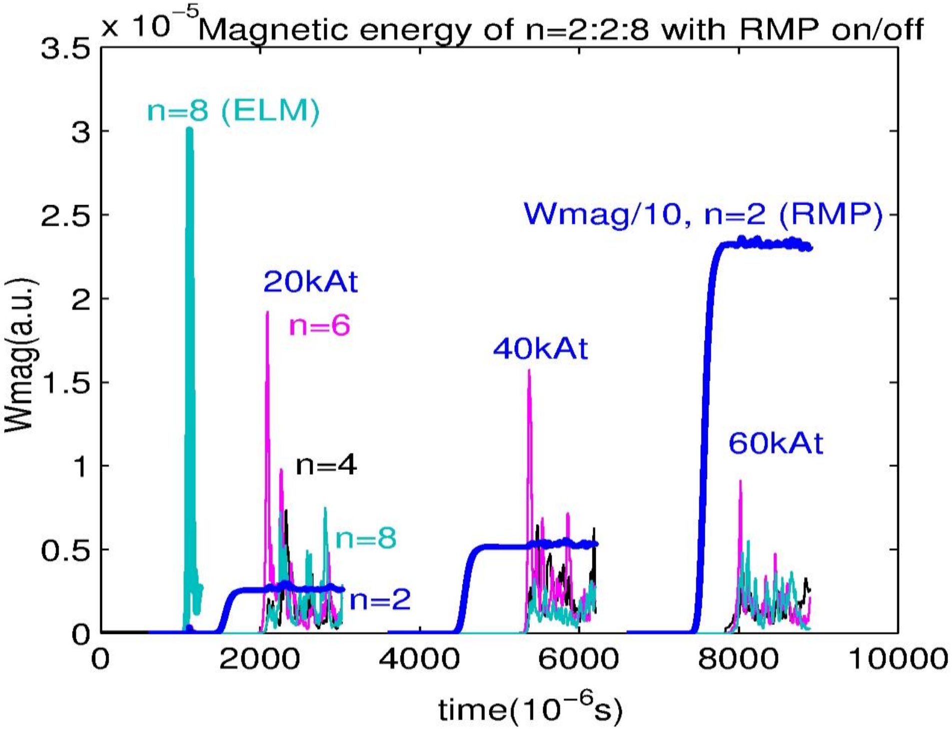

ELM mitigation by RMPs (n=2). Harmonics n=2,4,6,8.

Without RMP → large crash due to n=8.

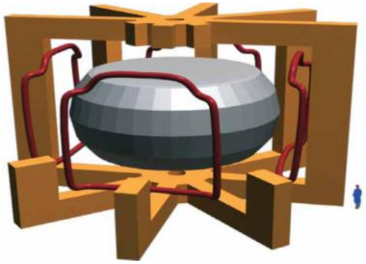

JET: ***n=2*** RMP
I_{coil}=20-80kAt

With RMP→ small relaxations due to n=2,4,6,8.

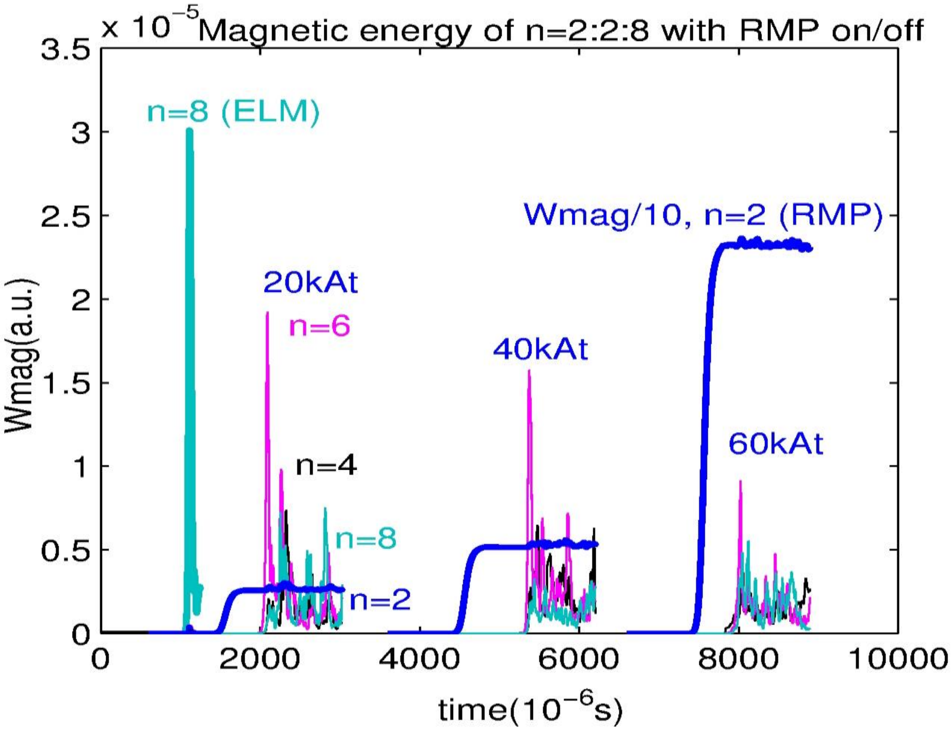

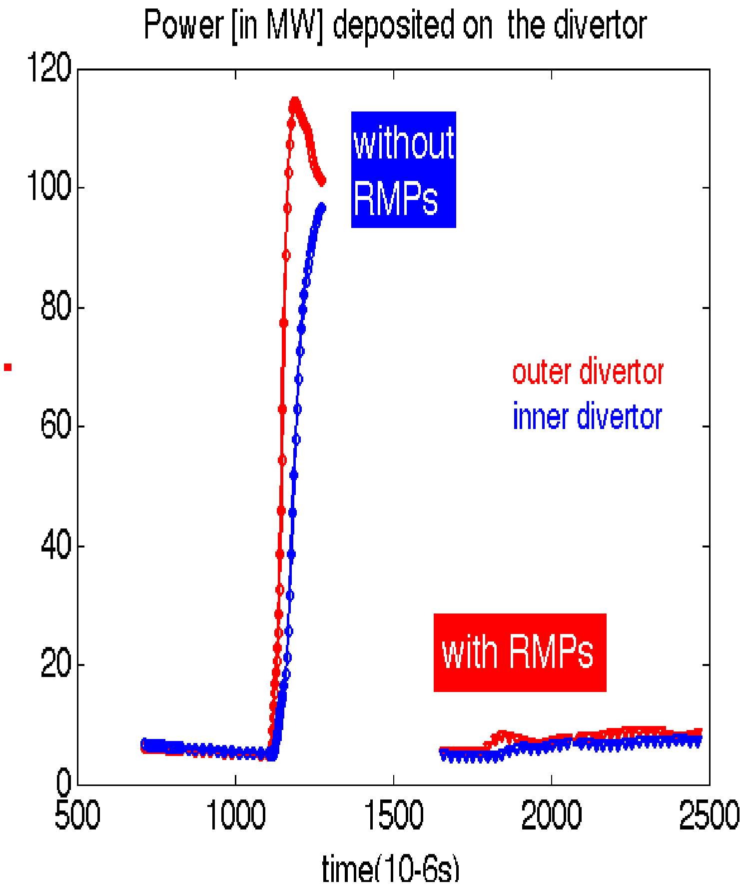

Power deposition divided by ~10 with RMPs

ELM/RMP coupling → redistribution of energy from n=8 to *even* n modes→ more continuous MHD activity

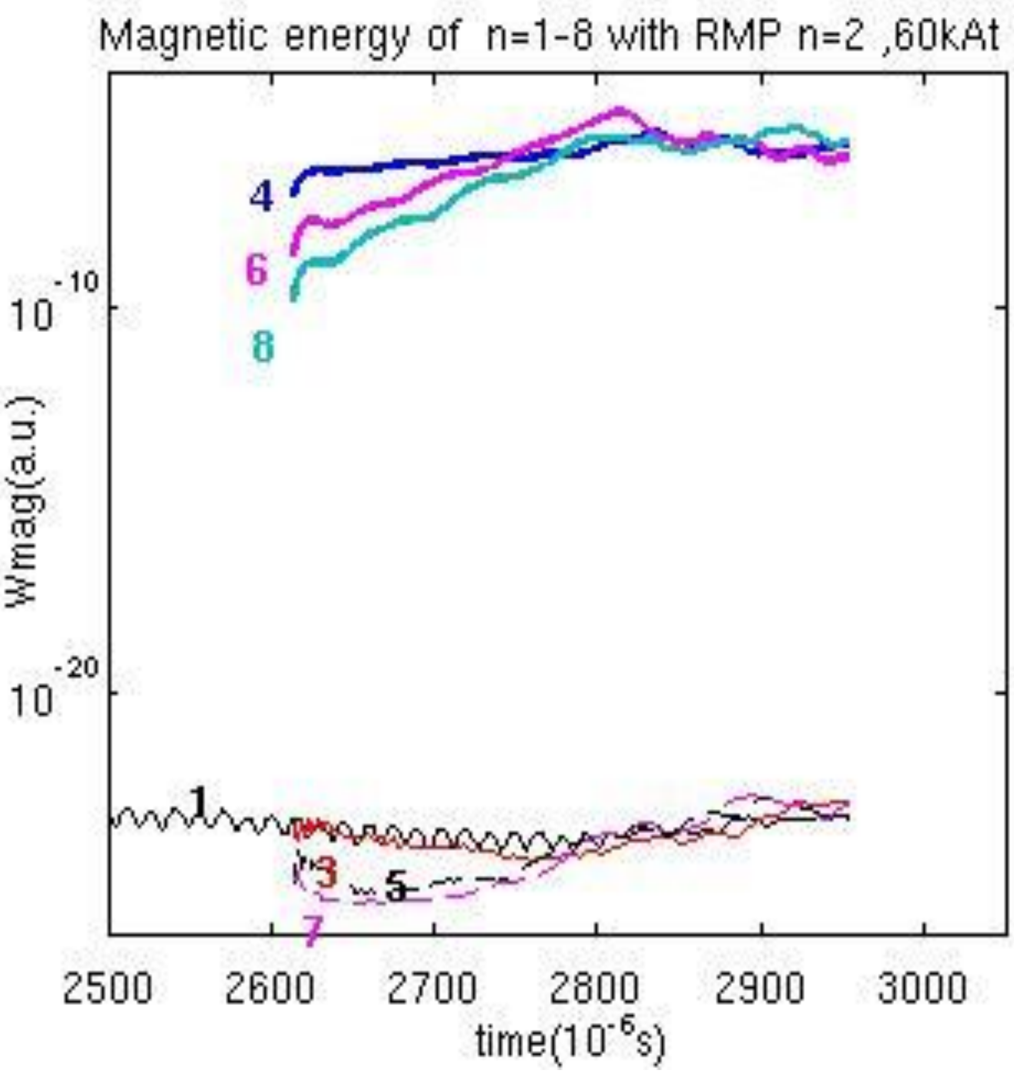

- Mitigated ELMs = even modes n=2,4,6,8 non-linearly driven by n=2 RMPs

- Initial magnetic energy of even modes (coupled with RMP) >>> odd modes (~remain at noise level)

Magnetic topology "transformed" by RMPs: from n=8 ballooning to n=4-6 islands (tearing parity)

No RMP, ELM(n=2-8) Mainly n=8

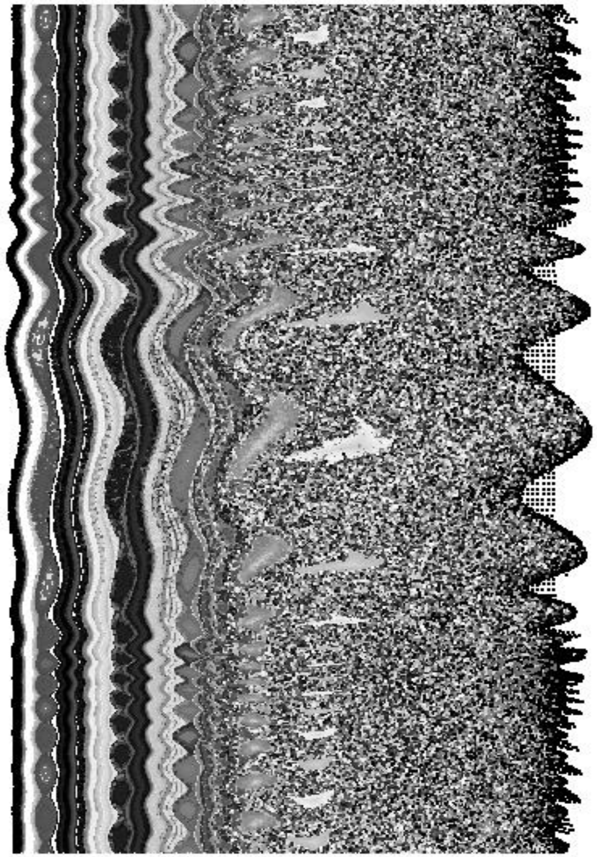

RMP(n=2) w/o ELMs

RMP(n=2) + ELMs (n=2-8)

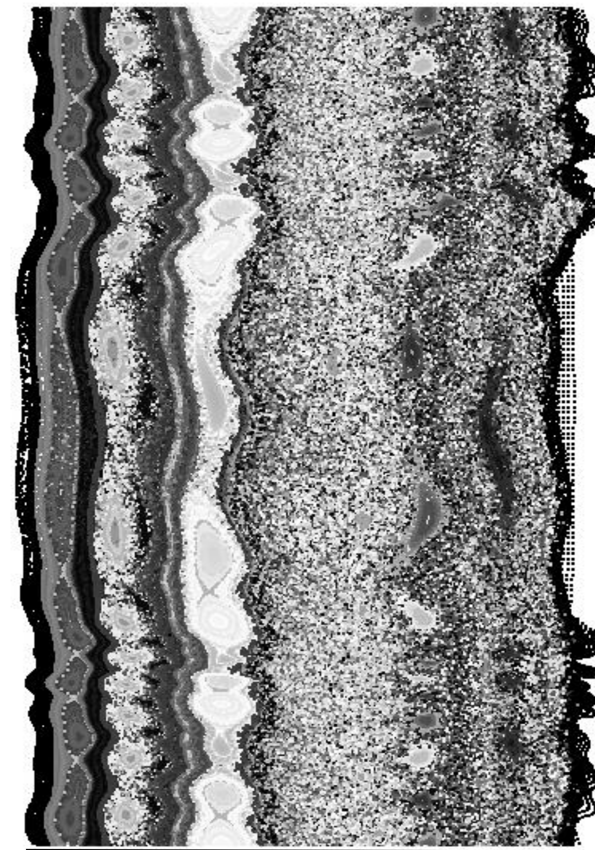

n=8 + n=2 →n=4-6 | 9/4; 14/6;15/6

[Bécoulet, Orain et al, PRL2014]

Preliminary results on ELM/RMP interaction in AUG: Depending on plasma response, no effect on ELM or stabilization

All modes from n=0-8 included

Preliminary results on ELM/RMP interaction in AUG: Depending on plasma response, no effect on ELM or stabilization

All modes from n=0-8 included

❖ Magnetic energy:

No RMP:
ELM grow and crash,
n=8 dominant

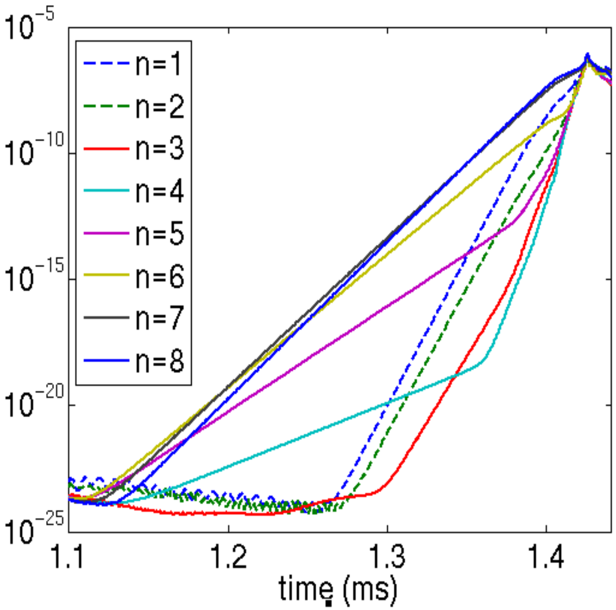

Preliminary results on ELM/RMP interaction in AUG: Depending on plasma response, no effect on ELM or stabilization

All modes from n=0-8 included

❖ Magnetic energy:

No RMP:
ELM grow and crash, n=8 dominant

Weak RMP penetration:
no toroidal coupling ELM/RMP
→ ELM crash

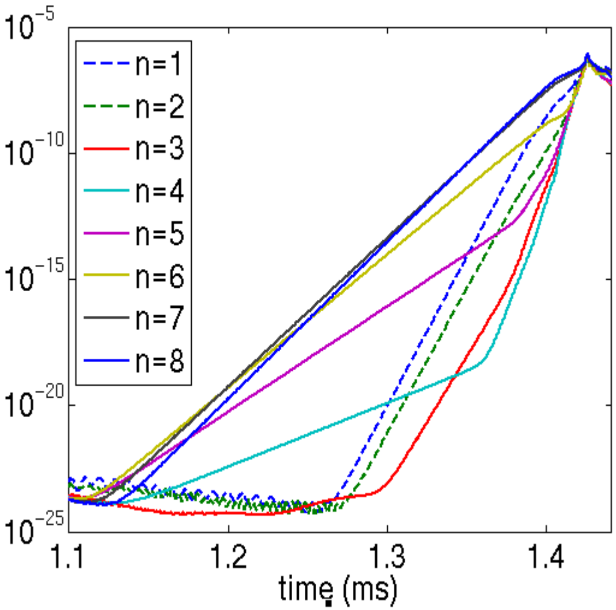

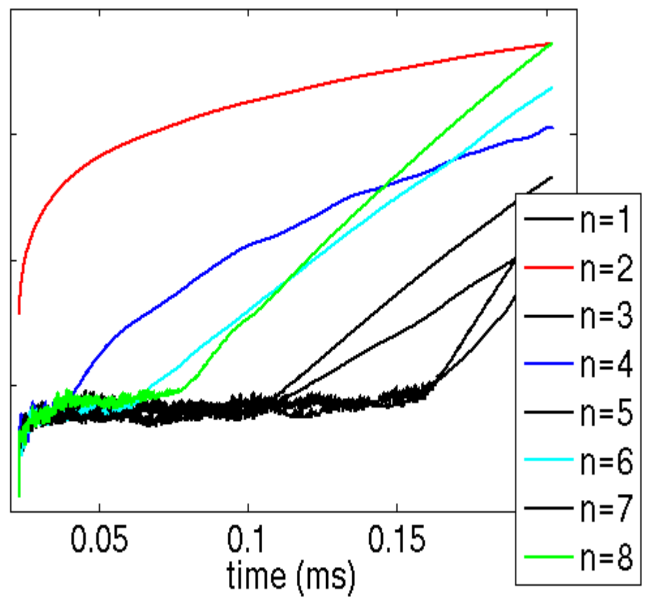

Preliminary results on ELM/RMP interaction in AUG: Depending on plasma response, no effect on ELM or stabilization

All modes from n=0-8 included

❖ Magnetic energy:

No RMP:
ELM grow and crash,
n=8 dominant

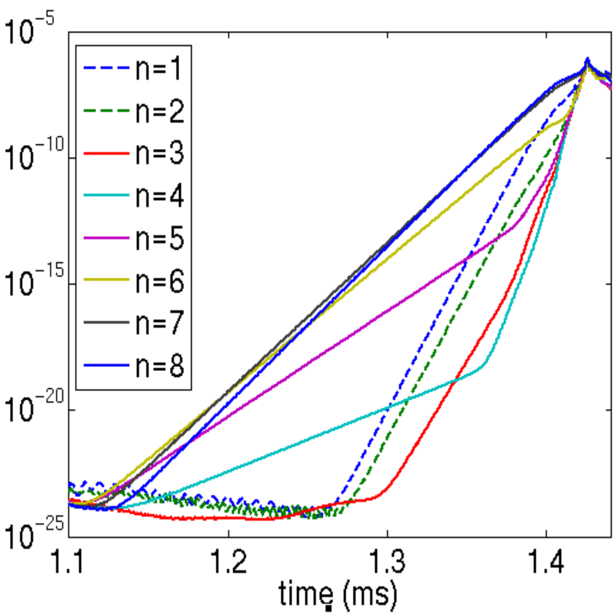

Weak RMP penetration:
no toroidal coupling
ELM/RMP
→ ELM crash

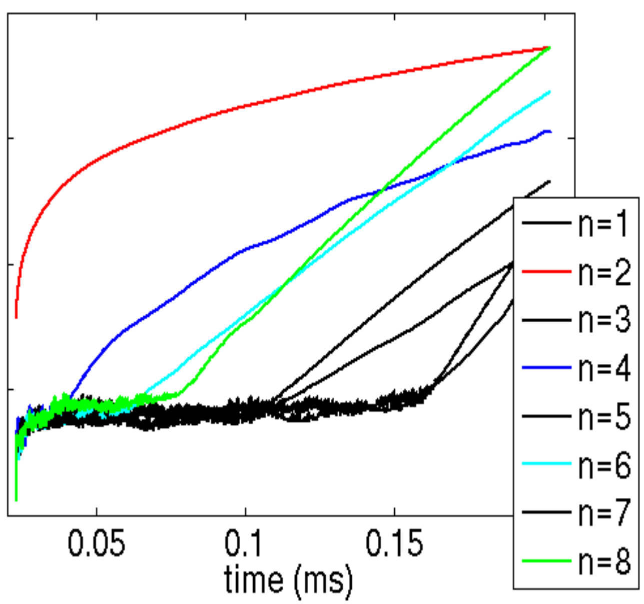

Large RMP penetration:
Medium-n even modes
coupled to n=2 RMP
→ ELM stabilization

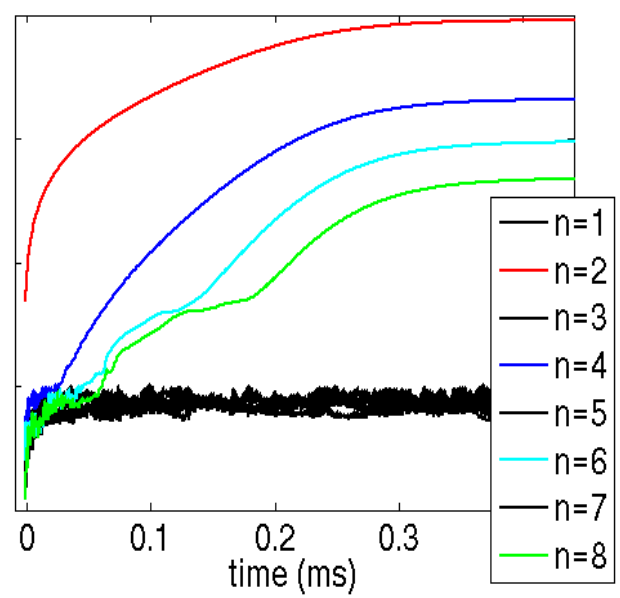

[F.Orain et al, IAEA2016]

❖ Growth rates of modes:

ΔΦ=+90°: growth rates coupled

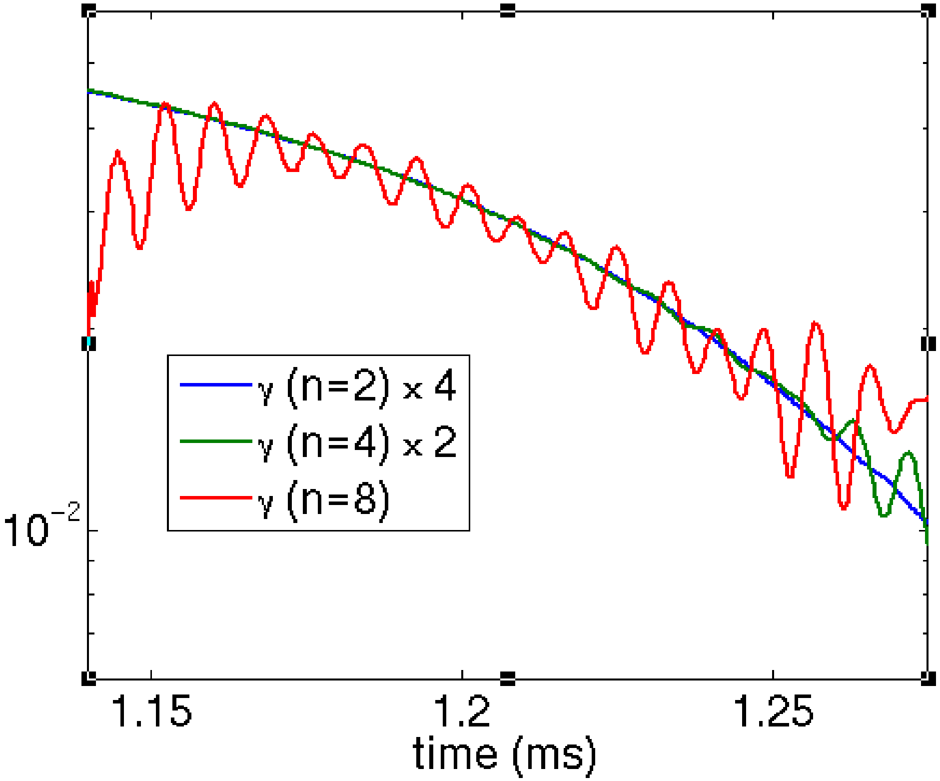

ΔΦ=-90°: growth rates not coupled

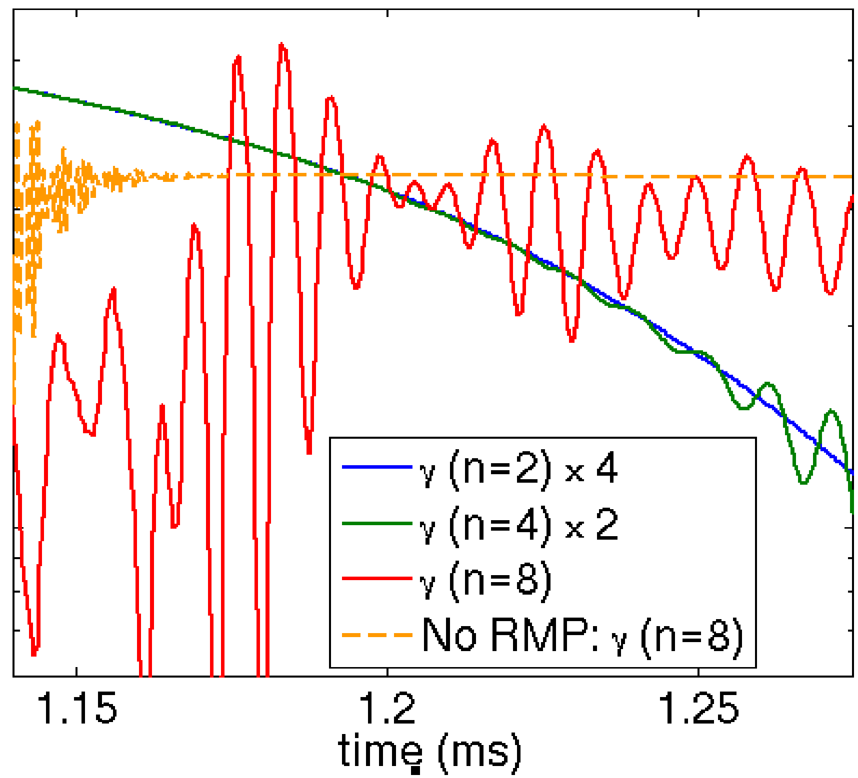

Now: 1/ Apply RMPs (3D equilibrium) then 2/ include ELMs

❖ Increasing ω* (and shear):

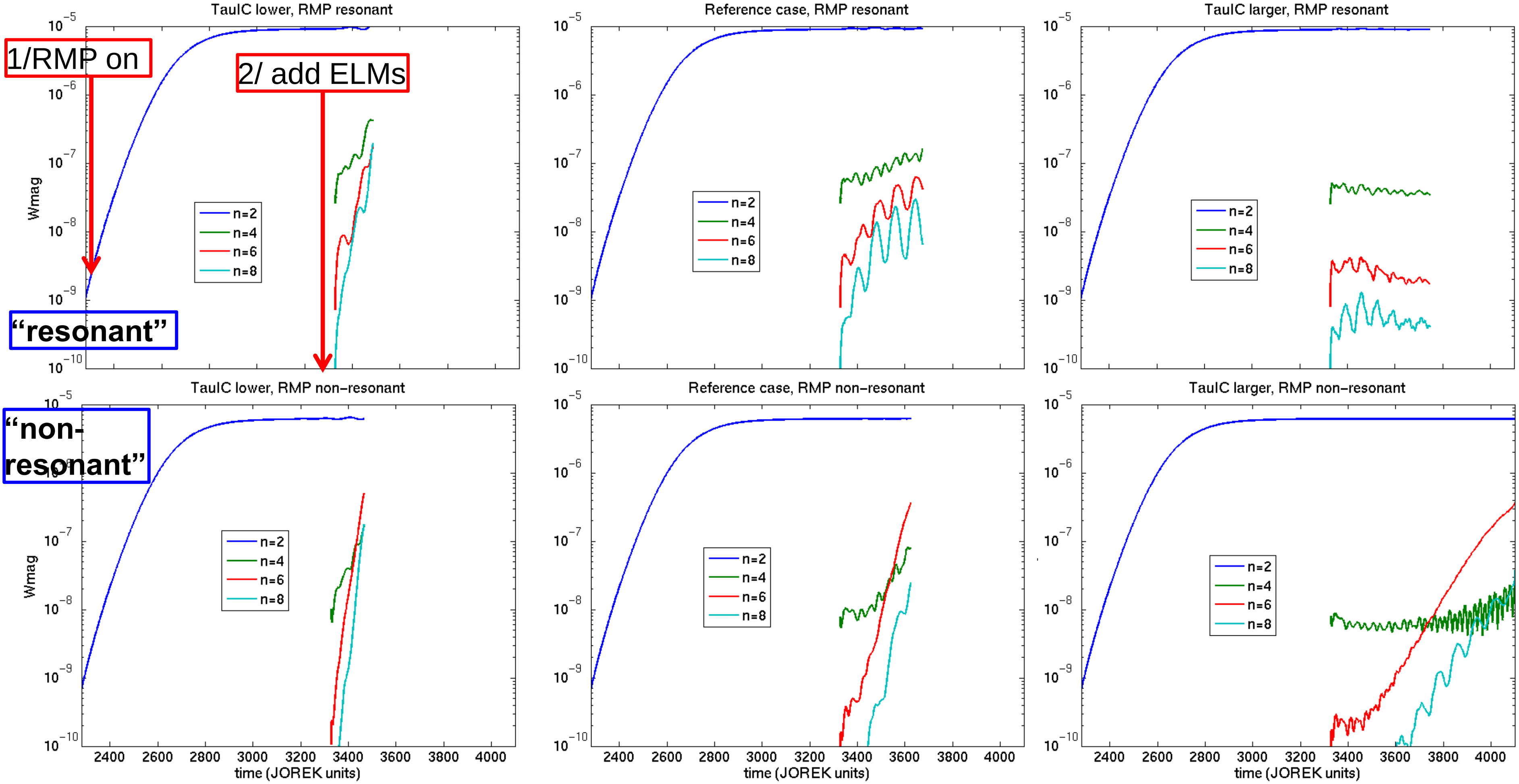

→ Larger perpendicular rotation stabilizes mitigated ELMs.

Other important parameters

❖ Viscosity ν / resistivity η:

→ η ++: destabilizing since makes ELMs more unstable

→ ν ++: stabilizing since increase RMP penetration

ELM mitigation/suppression=f(ν, η, ω) + RMP amplitude +other parameters?

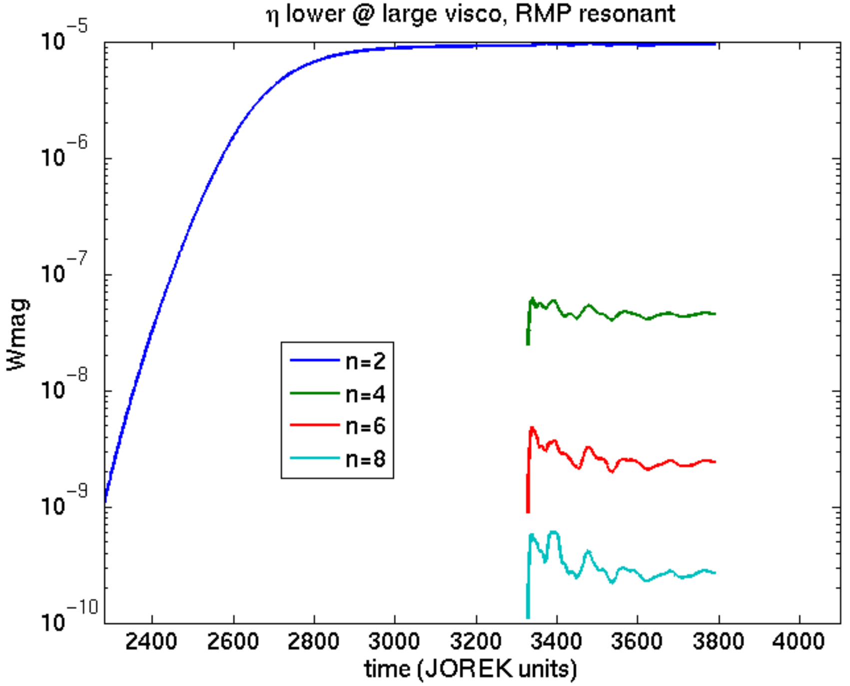

Conclusion/discussion on ELM control by RMPs

- 1st simulation of the ELM mitigation/ suppression by RMPs in JET-like study case:
  - Mechanism: energy cascade from high n to the non-linearly coupled n modes → more continuous MHD activity instead of a violent ELM crash

- Plasma response and ELM/RMP interaction modeled for experimental parameters of H-mode AUG discharges:
  - Strongest ELM mitigation related to largest kink response near X-point. Mechanism: coupling between *m>nq* edge kink component with *m* resonant component → amplification of resonant perturbation at the edge.
  - For small RMP penetration, no coupling of ELMs and RMPs → ELM crash similar to no RMP case. For large RMP penetration, coupling of medium-n modes with n=2 RMP → mitigation or stabilization of ELMs. Mitigated ELMs more easily stabilized at large viscosity, small resistivity and large poloidal rotation.

- Ongoing and future work:
  - Ongoing modeling to further understand ELM mitigation VS suppression.
  - Continue to investigate density pumpout.
  - Improved RMP model using JOREK-STARWALL.
  - ELM cycles with/without RMPs.

References

❖ Main publications:

- 2016: F. Orain *et al.*, Non-linear modeling of the plasma response to RMPs in Asdex Upgrade, *Nuclear Fusion 57, 022012*

- 2015: F. Orain *et al.*, Resistive reduced MHD modeling of multi-ELM cycles in tokamak X-point plasmas, *Physical Review Letters 114, 035001*

- 2015: F. Orain *et al.*, Non-linear MHD modeling of edge localized mode cycles and mitigation by resonant magnetic perturbations, *Plasma Phys. Controlled Fusion 57, 014020* (invited paper at 41st EPS conference on plasma physics, Berlin 2014)

- 2014: M. Becoulet, F. Orain *et al.*, Mechanism of Edge Localized Mode mitigation by Resonant Magnetic Perturbations, *Physical Review Letters 113, 115001*

- 2013: F. Orain *et al.*, Non-linear magnetohydrodynamic modeling of plasma response to resonant magnetic perturbations, *Physics of Plasmas 20, 102510*

- 2012: M. Becoulet, F. Orain *et al.*, Screening of resonant magnetic perturbations by flows in tokamaks, *Nuclear Fusion, 52(5), 054003*

Plasma response to RMPs: mechanism

- Ohm's law: $$\frac{1}{R^2}\frac{\partial \psi}{\partial t} = \eta \frac{J}{R^2} - \vec{B}\cdot\left(\nabla_{\parallel} u + \frac{\tau_{IC}}{\rho}\nabla_{\parallel} p\right)$$
- Linearization on resonant surface *q=m/n* (steady state):

$$\eta J_{nm} = -im\psi_{nm} R\left(\frac{\partial u_{oo}}{\partial \psi} - \frac{\tau_{IC}}{\rho_{00}}\frac{\partial p_{oo}}{\partial \psi}\right) \Rightarrow \eta J_{nm} = -b^{r}_{nm}\left(V_{E,\theta} + V^{e}_{p,\theta}\right)$$

- $V_{\perp,e}$ → induce response current to RMPs on resonant surfaces → magnetic field opposite to RMPs → **screening of RMPs**

RMPs in vacuum

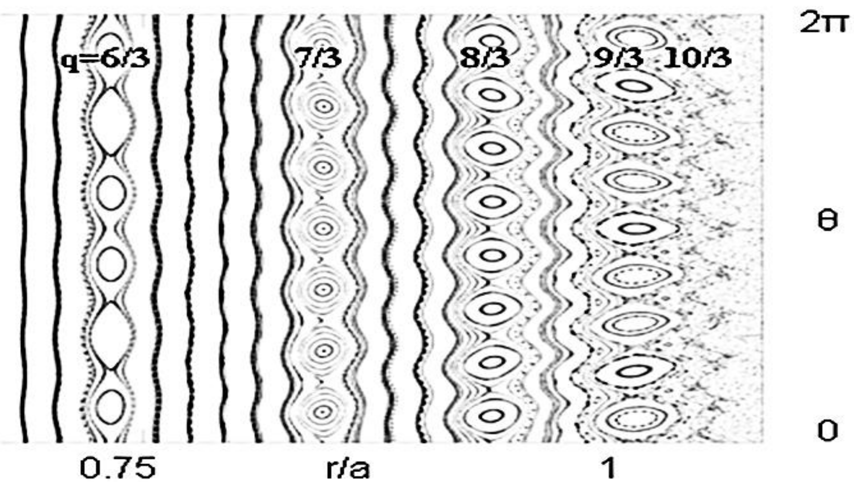

RMPs with plasma response

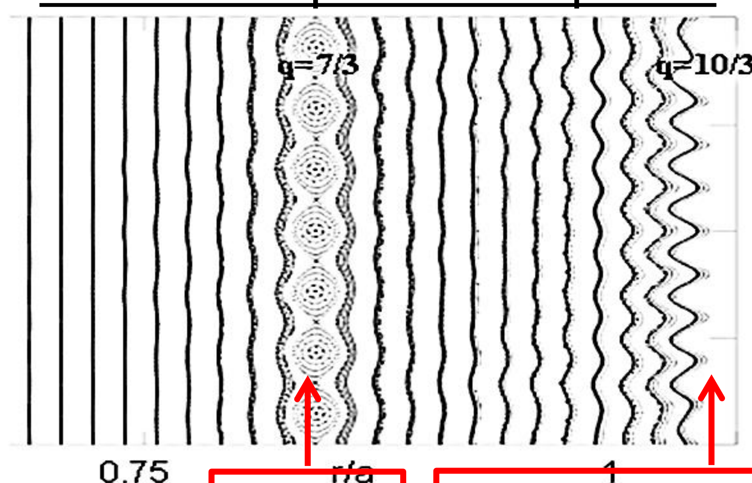

$V_{\perp e}=0$

High resistivity η

ω*>0: near-symmetric power deposition in inner/outer divertor targets

Experimentally: ELM power deposition:
either symmetry inner/outer divertor, either 2x more power on INNER divertor
[Pitts NF 2007, Eich PRL 2003]

Modeling without ω*:
Deposition mainly in OUTER divertor

ω*>0: Near-symmetric deposition in inner/outer divertor plates
→ Closer to experiments

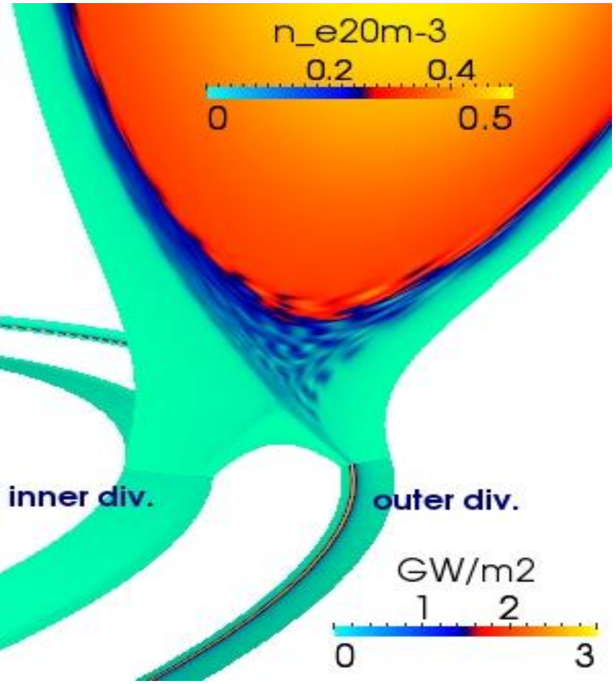

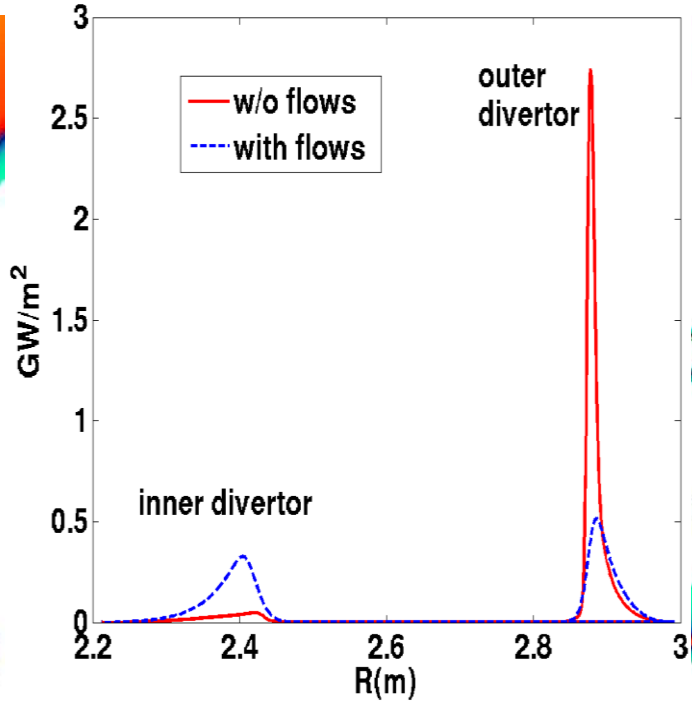

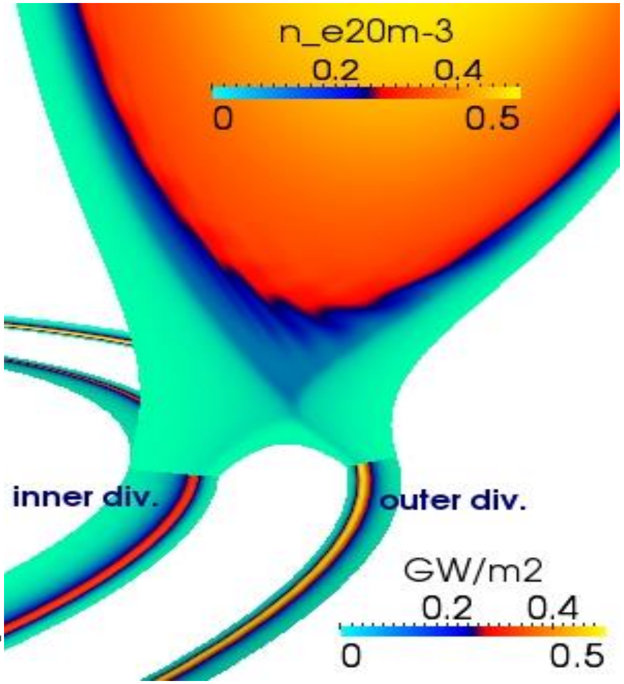

AUG experiments: ELM mitigation by n=2 RMP at low density→low ν*
Differential phase scan: study penetration = f($\Delta\Phi_{coils}$)

[Suttrop, Kirk et al, IAEA 2014]

$\Delta\Phi$ scan (by $-\pi$)

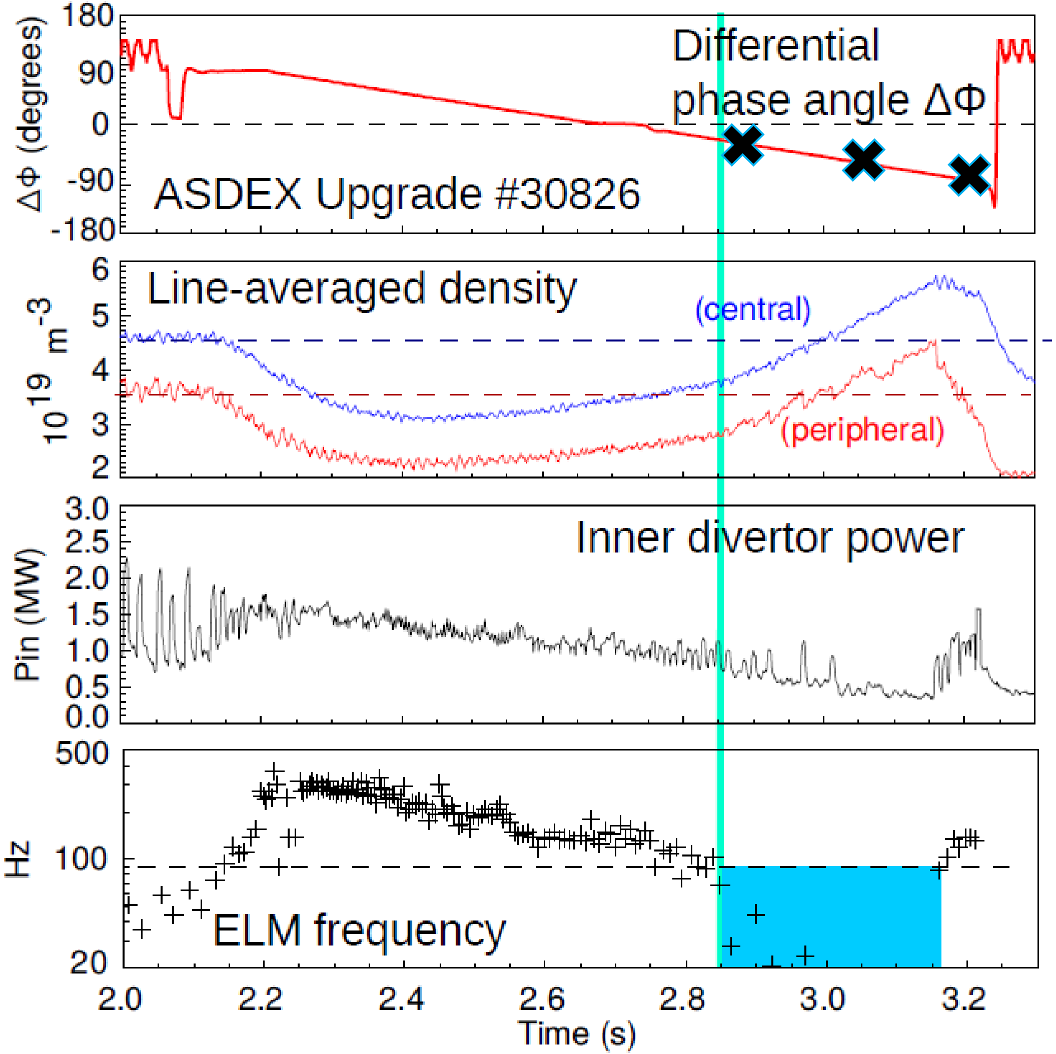

❖ Modeled coil configurations:

•$\Delta\Phi_{coils}$ = +90°
(shot #31128)
= +60°
= +30°

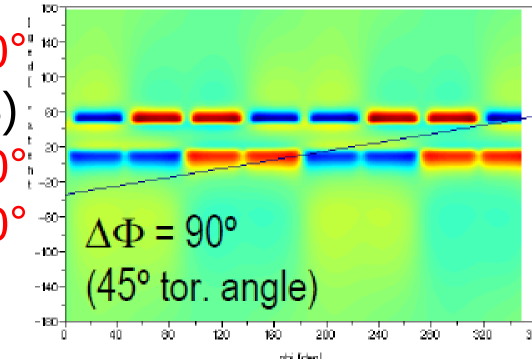

•$\Delta\Phi_{coils}$ = 0°
(even parity)

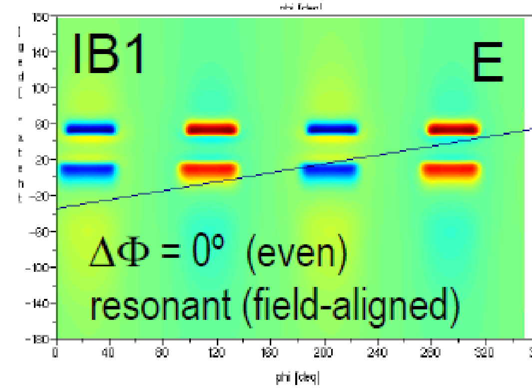

•$\Delta\Phi_{coils}$ = -30°
= -60°
= -90°